Universidade de São Paulo

Instituto de Física

Aspectos de complexidade em teoria quântica de campos e holografia

Felipe Soares Sá

Orientador: Prof. Dr. Diego Trancanelli

Tese de doutorado apresentada ao Instituto de Física como requisito parcial para a obtenção do título de Doutor em Ciências.

Banca Examinadora:

Prof(a). Dr(a). Diego Trancanelli (IFUSP)
Prof(a). Dr(a). Victor de Oliveira Rivelles (IFUSP)
Prof(a). Dr(a). Bertha María Cuadros Melgar (EEL USP)
Prof(a). Dr(a). Dmitry Melnikov (UFRN)
Prof(a). Dr(a). Alberto Tomas Faraggi Ugalde (UNAB - Chile)

São Paulo
2023

FICHA CATALOGRÁFICA
Preparada pelo Serviço de Biblioteca e Informação
do Instituto de Física da Universidade de São Paulo

Sá, Felipe Soares

Aspectos de complexidade em holografia. São Paulo, 2022.

Tese (Doutorado) – Universidade de São Paulo. Instituto de Física. Depto. de Física Matemática.

Orientador: Prof. Dr. Diego Trancanelli

Área de Concentração: Física de Alta Energia

Unitermos: 1. Complexidade; 2. Holografia; 3. Transição de Fase.

USP/IF/SBI-83/2022

University of São Paulo

Institute of Physics

Aspects of complexity in quantum field theory and holography

Felipe Soares Sá

Supervisor: Prof. Dr. Diego Trancanelli

Thesis submitted to the Physics Institute of the University of São Paulo in partial fulfillment of the requirements for the degree of Doctor of Science.

Examining Committee:

Prof(a). Dr(a). Diego Trancanelli (IFUSP)
Prof(a). Dr(a). Victor de Oliveira Rivelles (IFUSP)
Prof(a). Dr(a). Bertha María Cuadros Melgar (EEL USP)
Prof(a). Dr(a). Dmitry Melnikov (UFRN)
Prof(a). Dr(a). Alberto Tomas Faraggi Ugalde (UNAB - Chile)

São Paulo
2023

Acknowledgements

First of all, I would like to thank my family for all the support during these years and my dear girlfriend Simone that is always at my side, specially during the difficult pandemic times. I also need to thank Prof. Dr. Diego Trancanelli for advising me during my Ph.D. and my research partners and friends Viktor Jahnke and Marcos Cezar Ribeiro. I also need to say thank you to my great friends Carlos Vargas, Marcia Tenser and Gabriel Nagaoka for all these years of friendship, learning and support, and to my dear friend Daniel Teixeira that was a kind of second supervisor during all these years. Lastly, I am grateful to CNPq for the scholarship, without it this thesis would not exist.

Abstract

Complexity began to receive a lot of attention in high energy physics in the middle of the first decade of the XXI century, in the context of the study of black holes in AdS/CFT. The concept comes from computer science, where it emerged due to the need to classify which types of computational problems are feasible or not to be solved by a computer. Such a classification results in complexity classes.

Since its incorporation into physics, complexity has been studied from different angles. A possible path is the study of complexity from the point of view of holography. In this context, the growth of complexity in the CFT at the boundary is related to the growth of the interior of the AdS dual black hole in the interior. This relationship is based on the conjectures Complexity = Volume (CV) and Complexity = Action (CA).

A second path is the study of complexity in quantum systems, whether continuous or discrete. One can associate the idea that different states (or operators) of a quantum system have different complexities associated with them, that is, one can estimate the computational cost for the system to be in a given state. We also can think of complexity as a quantity which is sensitive to changes in system parameters. As a consequence, there is the possibility that complexity provides information about important properties of the system, for example, if it presents a chaotic behavior or if a given parameter change generates a phase transition.

Key-words: Complexity, Holography, Phase Transition.

Resumo

Complexidade começou a receber bastante destaque na Física de altas energias em meados da primeira década do século XXI no contexto do estudo de buracos negros em AdS/CFT. O conceito vem da ciência da computação, onde surgiu por conta da necessidade de se classificar quais tipos de problemas computacionais são factíveis de serem resolvidos por um computador ou não. Tal classificação é chamada de classes de complexidade.

Desde sua incorporação à Física, a Complexidade vem sendo estudada por diversos ângulos. Um caminho possível é o estudo da Complexidade do ponto de vista de holografia. Neste contexto, o crescimento da Complexidade na CFT da borda se relaciona com crescimento do interior do buraco negro AdS dual no interior. Tal relação se dá a partir das conjecturas Complexidade = Volume (CV) e Complexidade = Ação (CA).

Um segundo caminho é o do estudo da Complexidade em sistemas quânticos, sejam eles contínuos ou discretos. Pode-se associar a ideia de que diferentes estados (ou operadores) de um sistema quântico possuem diferentes complexidades associadas a eles, ou seja, pode-se então estimar o custo computacional para que o sistema esteja num dado estado e também temos agora a Complexidade como uma quantidade sensível a mudança de parâmetros do sistema. Como consequência, existe a possibilidade de que a Complexidade forneça informações sobre propriedades importantes do sistema, por exemplo, se este apresenta um comportamento caótico ou se uma dada alteração dos parâmetros geram uma transição de fase.
Palavras-chave: Complexidade, Holografia, Transição de Fase.

Contents

Chapter 1

Introduction

The most concrete realization of the holographic principle [1, 2] we have today is the so-called *AdS/CFT correspondence* (or *gauge/gravity duality*), which was proposed by Juan Maldacena in 1997 [3]. The main statement of the correspondence is that certain conformal field theories (CFTs) are equivalent to gravitational theories defined in a higher-dimensional curved geometry, the Anti-de Sitter (AdS) spacetime. The quantum field theory (QFT) degrees of freedom live in the asymptotic boundary of AdS, while the gravitational ones live in the interior, or bulk, of the space. Typically, both theories involved in the AdS/CFT correspondence display additional symmetries, such as supersymmetry, and their duality is characterized by matching observables computed on the two sides. The canonical example of the AdS/CFT correspondence is the duality between $\mathcal{N} = 4$ Super Yang-Mills (SYM) theory, the maximally superconformal quantum field theory in $3 + 1$ dimensions with gauge symmetry $SU(N)$, and type IIB superstring theory on $AdS_5 \times S^5$.

Arguably, the most interesting aspect of the AdS/CFT correspondence is its being an example of a *weak/strong duality*, meaning that the perturbative regime of one theory is mapped by the duality to the non-perturbative regime of the dual, and vice-versa. This opens up a particularly useful approach to physical processes that are hard to calculate in one formulation, but easier to obtain in the other one. Specifically, the AdS/CFT correspondence maps the strongly coupled regime of planar $\mathcal{N} = 4$ SYM theory to weakly coupled type IIB supergravity. This fact, plus the large amount of symmetries, makes it amenable to analytic computations.

The breakthrough provided by the AdS/CFT correspondence initiated a revolution in theoretical physics, that has involved several areas of research, from nuclear physics and the study of strongly coupled plasmas to condensed matter theory and the study of, for example, high temperature super-conductors. Moreover, the existence of the AdS/CFT correspondence provided an alternative way to study entanglement, a property of quantum systems which is not present in classical ones. The classical world does not accommodate the fact that it is possible to separate two non-interacting systems in such

way that they are not causally related anymore, but remain correlated, meaning that knowledge of one of the parts also implies knowledge about the other. This "peculiar" feature of the quantum world has been a source of great theoretical interest. The initial debate about the implications of such feature gave rise to the so-called Einstein-Podolsky-Rosen (EPR) paradox [4], paving the foundations for further investigations in subsequent years. With John Bell's work [5], the apparent paradox generated by the existence of entanglement was solved, improving the understanding of quantum correlations and their physical implications. Currently, the presence of entanglement as a real feature of quantum systems is not only natural, but central for the development of quantum optical and quantum computational applications, for instance.

It is easier to define and analyze quantum entanglement in simple cases involving a few number of qubits. Given a general bipartite system, the standard measure of quantum entanglement between two subsystems is called entanglement entropy (EE). Such quantity can be easily computed for a system of two qubits (Bell's pair), for instance, however its calculation can be rather involved for a many-body or a continuous system. In order to compute the EE for a QFT, e.g. for its ground state, some sort of sophisticated mathematical technique, such as the replica trick [6], is usually required. This scenario improved after the celebrated proposal by Shinsei Ryu and Tadashi Takayanagi of an holographic alternative to compute the entanglement entropy [7, 8]. The so-called holographic entanglement entropy proposal claims that the entanglement entropy associated with a spatial region in a QFT is given by the area of a particular extremal surface in the holographic dual geometry. The Ryu-Takayanagi proposal motivated Juan Maldacena and Leonard Susskind to purpose a conjecture which claims that "ER = EPR" [9]. In this conjecture, ER refers to a geometric construction named Einstein-Rosen bridge (ERB) which is a solution of the Einstein's equations, while EPR refers to the Einstein-Podolsky-Rosen experiment. The core of this conjecture is the holographic duality between entanglement in the boundary CFT and the wormhole geometry in the AdS bulk.

The fact that entanglement, which is a quantity very useful in quantum information, has acquired some relevance in the understanding of the structure of space-time, inspired the idea that further concepts from quantum information could be in some way useful to the comprehension of open problems in gravity as well. One example of such tools is the so-called *computational complexity*. In few words, computational complexity is a quantity that measures how difficult it is to implement a task. Problems or operations in quantum/classical computation can be classified as easy or hard according to the time that they require to be solved or implemented, which is equivalent to create complexity classes according to the necessary time required to accomplish such tasks [10].

Computational complexity became useful in high energy physics in the context of holography. It was pointed out by Susskind [11, 12] that a candidate for a complexity quantity from the boundary QFT perspective must describe the growth of an ERB at the

dual bulk side. On the one hand, classically, the ERB increases its volume indefinitely. In parallel, a black hole comes to thermal equilibrium really fast, a statement reflected in their saturation of the chaos bound [13], which supports the conjecture that they are in fact the fastest scramblers in nature [14]. This should hold for the dual boundary theory as well. On the other hand, all the time evolution seems to stops after a scrambling time t_*. These facts lead us to a question: is there any quantity in the dual boundary theory that can represent the boundless growth of the ERB? The answer is that the corresponding quantum state describing the ERB does not stop to evolve, which implies that its computational complexity will also keep evolving after the scrambling time. Summarizing, computational complexity is the candidate for a dual quantity that describes the growth of an ERB.

The first concrete association between complexity and some bulk geometrical quantity was the so-called Complexity=Volume (CV) conjecture [15, 16]. Such conjecture provided a relation between the complexity of the boundary state and the volume of a specific codimension-one Cauchy surface in the bulk. In a second moment, inspired by CV, it was conjectured in [17, 18] that the computational complexity is related to the classical bulk action computed over a region called Wheeler-DeWitt (WDW) patch. The so called Complexity=Action (CA) conjecture can be considered as an improved version of the CV conjecture.

An interesting fact about holographic complexity is that the computations on the bulk side were performed first. This is in the opposite direction of the holographic entanglement entropy version, for example. The entanglement entropy was a well-established concept in physics long before its holographic formulation by Ryu and Takayanagi. Consequently, the understanding of how to compute complexity in the QFT side became relevant. Following the seminal works on complexity in the context of quantum computation by Nielsen [19, 20, 21], the discussion about the corresponding formulation in QFT, motivated by the holographic complexity, started in [22]. Posteriorly, in [23], Nielsen's work was extended for continuous systems, particularly QFTs. This paper was a remarkable work in the area, providing the basis for future developments on the subject [24, 25, 26].

From the QFT side, it is possible to make a distinction between two types of complexity: complexity of states and complexity of operators. The complexity of states is associated to a defined *target state* that was obtained from a *reference state* by the action of a unitary operator. Here, these two states are the most important pieces of information, which makes this type of definition suitable to problems where a specific quantum state is being studied or has some centrality. On the other hand, the complexity of operators cares more with how a certain operator evolves from the identity by changing some parameter. Specifically, the time evolution operator is usually studied in this context since it provides us with two important pieces of information: the Hamiltonian and the

time evolution itself. In this sense, the complexity of operators works well for problems where the Hamiltonian is the main piece of information, instead of a specific quantum state.

This thesis is organized as follows. In Chapter 2, we are going to provide an overview about complexity in computer science, focusing on the classes of computational problem and their asymptotic behavior as well. In Chapter 3, the focus will be on holographic complexity, more specifically in the CA conjecture. We are going to consider the complexity for the Mateos-Trancanelli (MT) model, which is a solution of type IIB supergravity dual to a spatially anisotropic finite-temperature $\mathcal{N} = 4$ SYM plasma. Then, in Chapter 4, we will approach complexity in the context of QFTs, with emphasis on the complexity of the *thermofield double (TFD)* state for a charged scalar field theory. Additionally, the complexity of states for a chain of coupled fermionic oscillators will be considered as a second example. Lastly, the complexity of operators will be explained with the intention of studying bosonic or fermionic models that presents quantum phase transitions.

Chapter 2

Complexity in computer science

Computational complexity was already of interest to computer scientists in the early 1960's, prior to its relevance to the high energy community. We could say that computational complexity was born at that time [27]. Just to put things in perspective, Turing developed his theoretical computational model in 1936: the Turing Machine [28]. Since its idealization, the Turing machine proved to be the right theoretical model for computation. However, it fails to account the amount of computational resources, e.g. time or memory, needed by a computer to perform some task, a limitation that computational complexity theory was developed to overcome.

In this discussion about complexity in computer science, we are going to follow closely the discussion developed in the Nielsen & Chuang book [29], which is a standard reference for quantum computing. First of all, we need to think about the following relevant question: What is a computational problem? In order to handle this question, let us start with some crucial concepts. Whatever computation we are interested in, this is essentially made of three elements. The first one is named *input*, which is the information that needs to be provided for the computer so it can perform the desired computation. A simple example of an input is a list with two numbers. The second element is named *output*, which will be the result of the computation. In general, one does not want to be completely ignorant about the result of a computation. We may not be fully able to predict the result of the computation, however, it is desirable to know at least the data type of the output. For example, imagine that we want a specific name from a phone book and we ask a computer to search this specific name in a list for us. In this case, we expect the output to be the desired name or some message like "This name cannot be found". However, we do not expect a number as an output. Finally, the third element is named *algorithm*, which is the logical sequence that our computer will follow in order to obtain the output from the initial information provided by the input. These three elements together constitute a computational problem.

Without loss of generality, an input x is given by a sequence (or string) of bits,

namely

$$x \in \{0,1\}^n, \tag{2.1}$$

where n is the size of the input, which is essentially the number of the bits in the string. Bits are the fundamental pieces of classical computers assuming two possible values, 0 or 1. Any information in a classical computer is stored as a sequence of bits, also called a binary string. For example, the number 27 is stored as 11011 while the letter F is equivalent to 1000110. Following the same logic, the output from a computational problem is $y \in \{0,1\}^m$ with $m \neq n$. Notice that the sizes of the input and of the output do not need to match.

This notion of inputs and outputs as strings of binaries is quite useful to connect the concepts of algorithms and circuits. In a computational problem, the algorithm that we give to the computer in order to obtain the output from the input needs to be very specific and unambiguous. Different algorithms can build the bridge between the input and the output, which motivates computer scientists to keep seeking for more efficient algorithms. In this case, "more efficient" means algorithms that consume less computational resources (e.g. memory, processing time, etc). The sequence of instructions provided by an algorithm is implemented by a circuit. A circuit is a collection of wires and gates, which carry information around and perform simple operations on a finite number of bits. In Figure 2.1, we have an example of a simple circuit which is the application of the so-called NOT gate on a single bit. It flips the bit, taking 1 to 0 and 0 to 1. The wires carry the bit to and from the NOT gate, providing the information of the sequence of gates that act on a specific bit. More generally, a circuit may involve many input and

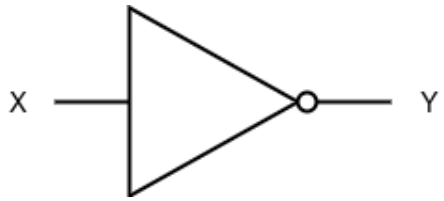

Figure 2.1: Symbol of the NOT gate. If $x = 0$, we have $y = 1$. On the other hand, for $x = 1$, then $y = 0$.

output bits, wires and logical gates. A logic gate is a function

$$f : \{0,1\}^n \to \{0,1\}^m \tag{2.2}$$

from some fixed number n of input bits to some fixed number m of output bits. For example, the NOT gate is a gate with one input bit and one output bit which computes

the function $f(a) = 1 \oplus a$, where a is a single bit, and $\oplus$ is modulo 2 addition

$$a \oplus b = \begin{cases} 0, & \text{if} \quad a = b \\ 1, & \text{if} \quad a \neq b \end{cases} ,$$

with a and b assuming the values 0 or 1. There are many other elementary logical gates which are useful for computation. A partial list includes the AND gate, the OR gate, the XOR gate, the NAND gate and the NOR gate. Each of these gates take two bits as input and produce a single bit as output. These logical gates can be put together to perform an enormous variety of computations. In fact, if we consider the entire list of logical gates, it is possible to compute any function given a n bits input and a m bits output [29].

We are going to talk more about logical gates and circuits later in the context of quantum computers. For now, let us approach some questions concerning algorithms in a different way. Despite the circuit being the fundamental sequence of operations that the computer will follow in order to perform the computation, we can also think about algorithms as a computer program built to accomplish some task. For example, consider a sorted list of names. It is completely possible for a modern computer to search for a specific name in this list. The question is how long the computer will take to perform this task. For a short list, it will be almost immediate. However, what happens if we keep increasing the size of the list, which is equivalent to adding more and more names to it? This is the kind of question that we are going to answer in the next pages.

2.1 Types of computational problems

Before we advance in the study of computational complexity in context of computer science, it is important to realize what are the different types of computational problems. We are not going to cover all of them, however it is safe to point out that they can be divided in four main categories [30]:

1. *Decision Problems:* Given an input x, the algorithm provides YES or NO as possible answers. The standard example of decision problem is the primality testing, where the algorithm needs to determine, given a positive integer n, if n is a prime number or not.

2. *Search Problems:* Differently from a Decision Problem, the answer of a Search Problem can be any kind of string. An important example of this category of computational problems is factoring. Given a positive integer n, the algorithm will provide a list of the prime factors of n. A second example of a search problem is an algorithm that searches for a specific entry in a dictionary. The answer will be the data related to this specific entry.

3. *Counting Problems:* Consider a problem R. The task of counting the number of solutions of R that respects some constraints is a Counting Problem. For example, given a graph G there is a set of subsgraphs of G called spanning trees, which are all the subgraphs G that includes every vertex of G and that are trees.[1] Then, the task related to find the spanning trees of G is a Counting Problem.

4. *Optimization Problems:* Given a set of possible solutions of a computational problem, the task of searching for the best solution among them is an Optimization Problem. As an example, let us consider again a graph G with n vertices. Then choose two specific vertices, which we will denote as u and v. A Counting Problem that could be applied on G is to figure out all the possible paths from u to v while a further Optimization Problem would be to select the shortest one among all such paths. A second example of an Optimization Problem is the Travelling Salesman Problem: given a list of cities and the distances between each pair of cities, find the shortest possible route that visits each city exactly once and returns to the origin city.

It is also important to point that in spite of the classification mentioned above, there is some arbitrariness in classifying computational problems. In fact, every problem can be seen as a search problem [30]. This does not mean that our classification in useless, but we need to be open minded about this question of classifying computational problems.

Equally important than understanding the types of computational problems is to figure out the computational resources required for a computer to accomplish some task. This is the main object of study for the computational complexity: quantify the time and resources required to solve computational problems.

2.2 Computational resources

Different models of computation lead to various resource requirements to accomplish the computation. Even in the case of a well-understood computational problem like addition of integers, differences between computational models may be of interest and may also produce distinct resource requirements. Consequently, as the first step to understand a problem, we would like to find a way of quantifying resource requirements which are independent of relatively simple changes in the computational model. A possible way to do this is by the introduction of the *asymptotic notation*, which is used to summarize the essential behavior of a function. This asymptotic notation can be used, for example, to summarize the number of time steps that are required by a given algorithm, without worrying too much about the exact time count.

[1] In graph theory, trees are graphs that do not have loops, i.e., their branches (or internal lines) do not loop back around and reconnect to itself.

The concept of time steps is essential in the analysis of circuits. If we are allowed to apply just one gate at each time step, the number of logical gates is equal the number of time steps. In this sense, we can quantify the time of execution of some algorithm by the number of gates applied. Then, this kind of circuit is running in *series*. On the other hand, if we are allowed to apply more than one gate at each time step, it is not correct to quantify the time of execution of the algorithm by the number of gates in the circuit. This kind of circuit is running in *parallel*. Another way to consider this idea of time steps is related to number of iterations that the algorithm needs in order to solve the desired task. Each iteration corresponds to one time step, which means that we are able to relate the number of iterations with the size of the input. If the size increases, the number of iterations also increases in some way. This correlation, as we will see soon, can be useful in order to study the complexity of some computational problem.

Suppose that we are interested in the number of time steps necessary to add two n-bit numbers. Perhaps a specific algorithm requires $3n + 5\log n + 16$ time steps to perform this task. However, in the limit of a large problem size the only term which matters is the $3n$ term. Furthermore, we neglect constant factors as being of secondary importance to the analysis of the algorithm. The essential behavior of the algorithm is summed up by saying that the number of operations required scales like n, where n is the number of bits in the numbers being added. The precise application of the asymptotic notation requires the analysis of three tools.

The first one is the so-called *big O notation*. This tool is used to set upper bounds on the behavior of a function. Suppose $f(n)$ and $g(n)$ are two functions on the non-negative integers. The function $f(n)$ is in the class of functions $O(g(n))$, or just $f(n)$ is $O(g(n))$, if there are constants c and n_0 such that for all values of n greater than n_0, $f(n) \leq cg(n)$. That is, for sufficiently large n, the function $g(n)$ is an upper bound on $f(n)$, up to an unimportant constant factor. The big O notation is particularly useful for studying the worst-case behavior of specific algorithms, where we are often satisfied with an upper bound on the resources consumed by an algorithm.

It is also interesting to set lower bounds on the resources required for a certain class of algorithms, e.g., the entire class of algorithms which can be used to multiply two numbers. For this task, the *big Ω notation* is useful. A function $f(n)$ is said to be $\Omega(g(n))$ if there exist constants c and n_0 such that for all n greater than n_0, $cg(n) \leq f(n)$. That is, for sufficiently large n, $g(n)$ is a lower bound on $f(n)$, up to an unimportant constant factor.

The last tool is called *big Θ notation* which is used to indicate that $f(n)$ behaves the same as $g(n)$ asymptotically, up to unimportant constant factors. That is, we say $f(n)$ is $\Theta(g(n))$ if it is both $O(g(n))$ and $\Omega(g(n))$.

Let us now consider some simple examples from [29]:

1. The function $f(n) = 2n$ is in the class $O(n^2)$, since $2n \leq n^2$ for all positive n.

2. The function $f(n) = 2^n$ is $\Omega(n^3)$, since $n^3 \leq 2^n$ for sufficiently large n.

3. The function $f(n) = 7n^2 + \sqrt{n}\log n$ is dominated by the term $7n^2$ for large values of n. As a consequence, for sufficiently large values of n, we have that $7n^2 \leq 7n^2 \leq 8n^2$. Then, the function $7n^2 + \sqrt{n}\log n$ is $\Theta(n^2)$.

As an example of the use of the asymptotic notation in the context of quantifying computational resources, let us consider the problem of sorting an n element list of names into alphabetical order. Many sorting algorithms are based upon the *compare-and-swap* operation: two elements of an n-element list are compared and swapped if they are in the wrong order. Considering that the compare-and-swap operation is the only allowed operation performed by the algorithm, how many of such operations are required in order to ensure that the list was correctly sorted?

In Python, a simple algorithm called *selection sort* uses the compare-and-swap operations to solve the sorting problem:

```
names =
['Einstein', 'Newton', 'Bohr', 'Heisenberg', 'Faraday', 'Curie', 'Feynman']

iterations = 0

for i in range(len(names)):
    for j in range(i+1,len(names)):
        if names[i] > names[j]:
            names[i], names[j] = names[j], names[i]

        iterations += 1

print(names)
print(iterations)
```

In the above example, we considered a list with seven names. However, the selection sort algorithm also works for a list of any size. As output, the algorithm will provide us with the sorted list and the number of iterations and the number of iterations, namely:

```
['Bohr', 'Curie', 'Einstein', 'Faraday', 'Feynman', 'Heisenberg', 'Newton']
21
```

This algorithm applies the compare-and-swap operations $n(n-1)/2$ times, which corresponds to the number of iterations. In the above case, the input size is $n = 7$, which provides $7(7-1)/2 = 21$ iterations, in accordance with what was presented in the above output. Lastly, we can say that the number of iterations used by the algorithm is $\Theta(n^2)$.

It is important to point out that there is at least one more efficient algorithm to handle sorting problems. The *heapsort* algorithm takes $O(n \log n)$ compare-and-swap operations to sort a list. In contrast with the selection sort algorithm, the heapsort splits the input list in a sorted and an unsorted region. Then, it iteratively shrinks the unsorted region by extracting the largest element from it and inserting it into the sorted region. This split in two distinct regions makes the heapsort an improved version of the selection sort algorithm. In fact, any algorithm based upon the compare-and-swap operation requires $\Omega(n \log n)$ of such operations. Thus, the sorting problem requires $\Theta(n \log n)$ compare-and-swap operations, in general.

2.3 Computational complexity

The main question in the study of computational complexity is the following: What time and space resources are required to perform a computation? Problems like addition and multiplication of numbers, or even sort an unsorted list, are considered as efficiently solvable because there are fast algorithms to accomplish these tasks, which means that theses algorithms do not consume too much space when they are running. On the other hand, there are many other problems that have no fast algorithm, at least so far, and are very unlikely to be solved.

In this sense of considering resources as the space and/or time required for the algorithm to run the task, *computational complexity* is the study of time and space resources required to solve computational problems. The task of computational complexity is to prove the existence of lower bounds on the resources required by the best possible algorithm that solves a problem, even if the desired algorithm is not explicitly known. In fact, computational complexity is complementary to the field of algorithm design. Ideally, the most efficient algorithms to accomplish a task would match perfectly with the lower bounds proved by computational complexity.

Consider a problem that takes n bits as input. For example, we might be interested to determinate if a particular n-bit number is prime or not. The main classification that is desirable to be made in computational complexity is between problems that can be solved using resources bounded by a polynomial function $Poly(n)$ or which require resources that grow faster than any polynomial function on n. For this latter case, we usually say that the resources required are exponential in the problem size $Exp(n)$.[2] In this sense, a problem is considered as *easy, tractable or feasible* if there is an algorithm for solving the problem using polynomial resources. On the other hand, a problem is *intractable or infeasible* if the best possible algorithm requires exponential resources.

Let us consider as an example the task of adding two numbers x_1 and x_2. Both

[2]Here we are not being so precise about the term exponential, since there are functions like $n^{\log n}$ which grow faster than any polynomial but they grow slower than any true exponential.

numbers have a binary string representation, i.e., $x_1 \in \{0,1\}^{n_1}$ and $x_2 \in \{0,1\}^{n_2}$ with $n_1 \neq n_2$ in general. The total size of the input is $n = n_1 + n_2$ and these two numbers can be added using a number of elementary operations that scales as $\Theta(n)$. This means that the algorithm which adds two numbers requires a polynomial, in this case linear, number of operations to perform its tasks. On the other hand, it is believed, although not mathematically proven, that the problem of factoring an integer into its prime factors is intractable. That is, the belief is that there is no algorithm which can factor an arbitrary n-bit integer using $O(Poly(n))$ operations.

It is important to notice that the polynomial versus exponential classification of an algorithm is sometimes tricky. For example, an algorithm that solves a problem using $2^{n/1000}$ operations is probably more useful than one which runs in n^{1000} operations. Only for very large input sizes ($n \approx 10^8$) the "efficient" polynomial algorithm will be preferable to the "inefficient" exponential algorithm [29]. In many cases, it may be more practical to choose the "inefficient" algorithm.

Computer scientists are not only interested in the polynomial versus exponential classification of problems. This is merely, for historical reasons, the simplest way of understanding how difficult a computational problem is. However, it is possible to make a better distinction between computational problems. We already know three tools that can be used to classify functions in different categories. This kind of process is quite useful for the study of computational complexity. Different computational problems may have the same asymptotic behavior, which means that the functions $f(n)$ related to these problems belong to the same Θ (or at least O) class of functions. This classification process will provide us with the notion of *complexity classes*. From now on, we will assume that the function $f(n)$ provides a running time of an algorithm based in the size n of the input. In this sense, n could be the size of an n-bit string in the addition problem of two integers or even the size of a list in the sorting problem. Whatever the interpretation of n is, we can consider the following complexity classes:

1. *Constant time* $O(1)$*:* The running time of the algorithm does not depend on the input size. A simple example of a task that runs in a constant time is to select a specific entry of a list or a matrix. The time an algorithm requires to perform this task will not change if the size of the input increases.

2. *Logarithmic time* $O(\log n)$*:* The running time of the algorithm increases slower than the input size. As an example, consider that we need to search for a name in a sorted dictionary. The algorithm does not need to check each word in the dictionary from the beginning until it finds the desired word. Instead, the algorithm can open the dictionary half way through and check if the word on that position is the one required. If it is not, the word is certainly either in the first or in the second half. As a result, half of the possibilities are eliminated in the first iteration. Then the

algorithm will keep repeating this process until it finds the required word. This *binary search* algorithm is far more efficient that searching all the entries in the dictionary.

3. *Linear time $O(n)$:* The running time of the algorithm increases at the same rate as the input size. The example of such computational problem is the unsorted list search. Differently from the sorted list case, the algorithm cannot take advantage of the fact that the list is sorted. Then, in the worst case, every word in the list needs to be checked. It is clear that the desired word can be found after the algorithm checks around 30% of the list, however, if the input size n is increased, this minimum percentage also will increase.

4. *Log-linear time $O(n \log n)$:* This kind of computational problem requires an algorithm that applies operations with total $\log n$ complexity on each input. The standard example of Log-linear time algorithms is the efficient sorting (Merge Sort), which is the computational problem of sort an unsorted list.

5. *Quadratic time $O(n^2)$:* Analogously to the previous case, these are computational problems that require operations with total complexity $O(n)$ on each input. This is the characteristic complexity of any algorithm that perform a double loop, for example, to check all the entries of a matrix.

6. *Polynomial time $O(Poly(n))$:* In this complexity class we accommodate computational problems with higher exponents (n^3, n^4, etc). A simple example of a Polynomial time algorithm is any loop inside loop implementation.

7. *Exponential time $O(Exp(n))$:* This complexity class accommodates problems that are considered hard to handle even for a small input size. If we increase the input size by one, the complexity is doubled or even tripled, based on whatever is the number that is being raised to the power n, so the complexity of the problems gets out of control pretty fast. As a consequence, problems with a fairly small input size might become computationally intractable, which means they are just not possible to do in a reasonable amount of time using modern computers. The standard example of an exponential complex problem is the Traveling Salesman Problem.

It is shown in Figure 2.2 the behavior of different complexity classes. It is important to notice that any fair and well-formulated computational problem can be handled by a modern computer if we are considering a very small input size. Take, for instance, the Traveling Salesman Problem. Surely it is important to solve this problem for a fairly small input size, however, what a company really wants is to solve this problem for thousands of cities. The conclusion here is that the discussion around computational complexity

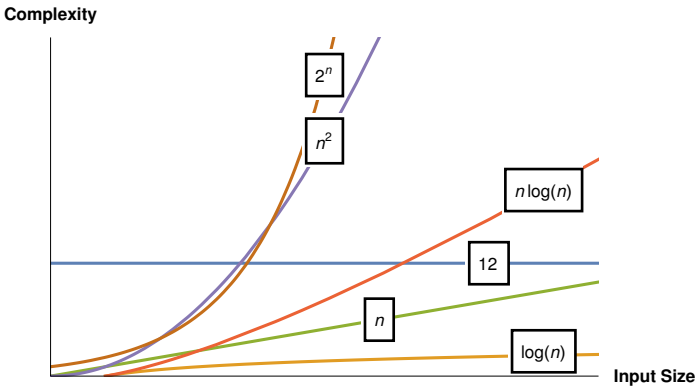

Figure 2.2: The growing of the different classes of computational complexity.

is relevant when the input size is very large. In this sense, the asymptotic notation fits perfectly in this discussion of complexity classes.

2.4 Decision problems: P vs NP

Previously it was pointed out that there are four categories of computational problems: Decision Problems, Search Problems, Counting Problems and Optimization Problems. Each of these categories of computational problems have their own characteristics and relevance. However, Decision Problems constitute the most important class of computational problems. The reason for such importance is that the main ideas of computational complexity are most easily and often formulated in terms of decision problems. There is also a simplest and elegant theory formulated for decision problems, which can be generalized quite naturally for more complex scenarios, and historically computational complexity arose primarily from the study of decision problems [29].

Just a quick review, in a Decision Problem, given an input x with size n, the algorithm provides YES or NO as possible outputs. For example, consider the computational problem of determining if a number is prime or not. We want to know what is the fastest algorithm that provides the answer. In a more quantitative way, it is said that a problem is in $TIME(f(n))$ if there exists an algorithm which solves the problem in a time $O(f(n))$, where n is the input size of x, also called as the length of x. Let us denote by $\mathbf{P}$ the collection of computational problems that can be solved in polynomial time, which means that they belong to $TIME(n^k)$ for some finite k. On the other hand, there are problems that require exponential time to be solved. Despite the fact that exponential times can become huge very quickly, computational problems in this category are still feasible at least until a certain input size. In this sense, let us name the collection of computational problems that can be solved in a finite amount of time by $\mathbf{R}$.

Let us consider three examples of computational problems related to $\mathbf{P}$ and $\mathbf{R}$. The first one is the $n \times n$ Chess, which is a decision problem that is not in $\mathbf{P}$. Given a

$n \times n$ board state, the algorithm will require an exponential amount of time to figure out if black or white will win. The second one is Tetris. Considering an initial arrangement of pieces and the sequence of pieces that are going to come, it is possible by trying all the possibilities to verify if the player can survive or not. The interesting fact about Tetris is that it is not known that it is in **P** or not. The last one is the Halting Problem. Given a computer program in any language (e.g.: Python, Java, etc), will this program sometime halt (or stop)? It could be very helpful to make an algorithm that is capable to say if the computer program will run forever or eventually will provide some output. The problem is that there is not an algorithm capable to perform such task for any computer program. Therefore, the Halting Problem is not in **R**.

Given the examples above, it is important to point that most of decision problems are uncomputable, which means that most of them are not in **R**. In order to prove this statement, let us work on a very clever argument. Consider that we have a certain amount of decision problems that we want to solve. We also know that the algorithms to solve these problems exist. Then, a relevant question here is: for any decision problem, is there an algorithm that solves it? An algorithm, for more complex that it could be, is ultimately a binary string. Any natural number can be represented as a binary string, which means that there is correspondence between an algorithm and a natural number. As a consequence, we can think of the space of all possible algorithms as the space of the natural numbers $\mathbb{N}$. Every algorithm is ultimately reduced to a natural number. On the other hand, a decision problem is a function that maps inputs to YES or NO (1 or 0). An input is also a binary string, in other words, a natural number. Then, a decision problem reduces to a function

$$f : \mathbb{N} \longrightarrow \{0, 1\}. \tag{2.3}$$

However, in the most general sense, a decision problem has an infinity of possible inputs, which results in an infinity amount of outputs that are 0 or 1. In order to encode a decision problem in binary language, it is necessary an infinite binary string. It is known that real numbers are many times encoded as infinite strings in binary language.[3] In this sense, decision problems are similar to real numbers in the same way that algorithms are ultimately natural numbers. Then, we can think in the space of all decision problems as the space of the real numbers $\mathbb{R}$. The conclusion here is that the space of decision problems is much bigger than the space of algorithms, or in other words, there are much more problems than algorithms to solve them. In general, every algorithm only solves one specific decision problem.

The interesting fact is that somehow most of the problems that someone can think of are solvable. However, mathematically speaking, most of the problems that someone could think of should not be solvable. With this idea in mind, there are some decision

[3]For example, the real number $\frac{1}{3}$ can be represented in binary language as 0.01010101..., where "." is called binary point.

problems that can be solved in polynomial time by what we could name as a "lucky algorithm". This kind of problems constitute a class of decision problems, just like **P**, **EXP** and **R**, called **NP**. Here, **NP** refers to nondeterministic polynomial problems. Any algorithm that solves a problems in **NP** does it by guessing. In this context, guessing means that the algorithm will try just one guess and it will achieve the right answer, without checking all the possibilities. One should notice that this method is not a realistic model of computation. While this nondeterministic model of computation is useful, it is not possible to apply it in a real computer, given that this method does not provide the notion of what is theoretically possible to be solved. The Tetris example illustrates very well the true meaning of these guessing that we are talking about. It was already pointed out that it is possible to solve Tetris in an exponential time by checking all the possibilities. However, Tetris is actually in **NP**. We do not need to check all the possibilities in order to answer the question "Do I survive or not?". Instead, the algorithm can make some guesses related to the incoming pieces. Eventually, there will be a sequence of choices that will provide the right answer for the problem. Here lies the central difference between a deterministic and a nondeterministic model of computation. Deterministic algorithms will always provides the answer for our decision problem. On the other hand, nondeterminitic algorithms may or may not work in addition of being highly sensitive to any change in the problem parameters. Looking back again to the Tetris case, if we change the initial arrangement of the pieces or even the sequence of incoming ones, the sequence of guesses that the algorithm makes will need to change.

Another way to think about **NP** is that this is the collection of decision problems whose solutions can be checked in polynomial time. In this sense, check means that if the answer of a decision problems is YES, it is possible to make an algorithm that can prove and check this answer in polynomial time. Likewise, every problem that could be solved in polynomial time can also be checked in polynomial time, which implies that **P** is inside of **NP**. This statement lead us to the following question: Is **P** equal to **NP**? In fact, at the time of writing, this question has no answer. More than that, this question is one of the famous Millennium Prize Problems. So far, what we have is a conjecture that says $\mathbf{P} \neq \mathbf{NP}$. This statement means that there are problems in **NP** that are not in **P**. Problems in **P** can be solved by a real computer without too much computational resources in comparison to problems that requires exponential time. On the other hand, problems in **NP** can be only solved by a theoretical computer, which makes **NP** a powerful model of computation in comparison to **P**. However, while the common sense may lead us too soon to this conclusion, we cannot prove such statement yet. Another way to think about $\mathbf{P} \neq \mathbf{NP}$ is by realizing that proving solutions is more difficult than checking solutions. For example, consider that we have a differential equation with no known solution. It is not difficult to convince ourselves that to develop a proof or even write an algorithm that provides all the solution of this equation is much harder than checking if a given solution

solves the differential equation.

Many puzzle games like Sudoku or Tetris are in somewhere between **P** and **NP** [31]. In order to make this statement more precise, we will refer to this region (or space of computational problems) as $\mathbf{NP}-\mathbf{P}$. Essentially, computational problems in $\mathbf{NP}-\mathbf{P}$ can be close to **P**, but not in **P**, or as far as possible of **P**. In this latter case, these problems are denoted as **NP**-hard. They are at least as hard as every problem in **NP**, including problems beyond $\mathbf{NP}-\mathbf{P}$ as well. In this sense, a computational problem is said to be **NP**-complete if it is in $\mathbf{NP} \cap \mathbf{NP}$-hard. The complete complexity zoo for decision problems is shown in Figure 2.3. The **NP**-complete problems are in the borderline of the **NP** space of problems. The same logic applies to decision problems in **EXP**. A problem is **EXP**-hard if it is as hard as every problem in **EXP**. There are also problems which are **EXP**-complete, for example, solving a chess table.

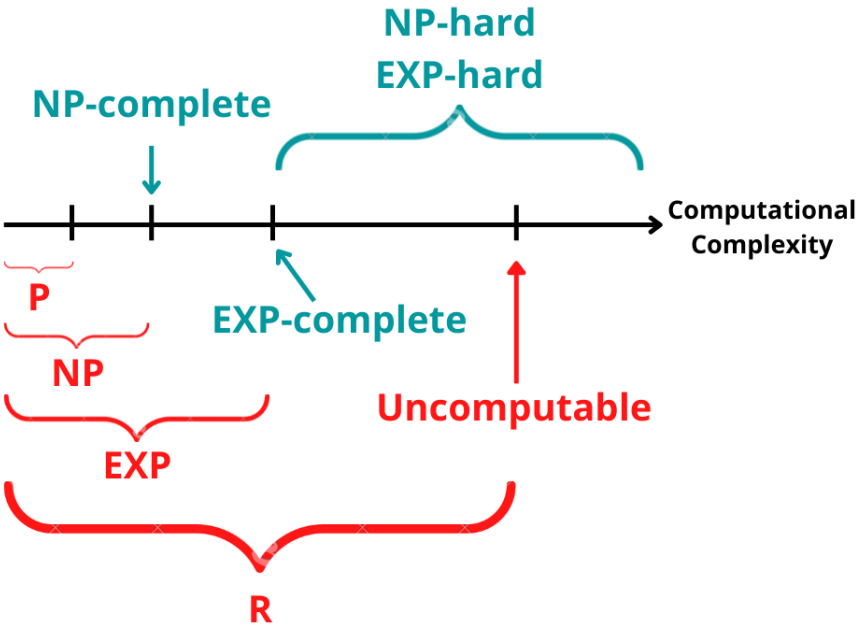

Figure 2.3: Complete scheme of complexity classes for decision problems.

A legitimate question in this discussion of **NP**-hard and **NP**-complete is how do we know that a computational problem is as hard as every problem in **NP**? What does this claim really means? In order to answer this question, let us first talk about *reductions*. This process is a method for designing algorithms. Consider a problem A that has no solution yet and a problem B whose solution is known, i.e., there is an algorithm that solves B. One alternative to answer problem A is try to convert it into problem B. If such process is possible, a reduction was performed and then it becomes possible to solve problem A using the same algorithm that solves problem B. Possibly, this reduction process will not provide the most efficient algorithm for the solution of the problem A, but at least there is a known way to solve it.

This reduction process is crucial in the classification of decision problems. First, the reduction has a preferred direction from simple problems to more complex problems. As a result, suppose that A is known to be **NP**-complete.[4] If it is possible to reduce A to B, it means that B is at least as hard as A. However, all the **NP**-complete problems can be reduced to each other, which provides a method to verify if a **NP**-hard problem is actually **NP**-complete.

With this brief discussion on **P** vs **NP**, we conclude this section on complexity in computer science. The next step will be holographic complexity. In the following section, we are going to understand the role that computational complexity plays in the context of high energy physics and its connection with the study of black holes.

[4] An example of a well known **NP**-complete problem is the 3-Partition problem [32].

Chapter 3

Holographic complexity

The standard physical setup for discussions of holographic complexity has been the eternal two-sided AdS black hole (see Figure 3.1). The bulk geometry is dual to the thermofield double state in the boundary theory [33], namely

$$|TFD\,(t_L, t_R)\rangle = \frac{1}{\sqrt{Z}} \sum_{n=0}^{\infty} e^{-\frac{\beta E_n}{2}} e^{-iE_n(t_L,t_R)} \,|n\rangle_L \,|n\rangle_R \,, \tag{3.1}$$

where L and R refers to the left and right boundaries, $\{|n\rangle\}$ are the energy states of one copy of the boundary theory and Z is the partition function. The TFD state is an entangled state between two copies of the boundary CFT. Its entanglement is responsible for the geometric connection in the bulk, i.e., the Einstein-Rosen bridge [9].

We already mentioned the question on the growth of the black hole interior in terms of boundary quantities. The conjectured holographic complexity seems to provide such an explanation, since a characteristic property of quantum complexity is that it continues to grow for very long times after the system has thermalized. Indeed, complexity is conjectured to continue to grow until a time scale which is exponential in the number of degrees of freedom of the system $\mathcal{C}_{max} \sim e^N$ [34].

There are two conjectures proposed for holographic complexity. The first one is the Complexity=Volume conjecture, which equates the complexity to the volume of the extremal/maximal time slice anchored at boundary times t_L and t_R [11, 12], namely

$$\mathcal{C}_V = \max \left[\frac{V\,(B)}{G_N \ell} \right], \tag{3.2}$$

where ℓ is a certain length scale associated with the geometry. The second one is the Complexity=Action conjecture [17, 18]. This conjecture relates the boundary complexity with the gravitational action evaluated on a region of space-time known as the Wheeler-DeWitt (WDW) patch, i.e., the region bounded by the null surfaces anchored at the

relevant times on the left and right boundaries, namely

$$\mathcal{C}_A = \frac{\mathcal{A}_{WDW}}{\pi}. \tag{3.3}$$

Also notice that the WDW patch is the domain of dependence of the maximal time slice appearing in the CV conjecture (see Figure 3.1). Focusing our attention to the CA

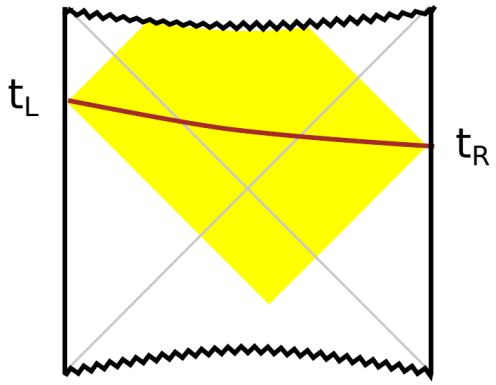

Figure 3.1: The Penrose diagram for a two sided AdS black hole. On the left and right boundaries, we have the two dual QFTs. According to the CV, the volume of the extremal curve (brown) connecting the two boundaries is the complexity of the boundary TFD state. Alternatively, following CA, the action over the WDW patch (yellow) is complexity of the boundary state. [35]

conjecture, it was pointed in [17, 18] that the late time growth rate of the complexity is proportional to $2M/\pi$, independently of the boundary curvature and the space-time dimension. Furthermore, it was suggested that this saturation of the growth rate is related to Lloyd's bound on the rate of computation by a system with energy M [36]. In the general case

$$\frac{d\mathcal{C}_A}{dt} \leq \frac{2E}{\pi}, \tag{3.4}$$

where E is the energy of the black hole. The above result is valid for other types of black holes than the neutral/static one.[1]

The saturation of the complexity growth leads us to the conjecture that black holes are the fastest computers in nature [18]. Such conjecture motivated physicists to verify if there are certain types of black holes whose holographic complexity violates Lloyd's bound. In [18], it was proposed a sequence of arguments that lead us to consider growth bound for the complexity. A similar conjecture was presented before by Lloyd in the context of computer science [36]. Computers are physical systems, so what they can do is limited by the laws of physics. Computers can't process information beyond some limit that is determined by it´s energy and number of degrees of freedom that it

[1]Here, neutral and static means that the black hole has no electric charge and angular momentum.

haves. Moreover, there are certain limits in physics that are described by speed of light c, the quantum scale $\hbar$ and the gravitational constant G that need to be respected by a computer. The same logic applies for complexity. In this sense, it was proposed in [18] that complexity growth should be limited by the energy of the system, namely

$$\frac{d\mathcal{C}_\psi}{dt} \leq \frac{2E_\psi}{\pi\hbar}, \tag{3.5}$$

where E_ψ is the average energy of system described by a state $|\psi\rangle$. The bound conjectured in (3.5) isn't only for quantum systems, it can be extended for black holes. By using the first law of thermodynamics, it's possible to rewrite (3.5) as

$$\frac{d\mathcal{C}}{dt} \leq \int_{gs}^{S} T dS, \tag{3.6}$$

with S being the black hole's entropy and T being its temperature. The gs in the integral refers to the ground state of the black hole. In order to approach more closely the saturation of the complexity growth, we are going to consider the complexity of an anisotropic black hole. The idea here is to study potential effects of the anisotropy on the complexity.

From now on, we will focus in a deeper understanding of the CA proposal. Our goal is to compute the holographic complexity of the Mateos-Trancanelli (MT) Model [37, 38]. The MT model is a solution of type IIB supergravity that was designed to model the effects of anisotropy in the quark-gluon plasma (QGP) created during heavy ion collisions. The anisotropy is present in the initial stages after the collision and it leads to different transverse and longitudinal pressures in the plasma. Additionally, above order $(a/T)^4$, where a is the anisotropy parameter and T is the temperature of the black brane, the boundary theory of the model presents a conformal anomaly.

3.1 Complexity = Action conjecture

The Complexity=Action conjecture was initially proposed in [17, 18], however, these preliminary works were focused in the late time behavior of the complexity in order to incorporate the concept of Lloyd's bound for complexity. Afterwards, the time-dependent complexity for the neutral and charged AdS-Schwarzschild black hole was computed, as well as for the BTZ black hole [23]. Since then, this work became the standard reference in the study of time-dependent complexity. Based on [23], it was computed in [39] the computational complexity for the MT Model up to order $(a/T)^2$. However, the derivation of complexity using CA in [39] was focused in bulk geometries described by metrics like

$$ds^2 = -G_{tt}(r)\, dt^2 + G_{rr}(r)\, dr^2 + G_{ij}(r)\, dx^i dx^j, \tag{3.7}$$

where r is the radial AdS coordinate and (t, x^i) are the boundary coordinates with $i = 1, 2, \ldots, d-1$, while the original one in [23] was performed for "Schwarzschild like" metrics. In the end, there is no extraordinary difference between the approaches, it is just a question of convenience. From now on, we are going to follow the steps of [39].

Consider a neutral black brane with a generic bulk action of the form

$$\mathcal{A} = \frac{1}{16\pi G} \int d^d x dr \sqrt{-g} \mathcal{L}\left(r, x\right). \tag{3.8}$$

In the (r, t, x^i) coordinate system, the boundary is located at $r = \infty$. We also assume the existence of a horizon at $r = r_H$, where G_{tt} has a zero and G_{rr} has a simple pole.

In the computations of holographic complexity, it is necessary to avoid the apparent singularity at $r = r_H$ and also use coordinates that cover the two sides of the geometry. Thus, we are going to use the Eddington-Finkelstein coordinates

$$u = t - r^*\left(r\right), \qquad v = t + r^*\left(r\right), \tag{3.9}$$

where $r^*\left(r\right)$ is the tortoise coordinate, given by

$$r^*\left(r\right) = \int dr \sqrt{\frac{G_{rr}\left(r\right)}{G_{tt}\left(r\right)}}, \tag{3.10}$$

in such way that the metric (3.7) becomes

$$ds^2 = -G_{uv}\left(r\right) du dv + G_{ij}\left(r\right) dx^i dx^j. \tag{3.11}$$

The CA conjecture claims that the complexity of the boundary state is given by the gravitational action evaluated in a region of the bulk known as the Wheeler-DeWitt (WDW) patch, namely

$$\mathcal{C}_A\left(t_L, t_R\right) = \frac{\mathcal{A}_{WDW}\left(t_L, t_R\right)}{\pi}, \tag{3.12}$$

where the WDW patch is the domain of dependence of any spatial slice anchored at a given pair of boundary times (t_L, t_R), as shown in Figure 3.2. Without any loss of generality, we consider the time evolution of holographic complexity for the symmetric configuration $t_L = t_R = t/2$. The action on the WDW patch is divergent because such region extends until the asymptotic boundaries of the space-time, which are located at $r = \infty$. In order to bypass this problem for now, we regularize this divergence by introducing a cutoff surface at $r = r_\infty$ close to the boundaries. Also, we introduce a cutoff surface $r = \varepsilon_0$ close to the past and future singularities. The gravitational action on the WDW patch can be written as

$$\mathcal{A}_{WDW} = \mathcal{A}_{bulk} + \mathcal{A}_{GHY} + \mathcal{A}_{joint}, \tag{3.13}$$

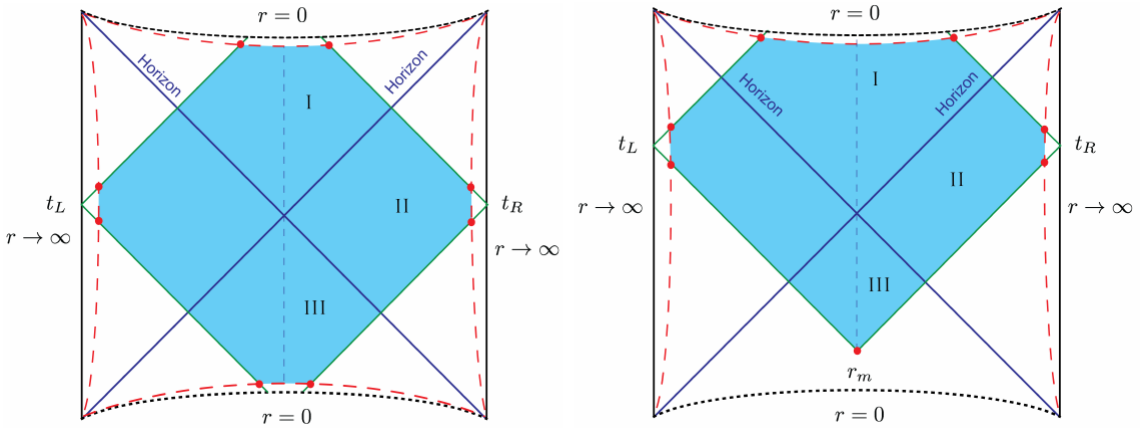

Figure 3.2: The WDW patch (blue region) in two different regimes. On the left, we have that $t < t_c$. In this situation, the WDW patch intersects both the future and past singularities. On the right, we have the regime $t > t_c$, where there is a additional null-null joint terms instead to the WDW patch intersect the past singularity. Figure from [23].

where

$$\mathcal{A}_{bulk} = \frac{1}{16\pi G}\int_{\mathcal{M}} d^{d+1}x\sqrt{-g}\mathcal{L}\,(x) \tag{3.14}$$

is the bulk action evaluated over a manifold $\mathcal{M}$, which in our case is the WDW patch. In order to have a well-defined variational principle, it is is necessary to introduce two additional terms to the $\mathcal{A}_{WDW}$. The first one is the Gibbons-Hawking-York (GHY) boundary term

$$\mathcal{A}_{GHY} = \frac{1}{8\pi G}\int_{\mathcal{B}} d^{d}x\sqrt{|h|}K, \tag{3.15}$$

where h is the determinant of the induced metric on $\mathcal{B}$, namely

$$h_{ij} = g_{\mu\nu}\frac{\partial x^{\mu}}{\partial \sigma^{i}}\frac{\partial x^{\nu}}{\partial \sigma^{j}}, \tag{3.16}$$

with σ^i being the coordinates on $\mathcal{B}$, and K is the trace of the extrinsic curvature

$$K = g^{\mu\nu}K_{\mu\nu}, \qquad K_{\mu\nu} = \nabla_{\mu}n_{\nu}. \tag{3.17}$$

The unit vector n_ν is normal to the surface $\mathcal{B}$. The GHY term is necessary when the boundary includes space-like and time-like segments, which we denoted as $\mathcal{B}$. In principle, there would be also a second boundary term for null-like segments. However, by following [40], this term is defined in terms of the parameter κ, analogous to K, which measure how much the null surface fails to be affinely parametrized. Then, we can set $\kappa = 0$, implying that it is not necessary to consider these null boundary terms. The second term is the joint term, which is necessary when the intersection between two boundary terms is not

smooth. This term can be written as

$$\mathcal{A}_{joint} = \frac{1}{8\pi G}\int_{\Sigma} d^{d-1}x\sqrt{G}\eta, \tag{3.18}$$

where $G = \det(G_{ij})$ and we are considering the intersection of a null-like segment with any another boundary segment, so it includes combinations of the type null/null, null/time-like and null/space-like. The WDW patch shown has no time-like/time-like, time-like/space-like or space-like/space-like intersections. Otherwise, we would have needed to consider additional joint terms for these kind of combinations.

As shown in Figure 3.2, the WDW patch intersects both the future and the past singularity at early times. At later times, which means $t > t_c$, the WDW patch no longer intersects the past singularity. This time scale separating these two regimes is given by

$$t_c = 2\left(r^*_\infty - r^*(0)\right), \qquad r^*_\infty = \lim_{r\to\infty} r^*(r). \tag{3.19}$$

Let us start focusing in the later time regime ($t > t_c$). Once the WDW patch no longer intersects with the past singularity, there are no surface and joint terms related to the past singularity. Instead, there is an additional joint term that comes from the intersection of two null boundaries. In order to compute the bulk contribution, due to the symmetry of the WDW patch, we can split the right side of the WDW patch in three regions, which we denote I, II and III. The total bulk action will be twice this value, once we need to consider the also the left side of the WDW patch. Then, the bulk action contribution from each of the part is

$$\begin{aligned}
\mathcal{A}^{I}_{bulk} &= \frac{V_{d-1}}{8\pi G}\int_{\varepsilon_0}^{r_h} dr\sqrt{-g}\left(\frac{t}{2} + r^*_\infty - r^*(r)\right)\mathcal{L}(r),\\
\mathcal{A}^{II}_{bulk} &= \frac{V_{d-1}}{8\pi G}\int_{r_h}^{r_\infty} dr\sqrt{-g}2\left(r^*_\infty - r^*(r)\right)\mathcal{L}(r),\\
\mathcal{A}^{III}_{bulk} &= \frac{V_{d-1}}{8\pi G}\int_{r_m}^{r_h} dr\sqrt{-g}\left(-\frac{t}{2} + r^*_\infty - r^*(r)\right)\mathcal{L}(r),
\end{aligned} \tag{3.20}$$

where $\mathcal{L}(r)$ is the on-shell Lagrangian. The joint point r_m refers to the intersection between the two null boundaries, which is given by

$$\frac{t}{2} - r^*_\infty + r^*(r_m) = 0. \tag{3.21}$$

The equation for the r_m can be solved numerically. Note that it is possible to recover the equation that gives the critical time t_c when we take the limit $r_m \to 0$ in the above equation. Then, summing all the three contributions in (3.20), we obtain that

$$\mathcal{A}_{bulk} = \mathcal{A}^0_{bulk} + \frac{V_{d-1}}{8\pi G}\int_{\varepsilon_0}^{r_m} dr\sqrt{-g}\left(\frac{t}{2} - r^*_\infty + r^*(r)\right)\mathcal{L}(r), \tag{3.22}$$

where $\mathcal{A}^0_{bulk}$ is the total bulk action in the $t < t_c$ regime, namely

$$\mathcal{A}^0_{bulk} = \frac{V_{d-1}}{2\pi G}\int_{r_h}^{r_\infty} dr\sqrt{-g}\left(r^*_\infty - r^*\left(r\right)\right)\mathcal{L}\left(r\right). \tag{3.23}$$

It was pointed in [23, 39] that the total bulk action has no time dependence in the regime $t < t_c$. Since we are going to study the time derivative of the complexity, in order to investigate violations of the Lloyd's bound (3.4), it is not necessary to pay too much attention to the early times regime.

The next step is to compute the GHY terms. For the later times regime, we have three boundaries, two at $r = r_\infty$ (two sides of the geometry) and the other at $r = \varepsilon_0$ (future singularity). In both cases the, outward-directed normal vector is of the form

$$n_\mu = \left(n_t, n_r, n_i\right) = b\left(0, 1, 0\right), \tag{3.24}$$

where b is some normalization constant in such way that $n^2 = 1$ for space-like vectors and $n^2 = -1$ for time-like vectors. Then, the space-like normal vector at $r = r_\infty$ is given

$$n^{(s)}_\mu = \left(0, \sqrt{G_{rr}\left(r_\infty\right)}, 0\right) \tag{3.25}$$

and the time-like normal vector at $r = \varepsilon_0$ is

$$n^{(t)}_\mu = \left(0, \sqrt{-G_{rr}\left(\varepsilon_0\right)}, 0\right). \tag{3.26}$$

The extrinsic curvature, in terms of a generic normal vector n_μ of the form (3.24) is

$$K = \nabla_\mu n^\mu = \frac{b}{2G_{rr}}\left(\frac{\partial_r G_{tt}}{G_{tt}} + \frac{\partial_r G}{G}\right)\Bigg|_{r=\varepsilon_0, r_\infty}, \tag{3.27}$$

where $b = \sqrt{\pm G_{rr}}$ depending if n_μ is space-like or time-like and $G = \det\left(G_{ij}\right)$. The induced metric on a surface of r constant is

$$ds^2_{ind} = -G_{tt}\left(r\right)dt^2 + G_{ij}\left(r\right)dx^i dx^j, \tag{3.28}$$

in such way that the GHY term becomes

$$\mathcal{A}_{GHY}\left(r\right) = \frac{V_{d-1}}{16\pi G}\chi\left(r\right)\int_{\mathcal{B}} dt, \qquad \chi = \sqrt{\frac{G_{tt}G}{G_{rr}}}\left(\frac{\partial_r G_{tt}}{G_{tt}} + \frac{\partial_r G}{G}\right), \tag{3.29}$$

with the integration over t depending of the boundary that is being considered. Then

$$\begin{aligned}
\mathcal{A}_{GHY}^{future}\left(\varepsilon_0\right) &= \frac{V_{d-1}}{8\pi G}\chi\left(\varepsilon_0\right)\left(\frac{t}{2}+r_\infty^*-r^*\left(\varepsilon_0\right)\right), \\
\mathcal{A}_{GHY}^{past}\left(\varepsilon_0\right) &= \frac{V_{d-1}}{8\pi G}\chi\left(\varepsilon_0\right)\left(-\frac{t}{2}+r_\infty^*-r^*\left(\varepsilon_0\right)\right), \\
\mathcal{A}_{GHY}\left(r_\infty\right) &= \frac{V_{d-1}}{8\pi G}\chi\left(r_\infty\right)\left(r_\infty^*-r^*\left(r_\infty\right)\right),
\end{aligned} \tag{3.30}$$

where we also computed the GHY term for the past singularity. We also obtain the GHY term for the $t < t_c$ regime:

$$\mathcal{A}_{GHY}^{0} = \frac{V_{d-1}}{8\pi G}\chi\left(r_\infty\right)\left(r_\infty^*-r^*\left(r_\infty\right)\right)+\frac{V_{d-1}}{4\pi G}\chi\left(\varepsilon_0\right)\left(r_\infty^*-r^*\left(\varepsilon_0\right)\right). \tag{3.31}$$

Finally, the total GHY term is the contribution of the future singularity plus the ones from the boundary at $r = r_\infty$, namely

$$\mathcal{A}_{GHY} = \frac{V_{d-1}}{8\pi G}\chi\left(\varepsilon_0\right)\left(\frac{t}{2}+r_\infty^*-r^*\left(\varepsilon_0\right)\right)+\mathcal{A}_{GHY}^{0}. \tag{3.32}$$

The last step is to compute the contribution from the joint terms. In the regime $t > t_c$, there are the null-null joint point at r_m, the null/space-like joint point- at $r = r_\infty$ and the null/time-like joint point at $r = \varepsilon_0$. For the null-null joint point, we have that

$$\mathcal{A}_{joint} = \frac{1}{8\pi G}\int_\Sigma d^{d-1}x\sqrt{G}\eta, \tag{3.33}$$

where η is defined in terms of the left and right null vectors which parametrize the null boundaries of the WDW patch, namely

$$\eta = \log\left|\frac{1}{2}k^L\cdot k^R\right|. \tag{3.34}$$

The vectors k^L and k^R are given by

$$k_\mu^L = -\alpha\partial_\mu\left(t-r^*\right), \qquad k_\mu^R = \alpha\partial_\mu\left(t+r^*\right), \tag{3.35}$$

in such way that

$$\eta = -\log\left|\frac{G_{tt}\left(r\right)}{\alpha^2}\right|. \tag{3.36}$$

Then, the null-null joint term is

$$\mathcal{A}_{joint}^{null} = -\frac{V_{d-1}}{8\pi G}\sqrt{G\left(r_m\right)}\log\left|\frac{G_{tt}\left(r_m\right)}{\alpha^2}\right|, \tag{3.37}$$

where r_m is given by (3.21). We still have to compute the joint contributions at $r = \varepsilon_0$ and $r = r_\infty$, however, it was pointed in [23] that for a large class of isotropic systems, the contribution from the asymptotic boundaries do not depend on time, while the contributions at $r = \varepsilon_0$ vanish. Then, we obtain that

$$\mathcal{A}^0_{joint} = \mathcal{A}^{bdry}_{joint} = \frac{V_{d-1}}{8\pi G} G\left(r_\infty\right) \log\left|G_{tt}\left(r_\infty\right)\right| \tag{3.38}$$

for the regime $t < t_c$, while for $t > t_c$ we have that

$$\mathcal{A}_{joint} = \mathcal{A}^{bdry}_{joint} - \frac{V_{d-1}}{8\pi G} \sqrt{G\left(r_m\right)} \log\left|\frac{G_{tt}\left(r_m\right)}{\alpha^2}\right|. \tag{3.39}$$

Summarizing the results, in the regime $t > t_c$, the action pieces computed over the WDW patch are

$$\begin{aligned}
\mathcal{A}_{bulk} &= \mathcal{A}^0_{bulk} + \frac{V_{d-1}}{8\pi G} \int_{\varepsilon_0}^{r_m} dr \sqrt{-g} \left(\frac{\delta t}{2} + r^*\left(r\right) - r^*\left(0\right)\right) \mathcal{L}\left(r\right) \\
\mathcal{A}_{GHY} &= \frac{V_{d-1}}{8\pi G} \chi\left(\varepsilon_0\right) \frac{\delta t}{2} + \mathcal{A}^0_{GHY} \\
\mathcal{A}_{joint} &= \mathcal{A}^0_{joint} - \frac{V_{d-1}}{8\pi G} \sqrt{G\left(r_m\right)} \log\left|\frac{G_{tt}\left(r_m\right)}{\alpha^2}\right|,
\end{aligned} \tag{3.40}$$

where we introduced the parameter $\delta t = t - t_c$, in such way that

$$\frac{\delta t}{2} + r^*\left(r_m\right) - r^*\left(0\right) = 0. \tag{3.41}$$

Then, the time derivative of each action term above is

$$\begin{aligned}
\frac{d\mathcal{A}_{bulk}}{dt} &= \frac{V_{d-1}}{16\pi G} \int_{\varepsilon_0}^{r_m} dr \sqrt{-g} \mathcal{L}\left(r\right) \\
\frac{d\mathcal{A}_{GHY}}{dt} &= \frac{V_{d-1}}{16\pi G} \chi\left(\varepsilon_0\right) \\
\frac{d\mathcal{A}_{joint}}{dt} &= \frac{V_{d-1}}{16\pi G} \left[\frac{1}{2}\sqrt{\frac{G_{tt}}{G G_{rr}}} G' \log\left|\frac{G_{tt}}{\alpha^2}\right| + \sqrt{\frac{G}{G_{rr} G_{tt}}} G'_{tt}\right]\Bigg|_{r=r_m},
\end{aligned} \tag{3.42}$$

in other words

$$\frac{d\mathcal{A}_{WDW}}{dt} = \frac{V_{d-1}}{16\pi G} \left[\int_{\varepsilon_0}^{r_m} dr \sqrt{-g} \mathcal{L}\left(r\right) + \chi\left(\varepsilon_0\right) + \left(\frac{1}{2}\sqrt{\frac{G_{tt}}{G G_{rr}}} G' \log\left|\frac{G_{tt}}{\alpha^2}\right| + \sqrt{\frac{G}{G_{rr} G_{tt}}} G'_{tt}\right)\Bigg|_{r=r_m}\right]. \tag{3.43}$$

This is the time derivative of the action on the WDW patch.

3.2 MT model

The Mateos-Trancanelli (MT) Model is a solution of type IIB supergravity which is dual to a spatially anisotropic finite-temperature $\mathcal{N} = 4$ Super Yang-Mills (SYM) plasma [37, 38]. The effective action for the model in five dimensions is given by

$$\mathcal{A} = \frac{1}{16\pi G_N}\int_{\mathcal{M}} d^5x\sqrt{-g}\left[R + \frac{12}{L^2} - \frac{1}{2}\left(\partial\phi\right)^2 - \frac{1}{2}e^{2\phi}\left(\partial\chi\right)^2\right] + S_{GHY}, \tag{3.44}$$

where ϕ, χ and $g_{\mu\nu}$ are the dilaton field, the axion field and the metric, respectively. The S_{GHY} is the already known boundary term on $\partial\mathcal{M}$ and G_N is the Newton's constant in five dimensions. From the action (3.44), we obtain the five Einstein equations and the dilation equation. Then, we can consider the following Ansatz for the metric, namely

$$ds^2 = e^{-\phi(r)/2}\left[-r^2F\left(r\right)B\left(r\right)dt^2 + \frac{dr^2}{r^2F\left(r\right)} + r^2\left(dx^2 + dy^2 + H\left(r\right)dz^2\right)\right], \tag{3.45}$$

where r is the AdS bulk coordinate and (t, x, y, z) are boundary gauge theory coordinates. The above solution has a horizon at $r = r_h$, where $F\left(r_h\right) = 0$, and the boundary is located at $r = \infty$, with $F = B = H = 1$ and $\phi = 0$. We set the AdS radius $L = 1$ for simplicity. The axion field is proportional to the coordinate z, i.e.,

$$\chi = az, \tag{3.46}$$

which introduce the anisotropy in the system by the parameter a. When $a = 0$, the solution (3.45) reduces to the gravity dual of $\mathcal{N} = 4$ SYM theory with gauge group $SU\left(N\right)$. Lastly, the H function is written in terms of the dilaton field, namely

$$H\left(r\right) = e^{-\phi(r)}. \tag{3.47}$$

This way, the six equations of motion can be written in terms of the functions $B\left(r\right)$ and $F\left(r\right)$, as well as the dilaton field $\phi\left(r\right)$. However, this system can be reduced to three differential coupled equations,[2] which can be solved analytically for small values of the anisotropy parameter ($a \ll T$). The strategy is to expand B, F and ϕ as a power series of a, that is

$$\begin{aligned} F\left(r\right) &= 1 - \frac{r_h^4}{r^4} + a^2F_2\left(r\right) + a^4F_4\left(r\right) + O\left(a^6\right), \\ B\left(r\right) &= 1 + a^2B_2\left(r\right) + a^4B_4\left(r\right) + O\left(a^6\right), \\ \phi\left(r\right) &= a^2\phi_2\left(r\right) + a^4\phi_4\left(r\right) + O\left(a^6\right), \end{aligned} \tag{3.48}$$

[2] Such procedure is detailed in [38].

where only even powers of a can appear due the symmetry $z \to -z$. Then, the equations of motion can be solved order by order until the desired power of a.

3.2.1 Solution order a^2

In [39] it was considered the analytic solutions until order a^2, which are given by

$$\begin{aligned} F(r) &= 1 - \frac{r_h^4}{r^4} + \frac{a^2}{24 r^4 r_h^2}\left[8 r^2 r_h^2 - 2 r_h^4 (4 + 5\log 2) + \left(3 r^4 + 7 r_h^4\right)\log\left(1 + \frac{r_h^2}{r^2}\right)\right], \\ B(r) &= 1 - \frac{a^2}{24 r_h^2}\left[\frac{10 r_h^2}{r^2 + r_h^2} + \log\left(1 + \frac{r_h^2}{r^2}\right)\right], \\ \phi(r) &= -\frac{a^2}{4 r_h^2}\log\left(1 + \frac{r_h^2}{r^2}\right). \end{aligned} \tag{3.49}$$

Once we have the solution for F, B and the dilaton ϕ, we are in position to compute some useful quantities. For example, from the Euclidean continuation of the metric, it is possible to compute the Hawking temperature

$$T_H = \frac{r_h^2 \sqrt{B(r_h)} F'(r_h)}{4\pi} = \frac{r_h}{\pi} + \frac{a^2}{48\pi r_h}(5\log 2 - 2), \tag{3.50}$$

as well as the Bekenstein-Hawking entropy

$$S = \frac{A_h}{4 G_N} = \frac{V_3 r_h^3}{4 G_N}\left(1 + \frac{5 a^2}{16 r_h^2}\log 2\right). \tag{3.51}$$

Then, we are able to compute the black brane's mass by the first law of thermodynamics, which provides

$$M(a) = \int T dS = \frac{V_3}{16\pi G_N}\left[3 r_h^4 + \frac{a^2 r_h^2}{4}(5\log 2 - 1)\right]. \tag{3.52}$$

The computation of the black brane's mass is crucial to compute the Lloyd's bound (3.4). Now we have all the ingredients to compute the holographic complexity for the MT model.

3.2.2 Late time behaviour

Let us first approach the solution computation of the complexity for the late time limit, where $r_m \to r_h$. Such situation is interesting due the fact that we expect the saturation of the Lloyd's bound in this limit. Thus, the time derivative of the WDW

patch in (3.43) becomes

$$\frac{d\mathcal{A}_{WDW}}{dt}=\frac{V_{d-1}}{16\pi G}\left[\int_{o}^{r_h}dr\sqrt{-g}\mathcal{L}\left(r\right)+\sqrt{\frac{G_{tt}G}{G_{rr}}}\left(\frac{\partial_r G_{tt}}{G_{tt}}+\frac{\partial_r G}{G}\right)\Big|_{r=\varepsilon_0}+\left(\sqrt{\frac{G}{G_{rr}G_{tt}}}G'_{tt}\right)\Big|_{r=r_h}\right], \tag{3.53}$$

where

$$\begin{aligned} G_{tt}\left(r\right)&=e^{-\phi(r)/2}r^2F\left(r\right)B\left(r\right),\\ G_{rr}\left(r\right)&=\frac{e^{-\phi(r)/2}}{r^2F\left(r\right)},\\ G\left(r\right)&=e^{-5\phi(r)/2}r^6. \end{aligned} \tag{3.54}$$

The final expression for the time derivative of the $\mathcal{A}_{WDW}$ is then

$$\frac{d\mathcal{A}_{WDW}}{dt}=\frac{V_3}{16\pi G_N}\left[3r_h^4+\frac{a^2r_h^2}{4}\left(5\log 2-1\right)\right]=2M\left(a\right),$$

which matches the mass of the black brane (3.52). Finally, the time derivative of the complexity saturates the Lloyd's bound, as was conjectured in [17, 18], i.e.

$$\frac{d\mathcal{C}_A}{dt}=\frac{2M}{\pi}. \tag{3.55}$$

Just a last comment, if we want to study the full time behavior of the holographic complexity, it is necessary to solve the equation (3.41) in order to obtain r_m as a function of δt. Then, we would be in position to place it in (3.43). Once the time derivative of the complexity is zero for $t<t_c$, the parameter δt is useful to describe the time behavior of $d\mathcal{C}_A/dt$ in the regime $t>t_c$. Such procedure was also done in [39] numerically. The result was that the time derivative of $\mathcal{C}_A$ violates the Lloyd's bound at initial times, approaching this bound from above at late times.

Chapter 4

Complexity in quantum many-body systems

The study of complexity in quantum computing is not something new. The pioneering studies by Nielsen and collaborators [19, 20, 21] provided an interesting formalism to quantify complexity for quantum systems. However, recent works in holography drew attention to the use of complexity in different areas of research. Since then, other proposals to compute computational complexity have been tried, as well as adaptations of Nielsen's *geometric* notion of complexity.

Let us try to set a timeline for the developments of computational complexity since holographic complexity was conjectured. Here we are going to focus on the study of complexity in quantum systems, either continuous (QFT) or discrete ones (spin chains). The initial question that was made after the rising of holographic complexity is if is it possible to obtain a method to compute complexity in QFT. The first proposal for complexity in QFT appeared in [22] where the author used Nielsen's formalism with the proper modifications required for continuous systems. Specifically, complexity was thought of as a line integral using the Fubini-Study metric [41]. After the works using the Fubini-Study metric, Nielsen's formalism become popular and it was used in [23], where the authors have further introduced a more general notion of metric than the previous one.

Before we continue, it is important to recall the two different notions of complexity already mentioned in the Introduction: complexity of states and complexity of operators. The first one measures the complexity between two quantum states of interest. The second one focuses on the complexity of a unitary operator that acts on a certain Hilbert space. Most commonly, this operator is taken as the time evolution operator $U(t)$. Each notion of complexity has its own pros and cons. The use of the complexity of states is recommended in a situation where we are interested in some property of the relevant states in a problem. For instance, by studying the complexity of distinct ground states as a function of their coupling constants it is possible to diagnose quantum phase transitions,

including topological nature, as one crosses a quantum critical point [42, 43, 44]. On the other hand, the complexity of operators is more advantageous in physical setups where the main information is in the Hamiltonian, as in the example of spin chains in condensed matter models.

4.1 Complexity of states

The so-called complexity of states measures the optimal coast to prepare a final state, let us denote it by target state $|\psi_T\rangle$, from an initial state, named reference state $|\psi_R\rangle$. This task can be accomplished by the action of a unitary operator U on the target state $|\psi_T\rangle$. At this point, it is interesting to make a parallel with the notion of complexity that it is already known from classical/quantum computing. If we consider a string of n qubits, the reference state can be chosen as

$$|\psi_R\rangle = \prod_{i=1}^{N} \otimes |0\rangle_i \,, \tag{4.1}$$

where $|0\rangle_i$ corresponds to the the spin down configuration for the i-th position (or lattice) of the string. Then, if we want to reach a certain configuration of this spin chain, which means to build a correspondent target state, in complexity language, we need to apply a set of elementary gates on $|\psi_R\rangle$. The sequence that these gates are applied constitute a quantum circuit, as is shown in Figure 4.1. At each time step s, there were applied a

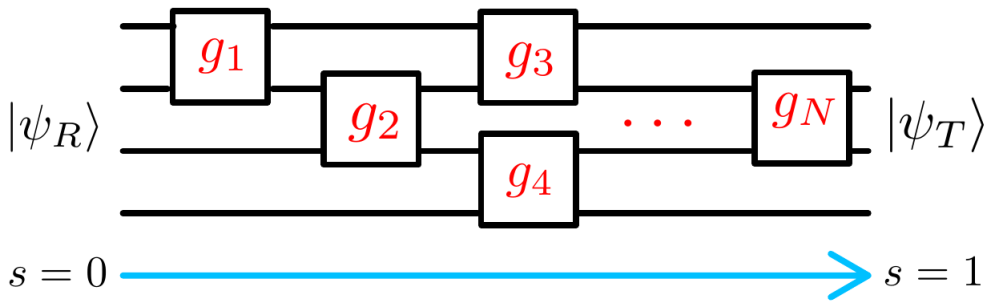

Figure 4.1: A general quantum circuit where $|\psi_T\rangle$ is obtained from $|\psi_R\rangle$ by applying a sequence of elementary gates g_i. We also can indicate the intermediate state $|\psi_n\rangle$ that is produced after every step, namely $|\psi_n\rangle = g_n g_{n-1} \cdots g_2 g_1$.

certain number of gates on some qubits. Here, it is important to make some assumptions. First, if we want to quantify complexity in a realistic way, it is reasonable that it does not exist a "super" quantum gate that implements the circuit in just one time step. Second, it is also reasonable to assume that one gate acts only on a few qubits, otherwise, most part of the circuit could be implemented fast and easily. In the standard quantum computing literature [45, 29], it is common to consider gates that act at most on three qubits. Lastly,

we assume that the quantum circuit runs in parallel, which means that more than one gate is allowed to act at each time step.

We are going to consider two cases for the complexity of states, both in the context of QFTs: the Fubini-Study method [22] for a complex scalar field theory and Nielsen's method [19, 20, 21] for fermions in 1+1. Both methods present some similarities. In fact, any method to compute complexity needs to follow essentially the same recipe. However, Nielsen's method presents a greater degree of generality, as we are going to see.

4.1.1 General properties for complexity of states

In order to present the basic elements that constitute the idea of computational complexity, let us keep in mind that we are trying to achieve a target state from a reference state by building a quantum circuit. In this sense, the concept of *circuit depth* is quite relevant. The quantum circuit takes a certain number of time steps to reach the target state from the reference state. So, this number of time steps is called depth of the circuit (see Figure 4.1). The concept of depth is important because the complexity of the target state is defined as the depth of the optimal quantum circuit required to build the target state from the reference state. This choice for complexity is quite intuitive: the bigger the circuit is, the more complex the task is. However, such choice only works if we consider circuits running in parallel. For circuits in series, which means only one gate acting at each time step, a better choice for complexity is the number of gates needed to implement the circuit.

There is nothing special about this reference state. Actually, any quantum state of the system can be chosen as the reference state, however, it is interesting to select a convenient one. In this context, convenient means "simple and unentangled". What one thinks to be a simple state is relative, nevertheless, simplicity in this context refers to a state that easily allows us to build other states by applying unitary operators on it. For example, in a spin chain, a good candidate for the simplest state was shown in 4.1. Sometimes the ground state of H can be picked as the simplest state. In general, the choice of target state will depend on additional information that will come from the system. Furthermore, the complexity associated to some state or process is not an absolute quantity, it will depend on the reference state. Then, it is useful and smart to consider the reference state as having zero complexity, agreeing with the choice of this state as reference.

The assumption about the absence of entanglement exist because of two reasons. First, to produce entanglement can be considered a task by itself, which means that there is a complexity associated to entanglement production. Second, the calculation of complexity associated to the ground state of the system is relevant in holography. For example, we denote by complexity of formation the additional complexity needed

to prepare the entangled thermofield double state for two copies of the boundary CFT compared to the complexity required to prepare the individual vacuum states of the two copies [46].

Back to the discussion of complexity in QFT, once the reference and target states are known, we reach the target state by the action of a set of unitary operators on the reference state. The complexity of such process (or state) corresponds to the minimum number of operations required to implement this task. In order to make this claim more precise, we need to determinate the set of elementary unitary operators. Let us denote this operator space by $\mathcal{G}$, whose elements will make the quantum circuit required to build the target state. Consider that the target and reference states are related by

$$|\psi_T\rangle = U(1)\,|\psi_R\rangle\,, \qquad U(0) = I, \tag{4.2}$$

where I is the identity operator. We introduced a parameter $s \in [0,1]$ such that $U(1)$ is the desired operator which provides the target state $|\psi_R\rangle$. Then, we now have the boundary conditions for the operator $U(s)$. However, this operator is expected to be the result of series of successive operations on $|\psi_T\rangle$, parameterized by s. Then, it is natural to think about a intermediate state

$$|\psi(s)\rangle = U(s)\,|\psi_R\rangle\,, \qquad U(s) = \overleftarrow{\mathcal{P}} \exp\left[-i\int_0^s G(s')\,ds'\right], \tag{4.3}$$

where $\overleftarrow{\mathcal{P}}$ denotes a path ordering such that the operators at smaller s are applied to the state first, as is shown in Figure 4.1.

With the expression for $U(s)$ in mind, it is natural to think that there are different ways to build $U(s)$, however, in order to compute the complexity of $|\psi_R\rangle$, we need to figure out the optimal operator U_{opt} that respects the boundary conditions (4.2). In Nielsen's work [19, 20, 21], the idea was to define a cost function $\mathcal{F}\left(U(s), \dot{U}(s)\right)$ which accomplishes all possible paths between $|\psi_T\rangle$ and $|\psi_R\rangle$. Then, the depth of the circuit acquires a more precise form

$$\mathcal{D}(U) = \int_0^1 \mathcal{F}\left(U(s), \dot{U}(s)\right) ds. \tag{4.4}$$

Now, the problem of finding the optimal circuit reduces to the problem of minimizing the functional (4.4). Once U_{opt} is known, the complexity of $|\psi_T\rangle$ is

$$\mathcal{C}\left(|\psi_T\rangle, |\psi_R\rangle\right) = \mathcal{D}(U_{opt}) = \min_{U(s)} \int_0^1 \mathcal{F}\left(U(s), \dot{U}(s)\right) ds. \tag{4.5}$$

In general, the cost function $\mathcal{F}$ is some local functional of the position $U(s)$ in the operator space $\mathcal{G}$ and a vector $\dot{U}(s)$ in the tangent space at this point. Then, a reasonable

cost function must satisfy a number of desirable features:

1. Continuity: $\mathcal{F}\left(U(s), \dot{U}(s)\right)$ should be continuous, i. e., $\mathcal{F} \in C^{\infty}$.
2. Positivity: $\forall U \in \mathcal{G}, \mathcal{F}\left(U(s), \dot{U}(s)\right) \geq 0$, where $\mathcal{F}\left(U(s), \dot{U}(s)\right) = 0$ only if U is the identity.
3. Positive Homogeneity: $\mathcal{F}\left(U(s), \lambda \dot{U}(s)\right) = \lambda \mathcal{F}\left(U(s), \lambda \dot{U}(s)\right), \forall \lambda \in \mathbb{R}$.
4. Triangle inequality: $\mathcal{F}\left(U, \dot{U} + \dot{U}'\right) \leq \mathcal{F}\left(U, \dot{U}\right) + \mathcal{F}\left(U, \dot{U}'\right)$ for all tangent vectors $\dot{U}$ and $\dot{U}'$.

The cost function in (4.4) that respects the properties above defines a length for a class of geometries known as Finsler manifolds. Now, more technically speaking, Nielsen proposes that the problem of finding an optimal circuit is equivalent to find the minimal path, i.e., the geodesic, on $\mathcal{G}$. Then, the complexity is identified as the length of this geodesic.

So far we just presented the formal recipe to compute complexity. Now, it is time to consider the necessary ingredients, that is, the operator space $\mathcal{G}$, the cost function $\mathcal{F}$ and the states chosen in the process (reference and target). The complexity is intimately connected to the choice of these ingredients. In the next sections, we are going to provide such ingredients and to consider two physical examples: the complexity of the TFD state for a charged scalar field theory and the complexity for $1+1$ fermionic QFT on a lattice.

4.2 Complexity: Fubini-Study metric

It was proposed in [22] to choose the Fubini-Study metric (or quantum information metric) [47] as the metric of the operator space $\mathcal{G}$. As a consequence, the cost function will be the line element in this space. The Fubini-Study metric is given by

$$ds_{FS} = \sqrt{\left|\partial_s |\psi(s)\rangle\right|^2 - \left|\langle\psi(s)| \partial_s |\psi(s)\rangle\right|^2}, \tag{4.6}$$

where $|\psi(s)\rangle$ is given by (4.3) and ∂_s is the derivative on the curve parameter s. The Fubini-Study metric represents a quantity that measures the distance between states in a parameterized Hilbert space $\mathcal{H}(s)$. This fact provides a reasonable motivation to consider (4.6) as the cost function for the complexity.[1] The expression in (4.6) is similar to the Riemannian metric, however, it is possible to consider a general version of (4.6), namely

$$ds_{FS}^{(p)} = \left|\left|\partial_s |\psi(s)\rangle\right|^p - \left|\langle\psi(s)| \partial_s |\psi(s)\rangle\right|^p\right|^{1/p}, \tag{4.7}$$

[1] For a complete review about the Fubini-Study metric, see [41, 45].

where $p \geq 1$. The case $p = 2$ leads to the standard Fubini-Study metric. Other values of p will provide a different measure for the operator space, which implies in a different complexity, even though the set of allowed gates keeps the same.

The next step would be to specify what is $|\psi(s)\rangle$, however, in order to accomplish that, we first need to obtain more details about the physical setup that we are handling. For the complexity using FS metric, we are going to consider the complexity of the TFD state for a complex scalar field theory [48]. This physical setup is interesting due to the presence of the additional $U(1)$ symmetry group, which implies a conserved electric charge. Such fact is interesting because there is the possibility to compare, at least at a qualitative level, the computation from the QFT side with the holographic side for charged AdS black holes.

4.2.1 TFD state for scalar field theory

Consider a complex scalar field theory in d dimensions whose Hamiltonian is given by

$$H = \int d^{d-1}x \left[\pi^\dagger \pi + \nabla\phi^\dagger \cdot \nabla\phi + m^2 \phi^\dagger \phi\right], \tag{4.8}$$

where m is the mass of the field $\phi(x)$ and $\pi(x) = \partial_0 \phi^\dagger$ is the conjugate momentum. In terms of the annihilation operators (a_k, b_k) and creation operators $\left(a_k^\dagger, b_k^\dagger\right)$ of the particle and anti-particle, respectively, the field $\phi(x)$ and its conjugate momentum have the following form:

$$\begin{aligned}
\phi(x) &= \int \frac{d^{d-1}k}{\sqrt{2\omega_k}} \left[a_k e^{-ikx} + b_k^\dagger e^{ikx}\right], \\
\pi(x) &= i \int d^{d-1}k \sqrt{\frac{\omega_k}{2}} \left[a_k^\dagger e^{ikx} - b_k e^{-ikx}\right],
\end{aligned} \tag{4.9}$$

where $\omega_k = \sqrt{k^2 + m^2}$. Another relevant quantity for our analysis is the $U(1)$ conserved charge

$$Q = iq \int d^{d-1}x \left[\phi^\dagger \partial_0 \phi - \phi \partial_0 \phi^\dagger\right], \tag{4.10}$$

where q is the electric charge of the field $\phi(x)$. From the canonical commutation relations

$$\left[\phi(t,\vec{x}), \pi(t,\vec{x}')\right] = \left[\phi^\dagger(t,\vec{x}), \pi^\dagger(t,\vec{x}')\right] = i\delta^{d-1}(\vec{x} - \vec{x}'), \tag{4.11}$$

we have that

$$\begin{aligned}
\left[a_{\vec{k}}, a_{\vec{k}'}^\dagger\right] &= \delta^{d-1}\left(\vec{k} - \vec{k}'\right), \\
\left[b_{\vec{k}}, b_{\vec{k}'}^\dagger\right] &= \delta^{d-1}\left(\vec{k} - \vec{k}'\right),
\end{aligned} \tag{4.12}$$

where all the other commutators involving a, $a^\dagger$, b and $b^\dagger$ are equal zero. We can use (4.9) to write H and Q in terms of the annihilation and creation operators, namely

$$\begin{aligned} H &= \int d^{d-1}k\omega_k \left[a_k^\dagger a_k + b_k^\dagger b_k + 1\right], \\ Q &= q\int d^{d-1}k \left[a_k^\dagger a_k - b_k^\dagger b_k\right]. \end{aligned} \tag{4.13}$$

The vacuum state $|0\rangle$ is such that

$$a_k|0\rangle = b_k|0\rangle = 0, \tag{4.14}$$

while excited states can be obtained by the application of $a_k^\dagger$ and $b_k^\dagger$ on $|0\rangle$, more precisely

$$|n_k, m_{k'}\rangle = \frac{\left(a_k^\dagger\right)^{n_k}}{\sqrt{n!}}\frac{\left(b_k^\dagger\right)^{n_k}}{\sqrt{m!}}|0\rangle\,. \tag{4.15}$$

The state $|n_k, m_{k'}\rangle$ has n particles with momentum $\vec{k}$ and m anti-particles with momentum $\vec{k}'$, while its energy and electric charge are $E = n_k\omega_k + m_{k'}\omega_{k'}$ and $Q = (n_k - m_{k'})\,q$, respectively.

After reviewing the basics of QFT related to this system, let us use the quantities obtained above to work on the computation of the complexity. Since we are interested in the TFD state for this theory, we need to consider two Hilbert spaces that initially are not entangled to each other. We can do that by considering two copies of the theory. Then, the Hilbert space becomes $\mathcal{H} = \mathcal{H}_L \otimes \mathcal{H}_R$, where $\mathcal{H}_L$and $\mathcal{H}_R$ denotes the left and right QFT, respectively. The basis for such spaces can be generated by the eigenstates of the total number operators $\mathcal{N}_k^L = a_k^{L\dagger}a_k^L + b_k^{L\dagger}b_k^L$ and $\mathcal{N}_k^R = a_k^{R\dagger}a_k^R + b_k^{R\dagger}b_k^R$. The vacuum of the system remains quite the same, however, we need to remember that $|0\rangle = |0_L\rangle \otimes |0_R\rangle$. Nevertheless, the decomposition of the Hilbert space is not unique. We can choose a different set of annihilation and creation operators A_k, $A_k^\dagger$, B_k and $B_k^\dagger$, in such way that $\mathcal{H} = \mathcal{H}_1 \otimes \mathcal{H}_2$. We also get a different "vacuum state" $|\Omega\rangle = |\Omega_1\rangle \otimes |\Omega_2\rangle$ which is annihilated by A_k^1, A_k^2, B_k^1 and B_k^2. The vacuum $|\Omega\rangle$ cannot be understood as the zero energy state, but rather as the state with no particles created by $A_k^\dagger$ and $B_k^\dagger$.

The set of operators a_k, $a_k^\dagger$, b_k, $b_k^\dagger$ and A_k, $A_k^\dagger$, B_k, $B_k^\dagger$ are connected by the so-called *Bogoliubov transformations*, namely

$$\begin{aligned} A_k^1 &= \cosh\theta_k a_k^L - \sinh\theta_k b_k^{R\dagger}, \\ A_k^2 &= \cosh\theta_k a_k^R - \sinh\theta_k b_k^{L\dagger}, \\ B_k^1 &= \cosh\theta_k b_k^L - \sinh\theta_k a_k^{R\dagger}, \\ B_k^2 &= \cosh\theta_k b_k^R - \sinh\theta_k a_k^{L\dagger}, \end{aligned} \tag{4.16}$$

which are transformations that preserve the algebra of the creation and annihilation operators. We can also write the particle and anti-particle number operator, namely, $N_k^1 = A_k^{1\dagger} A_k^1$ and $\overline{N}_k^1 = B_k^{1\dagger} B_k^1$, as

$$\begin{aligned} N_k^1 &= \cosh^2\theta_k a_k^{L\dagger} a_k^L - \cosh\theta_k \sinh\theta_k \left(a_k^{L\dagger} b_k^{R\dagger} + a_k^L b_k^R\right) + \sinh^2\theta_k b_k^R b_k^{R\dagger}, \\ \overline{N}_k^1 &= \cosh^2\theta_k b_k^{L\dagger} b_k^L - \sinh\theta_k \cosh\theta_k \left(a_k^{R\dagger} b_k^{L\dagger} + a_k^R b_k^L\right) + \sinh^2\theta_k a_k^R a_k^{R\dagger}. \end{aligned} \tag{4.17}$$

In a similar way

$$\begin{aligned} N_k^2 &= \cosh^2\theta_k a_k^{R\dagger} a_k^R - \cosh\theta_k \sinh\theta_k \left(a_k^{R\dagger} b_k^{L\dagger} + a_k^R b_k^L\right) + \sinh^2\theta_k b_k^L b_k^{L\dagger}, \\ \overline{N}_k^2 &= \cosh^2\theta_k b_k^{R\dagger} b_k^R - \sinh\theta_k \cosh\theta_k \left(a_k^{L\dagger} b_k^{R\dagger} + a_k^L b_k^R\right) + \sinh^2\theta_k a_k^L a_k^{L\dagger}, \end{aligned} \tag{4.18}$$

which implies that

$$\begin{aligned} \left(N_k^1 - \overline{N}_k^2\right)|\Omega\rangle &= \left(a_k^{L\dagger} a_k^L - b_k^{R\dagger} b_k^R\right)|\Omega\rangle = 0, \\ \left(\overline{N}_k^1 - N_k^2\right)|\Omega\rangle &= \left(b_k^{L\dagger} b_k^L - a_k^{R\dagger} a_k^R\right)|\Omega\rangle = 0. \end{aligned} \tag{4.19}$$

The expressions in (4.19) led us to two other important results:

$$\begin{aligned} \left(\mathcal{N}_k^L - \mathcal{N}_k^R\right)|\Omega\rangle &= 0, \\ \left(Q_L + Q_R\right)|\Omega\rangle &= 0. \end{aligned} \tag{4.20}$$

In order to take advantage of the results right above, let us expand $|\Omega\rangle$ in basis generated by the eigenstates of $\mathcal{N}_k^L$ and $\mathcal{N}_k^R$, namely

$$|\Omega\rangle = \prod_{\vec{k}_i} \sum_{n,m} C_{n,m} \left|n_{k_i}, q\right\rangle_L \left|m_{k_i}, -q\right\rangle_R. \tag{4.21}$$

In order to satisfy the second equation in (4.20), we are already considering that the states on the left have positive electric charge, while the state on the right have $-q$. Also, $\prod_{\vec{k}_i}$ means that we are considering the product state between all the possible values of $\vec{k}$.[2] As a direct consequence of the first equation in (4.19), we obtain

$$\left(\mathcal{N}_k^L - \mathcal{N}_k^R\right)|\Omega\rangle = \prod_{\vec{k}_i} \sum_{n,m} C_{n,m} \left(n_k - m_k\right) \left|n, q\right\rangle_a \left|m, -q\right\rangle_b = 0, \tag{4.22}$$

which implies that $C_{n,m} = \delta_{nm}$. Also, we can apply A_k^1 on $|\Omega\rangle$ in order to obtain the following recurrence relation:

$$C_{n+1} = \tanh\theta_k C_n. \tag{4.23}$$

[2] In (4.21), we are discretizing the possible values of $\vec{k}$ just as a matter of notation.

The recurrence relation (4.23) leads us to rewrite C_n as

$$C_n = e^{n \ln(\tanh \theta_k)}, \tag{4.24}$$

allowing us to rewrite $|\Omega\rangle$, namely

$$|\Omega\rangle = \prod_{\vec{k}_i} \sum_{n=0}^{\infty} e^{n \ln\left(\tanh \theta_{k_i}\right)} |n_{k_i}, q\rangle_L |n_{k_i}, -q\rangle_R . \tag{4.25}$$

Another useful way to represent $|\Omega\rangle$ is by noticing that

$$|n_k, q\rangle_L |n_k, -q\rangle_R = \frac{\left(a_k^{L\dagger} b_k^{R\dagger}\right)^n}{n!} |0\rangle , \tag{4.26}$$

since we want the simplest state that respects (4.20). Then, we have that

$$|\Omega\rangle = \exp\left(\sum_{k_i} \tanh \theta_{k_i} a_{k_i}^{L\dagger} b_{k_i}^{R\dagger}\right) |0\rangle . \tag{4.27}$$

The expression for the vacuum $|\Omega\rangle$ in (4.25) was built only with general properties of the Bogoliubov transformations (4.16). Such fact is interesting because we have a free parameter θ_k, which can provide different interpretations for the non-canonical Hilbert space decomposition.

The next step is to figure out the parameter θ_k in order to $|\Omega\rangle$ becomes the TFD state. This can be done by a direct comparison to the usual formula for the TFD state, namely

$$|TFD\rangle = \sum_{n=0}^{\infty} e^{-\beta E_n/2} |n\rangle_L |n\rangle_R , \tag{4.28}$$

where E_n is the energy of simple state $|n, q\rangle$. Consider the total Hamiltonian of the system with the addition of a chemical potential μ, namely

$$H = H_L + H_R + \mu \left(Q_L - Q_R\right) . \tag{4.29}$$

If we apply H on one of the basis state in (4.25), we obtain

$$H |n, q\rangle_L |n, -q\rangle_R = 2n \left(\omega_k + \mu q\right) |n, q\rangle_L |n, -q\rangle_R , \tag{4.30}$$

which implies that

$$\tanh \theta_k = e^{-\frac{\beta}{2}(\omega_k + \mu q)}. \tag{4.31}$$

The charged TFD state is then

$$|TFD_q\rangle = \exp\left(\int d^{d-1}k e^{-\frac{\beta}{2}(\omega_k+\mu q)} a_k^{L\dagger} b_k^{R\dagger}\right)|0\rangle\,. \tag{4.32}$$

In order to understand the time dependence of the complexity, we need to consider a time dependent TFD state, which means that we need to apply the time evolution operator on that. In terms of the creation and annihilation operator, the Hamiltonian (4.29) has the following form:

$$H = \int d^{d-1}k \left[(\omega_k+\mu q)\left(a_k^{L\dagger}a_k^L + b_k^{R\dagger}b_k^R + 1\right) + (\omega_k-\mu q)\left(b_k^{L\dagger}b_k^L + a_k^{R\dagger}a_k^R + 1\right)\right]. \tag{4.33}$$

The creation and annihilation operators that appears in H commute to each other, which allow us to ignore the second term in (4.33) because it just contributes to the time evolution of the TFD state as an overall phase. Then, the time evolution operator is given by

$$U_T(t) = \exp\left(-i\int d^{d-1}k\,(\omega_k+\mu q)\left(a_k^{L\dagger}a_k^L + b_k^{R\dagger}b_k^R + 1\right)t\right), \tag{4.34}$$

Using the inverse Bogoliubov transformations

$$\begin{aligned}
a_k^L &= \cosh\theta_k A_k^1 + \sinh\theta_k B_k^{2\dagger},\\
a_k^R &= \cosh\theta_k A_k^2 + \sinh\theta_k B_k^{1\dagger},\\
b_k^L &= \cosh\theta_k B_k^1 + \sinh\theta_k A_k^{2\dagger},\\
b_k^R &= \cosh\theta_k B_k^2 + \sinh\theta_k A_k^{1\dagger},
\end{aligned} \tag{4.35}$$

the Hamiltonian (4.33) becomes

$$H = \int d^{d-1}k\,(\omega_k+\mu q)\left[\cosh 2\theta_k\left(A_k^{1\dagger}A_k^1 + B_k^2 B_k^{2\dagger}\right) + \sinh 2\theta_k\left(A_k^1 B_k^2 + A_k^{1\dagger}B_k^{2\dagger}\right)\right]. \tag{4.36}$$

The time dependent TFD state is then

$$|TFD_q(t)\rangle = e^{-iHt}|TFD_q\rangle\,, \tag{4.37}$$

where we are considering H given by (4.36).

4.2.2 The operator space

The time dependent TFD state is obtained from (4.32) by the application of the time evolution operator. Since we are interested in $|TFD_q(t)\rangle$ as the target state, it is intuitive to consider $|TFD_q\rangle$ as the reference state. Then, the complexity that will be obtained is time dependent and it essentially measures the computational cost to evolve

the TFD state in time. Consider the operator $U(s)$ as the one that implements the time evolution on our reference state. We already obtained in (4.34) that $U(1) = U_T(t)$, which is the boundary condition for $s = 1$. Now, we need to figure out what is the operator space where $U(s)$ lives. In order to do that, let us rewrite (4.36) as

$$H = \int d^{d-1}k \, (\omega_k + \mu q) \left[2\cosh 2\theta_k L_k^{(0)} + \sinh 2\theta_k \left(L_k^{(+)} + L_k^{(-)} \right) \right], \tag{4.38}$$

where

$$\begin{aligned} L_k^{(0)} &= \frac{1}{2} \left(A_k^{1\dagger} A_k^1 + B_k^2 B_k^{2\dagger} \right), \\ L_k^{(+)} &= A_k^{1\dagger} B_k^{2\dagger}, \\ L_k^{(-)} &= A_k^1 B_k^2. \end{aligned} \tag{4.39}$$

The set of operators $\left\{ L_k^{(0)}, L_k^{(+)}, L_k^{(-)} \right\}$ are the generators of an $SU(1,1)$ Lie algebra with the following commutation relations:

$$\begin{aligned} \left[L_k^{(+)}, L_k^{(-)} \right] &= -2L_k^{(0)}, \\ \left[L_k^{(0)}, L_k^{(\pm)} \right] &= \pm L_k^{(\pm)}. \end{aligned} \tag{4.40}$$

Then, it is possible to rewrite the time evolution operator as

$$U_T(t) = \exp \left[\int d^{d-1}k \left(\alpha_k^{(0)}(t) \, L_k^{(0)} + \alpha_k^{(+)}(t) \, L_k^{(+)} + \alpha_k^{(-)}(t) \, L_k^{(-)} \right) \right], \tag{4.41}$$

with

$$\begin{aligned} \alpha_k^{(\pm)}(t) &= -i \, (\omega_k + \mu q) \, t \sinh 2\theta_k, \\ \alpha_k^{(0)}(t) &= -2i \, (\omega_k + \mu q) \, t \cosh 2\theta_k. \end{aligned} \tag{4.42}$$

Since the time evolution operator has an exponential decomposition in terms of $SU(1,1)$ generators, it is reasonable to assume that the operator $U(s)$, which connects the target and reference state, is an element of the $SU(1,1)$ group.

Let us come back quickly to some general aspects of the complexity calculation. The intermediate state $|\psi(s)\rangle$ in (4.3) is built from $|\psi_R\rangle$ by the action of some unitary operator $U(s)$ in such way that $|\psi(1)\rangle = |\psi_T\rangle$. Since $U(s)$ is an element of $SU(1,1)$ group, it can be written as

$$U(s) = \exp \left[\int d^{d-1}k \left(\beta_k^{(0)}(s) \, L_k^{(0)} + \beta_k^{(+)}(s) \, L_k^{(+)} + \beta_k^{(-)}(s) \, L_k^{(-)} \right) \right], \tag{4.43}$$

where $U(s)$ must match $U_T(t)$ when $s = 1$. The elements of $SU(1,1)$ have the following

well-known decomposition [49]

$$U(s)=\exp\left[\int d^{d-1}k\gamma_k^{(+)}(s)\,L_k^{(+)}\right]\exp\left[\int d^{d-1}k\log\left(\gamma_k^{(0)}\right)L_k^{(0)}\right]\left[\int d^{d-1}k\gamma_k^{(-)}(s)\,L_k^{(-)}\right], \tag{4.44}$$

where

$$\begin{aligned}\gamma_k^{(\pm)}&=\frac{2\beta_k^{(\pm)}\sinh\eta_k}{2\eta_k\cosh\eta_k-2\beta_k^{(0)}\sinh\eta_k},\\ \gamma_k^{(0)}&=\left(\cosh\eta_k-\frac{\beta_k^{(0)}}{2\eta_k}\sinh\eta_k\right)^{-2},\\ \eta_k^2&=\frac{\beta_k^{(0)2}}{4}-\beta_k^{(+)}\beta_k^{(-)}.\end{aligned} \tag{4.45}$$

The expression (4.44) is quite useful because it is possible to figure out that

$$\begin{aligned}L_k^{(-)}\left|TFD_q\right\rangle&=0,\\ L_k^{(0)}\left|TFD_q\right\rangle&=\frac{1}{2}\left|TFD_q\right\rangle,\end{aligned} \tag{4.46}$$

which shows that only $L_k^{(+)}$ has a non-trivial contribution for the operator $U(s)$. As a result, the intermediate state becomes

$$\left|\psi(s)\right\rangle=\exp\left[\int d^{d-1}k\log\left(\sqrt{\gamma_k^{(0)}(s)}\right)\right]\exp\left[\int d^{d-1}k\gamma_k^{(+)}(s)\,L_k^{(+)}\right]\left|TFD_q\right\rangle, \tag{4.47}$$

where by imposing the normalization condition on $\left|\psi(s)\right\rangle$, we obtain

$$\left|\gamma_k^{(0)}\right|=1-\left|\gamma_k^{(+)}\right|^2. \tag{4.48}$$

Applying the normalization condition (4.48) in (4.47), we obtain the final expression for the intermediate state $\left|\psi(s)\right\rangle$, namely

$$\left|\psi(s)\right\rangle=\exp\left[\int d^{d-1}k\left(\log\left(\sqrt{1-\left|\gamma_k^{(+)}\right|^2}\right)+\gamma_k^{(+)}(s)\,L_k^{(+)}\right)\right]\left|TFD_q\right\rangle \tag{4.49}$$

Once we built $\left|\psi(s)\right\rangle$, we are in condition to compute the line element in operator space provided by the Fubini-Study metric in (4.6). By computing the s derivative of $\left|\psi(s)\right\rangle$, we obtain that

$$\partial_s\left|\psi(s)\right\rangle=\int d^{d-1}k\left(\frac{\partial_s\left|\gamma_k^{(+)}\right|^2}{2\left(1-\left|\gamma_k^{(+)}\right|^2\right)}+\partial_s\gamma_k^{(+)}(s)\,L_k^{(+)}\right)\left|\psi(s)\right\rangle. \tag{4.50}$$

The next step is to place (4.49) and (4.50) in (4.6). Then, we obtain

$$ds_{FS}^2 = \int d^{d-1}k' \int d^{d-1}k \partial_s \gamma_{k'}^{(+)*}(s)\, \partial_s \gamma_k^{(+)}(s) \left[\left\langle L_{k'}^{(-)} L_k^{(+)} \right\rangle - \left\langle L_{k'}^{(-)} \right\rangle \left\langle L_k^{(+)} \right\rangle \right], \quad (4.51)$$

where $\langle\rangle$ means the expectation value of an operator with relation to the state $|\psi(s)\rangle$. It is possible to show that

$$\left\langle L_k^{(+)} \right\rangle = \left\langle L_k^{(-)} \right\rangle = 0, \quad (4.52)$$

where it was necessary to use

$$\langle TFD_q| L_k^{(+)} |TFD_q\rangle = \langle TFD_q| L_k^{(-)} |TFD_q\rangle = 0. \quad (4.53)$$

In a similar way, the second expectation value in (4.51) is

$$\left\langle L_k^{(-)} L_k^{(+)} \right\rangle = \left[1 - \left| \gamma_k^{(+)}(s) \right|^2 \right] \left[\sum_{n=0}^{\infty} (n+1)^2 \left(\left| \gamma_k^{(+)}(s) \right|^2 \right)^n \right] \delta^{d-1}\left(\vec{k} - \vec{k}' \right). \quad (4.54)$$

By solving the infinity sum above, namely

$$\sum_{n=0}^{\infty} (n+1)^2 \left(\left| \gamma_k^{(+)}(s) \right|^2 \right)^n = \frac{1}{\left(1 - \left| \gamma_k^{(+)}(s) \right|^2 \right)^3}, \quad (4.55)$$

we obtain the final expression for the Fubini-Study metric

$$ds_{FS} = \sqrt{\int d^{d-1}k \left[\frac{\left| \partial_s \gamma_k^{(+)}(s) \right|}{1 - \left| \gamma_k^{(+)}(s) \right|} \right]^2}. \quad (4.56)$$

The expression above is essentially the complexity of the charged $|TFD_q(t)\rangle$, however, in [48] it was considered the Fubini-Study metric in (4.7) with $p = 1$, which leads to

$$\mathcal{C} = \min_{\gamma_k^{(+)}(s)} \int_0^1 ds \int d^{d-1}k \left[\frac{\left| \partial_s \gamma_k^{(+)}(s) \right|}{1 - \left| \gamma_k^{(+)}(s) \right|^2} \right]. \quad (4.57)$$

The complexity of the $|TFD_q(t)\rangle$ now depends essentially on $\gamma_k^{(+)}(s)$, which is related to the coefficients $\left\{ \beta_k^{(0)}(s), \beta_k^{(+)}(s), \beta_k^{(-)}(s) \right\}$ from (4.43) by the relations in (4.45). Also, the operator $U(s)$ in (4.43) must match the time evolution operator $U_T(t)$ for $s = 1$. This condition is equivalent to impose that the set of coefficients $\left\{ \beta_k^{(0)}(s), \beta_k^{(+)}(s), \beta_k^{(-)}(s) \right\}$ is equal to the coefficients $\left\{ \alpha_k^{(0)}(t), \alpha_k^{(+)}(t), \alpha_k^{(-)}(t) \right\}$

in (4.41) for $s = 1$. The conditions above provide the following way to write $\gamma_k^{(+)}(s)$:

$$\gamma_k^{(+)}(s) = -i\frac{\sinh 2\theta_k \sin \Delta}{\cos \Delta + i \cosh 2\theta_k \sin \Delta},$$
$$\Delta = (\omega_k + \mu q)\, ts. \tag{4.58}$$

The expression for $\gamma_k^{(+)}(s)$ in (4.58) satisfies all the boundary conditions and the necessary matches between $U(s)$ and $U_T(t)$ at $s = 1$. By computing

$$\left|\partial_s \gamma_k^{(+)}(s)\right| = \frac{\sinh 2\theta_k (\omega_k + \mu q)\, t}{\cos^2 \Delta + \cosh^2 2\theta_k \sin^2 \Delta} \tag{4.59}$$

and

$$1 - \left|\gamma_k^{(+)}(s)\right|^2 = \frac{1}{\cos^2 \Delta + \cosh^2 2\theta_k \sin^2 \Delta}, \tag{4.60}$$

we obtain

$$\mathcal{C}(t) = \int_0^1 ds \int d^{d-1}k \sinh 2\theta_k (\omega_k + \mu q)\, t. \tag{4.61}$$

4.2.3 Computing the complexity

The last step is to solve the integrals in (4.61). The one in s is quite direct, allowing us to rewrite the expression for the complexity as

$$\mathcal{C}(t) = \int d^{d-1}k \sinh 2\theta_k (\omega_k + \mu q)\, t. \tag{4.62}$$

Now, remember that the parameter θ_k and the quantity $\omega_k + \mu q$ are related by

$$\tanh \theta_k = e^{-\frac{\beta}{2}(\omega_k + \mu q)}, \tag{4.63}$$

which implies that

$$\cosh^2 \theta_k = \frac{1}{1 - e^{-\beta(\omega_k + \mu q)}},$$
$$\sinh^2 \theta_k = \frac{e^{-\beta(\omega_k + \mu q)}}{1 - e^{-\beta(\omega_k + \mu q)}}. \tag{4.64}$$

Then, the expression for $\mathcal{C}(t)$ becomes

$$\mathcal{C}(t) = 2t \int d^{d-1}k \frac{e^{-\frac{\beta}{2}(\omega_k + \mu q)}}{1 - e^{-\beta(\omega_k + \mu q)}} (\omega_k + \mu q). \tag{4.65}$$

If we consider the massless case, which means $\omega_k = |k| = k$, the expression for $\mathcal{C}(t)$ can be written as

$$\mathcal{C}(t) = 2t\Omega_{k,d-2} \sum_{n=0}^{\infty} \int dk k^{d-2} (k + \mu q)\, e^{-\left(n+\frac{1}{2}\right)\beta(k+\mu q)}, \tag{4.66}$$

where $\Omega_{k,d-2}$ is the $d-2$ sphere volume. By solving the integral em in k, the expression right above becomes

$$\mathcal{C}(t) = 2\beta^{-d} t \Omega_{k,d-2} \Gamma(d-1) \sum_{n=0}^{\infty} \frac{e^{-\left(n+\frac{1}{2}\right)\beta\mu q}}{\left(n+\frac{1}{2}\right)^{d}} \left(d-1+\left(n+\frac{1}{2}\right) q\beta\mu\right). \tag{4.67}$$

In order to obtain an analytic form for (4.67), let us consider the case where $\beta\mu q \ll 1$, which leads to a considerable simplification of $\mathcal{C}(t)$:

$$\mathcal{C}(t) = 2\beta^{-d} t \Omega_{k,d-2} \Gamma(d-1) \sum_{n=0}^{\infty} \left((d-1)\left(n+\frac{1}{2}\right)^{-d} - (d-2)\left(n+\frac{1}{2}\right)^{-(d-1)} \beta\mu q\right). \tag{4.68}$$

The sums in the above expression converge in such way that the expression for $\mathcal{C}(t)$ is now written in terms of gamma functions $\Gamma(d)$ and Riemann zeta functions $\zeta(d)$, namely

$$\mathcal{C}(t) = 2\beta^{-d} t \Omega_{k,d-2} \left[\Gamma(d)\left(2^{d}-1\right)\zeta(d) - (d-2)\Gamma(d-1)\left(2^{d-1}-1\right)\zeta(d-1)\beta\mu q\right]. \tag{4.69}$$

Despite the complicated functions that appears in the expression for the complexity, notice that the total energy for the neutral scalar field is

$$E = \int d^{d-1}k \frac{\sum_{n_k=0}^{\infty} n_k k e^{-\beta n_k k}}{\sum_{n_k=0}^{\infty} e^{-\beta n_k k}} = \int d^{d-1}k \frac{k e^{-\beta k}}{1-e^{-\beta k}} = \Omega_{k,d-2}\beta^{-d}\Gamma(d)\zeta(d), \tag{4.70}$$

while the total charge is

$$Q = \int d^{d-1}k \frac{q e^{-\beta n_k (k+\mu q)}}{1-e^{-\beta n_k (k+\mu q)}} = q\Omega_{k,d-2}\beta^{-(d-1)}\Gamma(d-1)\zeta(d-1), \tag{4.71}$$

which leads to

$$\mathcal{C}(t) = 2t\left[\left(2^{d}-1\right)E - (d-2)\left(2^{d-1}-1\right)\mu Q\right]. \tag{4.72}$$

It is expected that using CA [18], the holographic complexity for the charged AdS black hole approaches at late times as

$$\frac{d\mathcal{C}_A}{dt} = \frac{2}{\pi}(M-\mu Q), \tag{4.73}$$

which is the conjectured Lloyd's bound for this kind of black hole [18]. We have here a qualitative agreement between the complexity computed by the QFT side and the conjectured bound. In a more quantitative analysis, it can be pointed out a violation of the Lloyd's bound in (4.72). However, even in holographic computation there is an apparent violation of this bound for the charged AdS black hole [18, 50].

4.3 Nielsen's approach

In this section we are going to introduce the Nielsen's method for computing complexity. Many of the necessary concepts to precisely define complexity were already introduced in the previous section. Just as a quick review, we need essentially the same ingredients of the Fubini-Study method: the reference state $|\psi_R\rangle$, the target state $|\psi_R\rangle$ and the operator $U(s)$ which connects these two states. We also keep having the intermediate states $|\psi(s)\rangle$ and the same boundary conditions for $U(s)$ presented in (4.2) and (4.3).

Let us start to talk about the differences. Consider that the reference and target states are connected by the following unitary operator:

$$U(s) = \overleftarrow{P} \exp\left[-i \int_0^s ds' Y^I(s') L_I\right], \tag{4.74}$$

where we are already considering that the set of operators L_I forms a basis for some Lie algebra $\mathfrak{g}$ and $I = 1, 2, \cdots, \dim \mathfrak{g}$. The coefficients $Y^I(s)$ are called control functions. Making again an analogy to quantum circuits, the $Y^I(s)$ functions essentially measure how much each generator L_I contributes to the circuit at each step s. Similarly to the Fubini-Study case, we need to specify the group manifold where $U(s)$ belongs to, which is essentially our operator space. By differentiating (4.74) with respect to s, we obtain

$$Y^I(s) L_I = (\partial_s U(s)) U^{-1}(s). \tag{4.75}$$

It would be interesting to isolate $Y^I(s)$ on the left-hand side of (4.75), leading to the possibility to determinate $Y^I(s)$ from specific properties of the group. For example, if we consider the $S\mathcal{U}(2)$ group, we could use the trace properties of the Pauli matrices and the fact that there is a well-known general matrix form for the elements of $S\mathcal{U}(2)$ to figure out what $Y^I(s)$ is. For higher dimensional cases, we can introduce the Cartan-Killing form

$$K(X, Y) = \mathrm{Tr}\left(\mathrm{adj}_X \mathrm{adj}_Y\right). \tag{4.76}$$

In the above expression, adj_X means adjoint representation of $X \in \mathfrak{g}$, given by

$$(\mathrm{adj}_X)^M_N = x^K f^M_{KN}, \tag{4.77}$$

where x^K are the coefficients of the expansion $X = x^I L_I$. Notice also that

$$\left(\mathrm{adj}_{L_I}\right)^M_N = f^M_{IN}, \tag{4.78}$$

which provides the Cartan-Killing metric of $\mathfrak{g}$, namely

$$K_{IJ} = K(L_I, L_J) = f^M_{IN} f^N_{JM}, \tag{4.79}$$

where f_{IJ}^{L} is the structure constant of the Lie algebra, defined as

$$[L_I, L_J] = f_{IJ}^{K} L_k. \tag{4.80}$$

Then, we can multiply (4.75) by L_J and then trace it. As a result, we obtain

$$Y^I(s)\, K_{IJ} = \left[\left(\partial_s U(s)\right) U^{-1}(s)\right]_N^M f_{JM}^N, \tag{4.81}$$

where we need to consider some $\dim \mathfrak{g} \times \dim \mathfrak{g}$ representation of $\left(\partial_s U(s)\right) U^{-1}(s)$.

The introduction of the Cartan-Killing metric allows us to define the following line element

$$ds^2 = K_{IJ} Y^I(s)\, Y^J(\sigma)\,, \tag{4.82}$$

in such way that we could consider the cost function (4.13) as

$$\mathcal{D}(U) = \int_0^1 ds \sqrt{K_{IJ} Y^I(s)\, Y^J(s)}. \tag{4.83}$$

Then, the complexity of the target state is

$$\mathcal{C} = \mathcal{D}(U_{opt}) = \min_{Y^I(s)} \int_0^1 ds \sqrt{K_{IJ} Y^I(s)\, Y^J(s)}. \tag{4.84}$$

Now, we have essentially the problem of computing complexity in terms of the information that comes from the Lie algebra $\mathfrak{g}$. Next, we are going to consider the complexity between ground states connected by Bogoliubov transformations in a fermionic field theory. In special, we are going to focus on the toy model for fermions on a lattice presented in [26].

4.3.1 Free fermions in 1+1

Let us start considering the Dirac Lagrangian in d dimensions

$$\mathcal{L} = \bar{\psi}\left(i\gamma^\mu \partial_\mu - m\right)\psi, \tag{4.85}$$

where $\overline{\psi} = \psi^\dagger \gamma^0$ is the adjoint spinor and γ^μ are the gamma matrices. The conjugate momentum is given by

$$\Pi(x) = \frac{\mathcal{L}}{\partial\left(\partial_0 \psi(x)\right)} = i\psi^\dagger(x)\,, \tag{4.86}$$

while the Hamiltonian is

$$H = \int d^{d-1}x \left[-i\bar{\psi}\gamma^i \partial_i \psi + m\bar{\psi}\psi\right]. \tag{4.87}$$

Let us focus on Majorana fermions in $1+1$ dimensions, which allows us to consider a purely imaginary representation for the gamma matrices, namely

$$\gamma^0 = \begin{pmatrix} 0 & -i \\ i & 0 \end{pmatrix}, \qquad \gamma^1 = \begin{pmatrix} 0 & i \\ i & 0 \end{pmatrix}, \tag{4.88}$$

while our Majorana spinor can be written as

$$\psi = \begin{pmatrix} \psi^1 \\ \psi^2 \end{pmatrix}, \tag{4.89}$$

where the two spinor components ψ^1 and ψ^2 are real Grassmann variables. It is possible to rewrite the Hamiltonian (4.87) in terms of the spinor components, namely

$$H = \int dx \left[-i \left(\psi^1 \partial_x \psi^1 - \psi^2 \partial_x \psi^2 \right) - im \left[\psi^1, \psi^2 \right] \right]. \tag{4.90}$$

By defining the complex Grassmann variables

$$\Psi = \frac{\psi^1 - i\psi^2}{\sqrt{2}}, \qquad \Psi^\dagger = \frac{\psi^1 + i\psi^2}{\sqrt{2}}, \tag{4.91}$$

the Hamiltonian becomes

$$H = \int dx \left[-i \left(\Psi \partial_x \Psi + \Psi^\dagger \partial_x \Psi^\dagger \right) + m \left[\Psi^\dagger, \Psi \right] \right]. \tag{4.92}$$

We can regulate this Hamiltonian by placing it on a lattice with spacing δ. As a result, we obtain

$$H = \sum_{n=0}^{N-1} \left[-i \left(\Psi_n \Psi_{n+1} + \Psi_n^\dagger \Psi_{n+1}^\dagger \right) + \omega \left[\Psi_n^\dagger, \Psi_n \right] \right], \tag{4.93}$$

where $\omega = \delta m$. Now, considering periodic boundary conditions $\Psi_n = \Psi_{n+N}$, the discrete Fourier transform is

$$\Psi_n = \frac{1}{\sqrt{N}} \sum_{k=0}^{N-1} \Psi_k e^{2\pi i n k/N} \tag{4.94}$$

and its inverse transformation

$$\Psi_k = \frac{1}{\sqrt{N}} \sum_{n=0}^{N-1} \Psi_n e^{-2\pi i n k/N}. \tag{4.95}$$

From the canonical quantization conditions

$$\left\{ \Psi_n, \Psi_m^\dagger \right\} = \delta_{nm}, \qquad \left\{ \Psi_n, \Psi_m \right\} = \left\{ \Psi_n^\dagger, \Psi_m^\dagger \right\} = 0, \tag{4.96}$$

we obtain

$$\left\{\Psi_k, \Psi_{k'}^\dagger\right\} = \delta_{kk'}, \qquad \{\Psi_k, \Psi_{k'}\} = \left\{\Psi_k^\dagger, \Psi_{k'}^\dagger\right\} = 0, \tag{4.97}$$

which is the well-known algebra of the creation and annihilation operators. By placing (4.94) in H, we obtain that

$$H = \sum_{k=0}^{N-1} \left[-i\left(\Psi_k \Psi_{-k} e^{-2\pi i k/N} + \Psi_k^\dagger \Psi_{-k}^\dagger e^{2\pi i k/N}\right) + \omega\left[\Psi_k^\dagger, \Psi_k\right]\right]. \tag{4.98}$$

From the fact that $\Psi_k = \Psi_{k+N}$, it is possible to rearrange the Hamiltonian in such way that

$$H = \omega\left[\Psi_0^\dagger, \Psi_0\right] + \sum_{k=1}^{\frac{N-1}{2}} \left[\omega\left[\Psi_{N-k}^\dagger, \Psi_{N-k}\right] + \omega\left[\Psi_k^\dagger, \Psi_k\right] + g(k)\left(\Psi_k^\dagger \Psi_{N-k}^\dagger - \Psi_k \Psi_{N-k}\right)\right], \tag{4.99}$$

where

$$g(k) = 2\sin\left(\frac{2\pi i k}{N}\right). \tag{4.100}$$

Lastly, it is possible to redefine the variables in H as

$$\begin{aligned} a_k &= \Psi_k, \qquad a_k^\dagger = \Psi_k^\dagger, \\ b_k &= \Psi_{N-k}, \qquad b_k^\dagger = \Psi_{N-k}^\dagger, \end{aligned} \tag{4.101}$$

leading us to a interesting expression for H, namely

$$H = \sum_{k=1}^{\frac{N-1}{2}} H_k + \omega\left[\Psi_0^\dagger, \Psi_0\right], \tag{4.102}$$

with

$$H_k = \omega\left[b_k^\dagger, b_k\right] + \omega\left[a_k^\dagger, a_k\right] + g(k)\left(a_k^\dagger b_k^\dagger - a_k b_k\right). \tag{4.103}$$

For each mode k, we have a Hamiltonian H_k that describes two coupled fermionic oscillators. This allow us to consider the complexity of a single pair of coupled fermionic oscillators, in such way that will be possible to generalize the result for the entire lattice.

4.3.2 Coupled fermionic oscillators

Consider two coupled fermionic oscillators, whose Hamiltonian is given by

$$H = \omega\left[b^\dagger, b\right] + \omega\left[a^\dagger, a\right] + g\left(a^\dagger b^\dagger - ab\right). \tag{4.104}$$

Let us consider the Bogoliubov transformations

$$\begin{aligned} A &= \cos\theta a + \sin\theta b^\dagger, \\ A^\dagger &= \cos\theta a^\dagger + \sin\theta b, \\ B &= \cos\theta b - \sin\theta a^\dagger, \\ B^\dagger &= \cos\theta b^\dagger - \sin\theta a, \end{aligned} \tag{4.105}$$

and the inversion transformations

$$\begin{aligned} a &= \cos\theta A - \sin\theta B^\dagger, \\ a^\dagger &= \cos\theta A^\dagger - \sin\theta B, \\ b &= \cos\theta B + \sin\theta A^\dagger, \\ b^\dagger &= \cos\theta B^\dagger + \sin\theta A, \end{aligned} \tag{4.106}$$

which preserve the anti-commutation relations, in such way that

$$H = \left[\omega\cos(2\theta) + \frac{g}{2}\sin(2\theta)\right]\left(\left[A^\dagger, A\right] + \left[B^\dagger, B\right]\right) + \left[\omega\sin(2\theta) - \frac{g}{2}\cos(2\theta)\right]\left([A, B] - \left[A^\dagger, B^\dagger\right]\right). \tag{4.107}$$

To obtain a diagonal Hamiltonian, we need to set the transformation parameters in order to cancel the second term in (4.107), namely

$$\tan(2\theta) = \frac{g}{2\omega}. \tag{4.108}$$

As a direct consequence

$$\cos(2\theta) = \frac{2\omega}{\sqrt{4\omega^2 + g^2}}, \qquad \sin(2\theta) = \frac{g}{\sqrt{4\omega^2 + g^2}}, \tag{4.109}$$

resulting in

$$H = \lambda\left(\left[A^\dagger, A\right] + \left[B^\dagger, B\right]\right), \tag{4.110}$$

where

$$\lambda = \frac{1}{2}\sqrt{4\omega^2 + g^2}. \tag{4.111}$$

Similarly to the Fubini-Study case, the fact that the new vacuum $|\Omega\rangle$ has no particles provides the following recurrence condition:

$$\left(A^\dagger A - B^\dagger B\right)|\Omega\rangle = \left(a^\dagger a - b^\dagger b\right)|\Omega\rangle = 0. \tag{4.112}$$

The above expression shows that $|\Omega\rangle$ has the same number of particles and anti-particles created by $a^\dagger$ and $b^\dagger$, respectively. Then, the decomposition of $|\Omega\rangle$ in the old basis is given

by

$$|\Omega\rangle = C_{00}\,|00\rangle + C_{11}\,|11\rangle\,. \tag{4.113}$$

By applying A and B on $|\Omega\rangle$, we obtain the coefficients α and β, namely

$$|\Omega\rangle = \cos\theta\,|00\rangle + i\sin\theta\,|11\rangle\,. \tag{4.114}$$

Now, let us take advantage of the fact that our system lives in a four-dimensional Hilbert space $\mathcal{H}_2 \otimes \mathcal{H}_2$, allowing us to choose

$$|0\rangle = \begin{pmatrix} 1 \\ 0 \end{pmatrix}, \qquad |1\rangle = \begin{pmatrix} 0 \\ 1 \end{pmatrix}, \tag{4.115}$$

in such way that

$$|00\rangle = \begin{pmatrix} 1 \\ 0 \\ 0 \\ 0 \end{pmatrix}, \qquad |11\rangle = \begin{pmatrix} 0 \\ 0 \\ 0 \\ 1 \end{pmatrix}, \qquad |01\rangle = \begin{pmatrix} 0 \\ 1 \\ 0 \\ 1 \end{pmatrix}, \qquad |10\rangle = \begin{pmatrix} 0 \\ 0 \\ 1 \\ 0 \end{pmatrix}. \tag{4.116}$$

In this matrix representation, the vacuum $|\Omega\rangle$ has the form

$$|\Omega\rangle = \begin{pmatrix} \cos\theta \\ 0 \\ 0 \\ i\sin\theta \end{pmatrix} = U_{(4\times4)} \begin{pmatrix} 1 \\ 0 \\ 0 \\ 0 \end{pmatrix}, \tag{4.117}$$

where

$$U_{(4\times4)} = \begin{pmatrix} \cos\theta & 0 & 0 & i\sin\theta \\ 0 & \cos\theta & 0 & 0 \\ 0 & 0 & \cos\theta & 0 \\ i\sin\theta & 0 & 0 & \cos\theta \end{pmatrix}. \tag{4.118}$$

Nevertheless, the operator U changes only the first and fourth component of $|00\rangle$, in such way that we can consider this problem using 2×2 matrices, namely

$$\begin{pmatrix} \cos\theta \\ i\sin\theta \end{pmatrix} = U_{(2\times2)} \begin{pmatrix} 1 \\ 0 \end{pmatrix}. \tag{4.119}$$

Then, the complexity of $|\Omega\rangle$ will be computed considering a 2×2 unitary matrix. Actually, it is possible to extract the $U(1)$ phase e^{iy} and consider that $U(s) \in U(1) \times$

$SU(2)$, which has the following general form

$$U(s) = e^{iy(s)} \begin{pmatrix} \alpha(s) & -\beta^*(s) \\ \beta(s) & \alpha^*(s) \end{pmatrix}, \qquad |\alpha|^2 + |\beta|^2 = 1, \tag{4.120}$$

where $\alpha, \beta \in \mathbb{C}$. Another way to express $U(s)$ is by considering α, β as $\alpha = a + ib$ and $\beta = c + id$, in such way that

$$U = e^{iy} \begin{pmatrix} a + ib & -c + id \\ c + id & a - bi \end{pmatrix}, \tag{4.121}$$

with

$$a^2 + b^2 + c^2 + d^2 = 1. \tag{4.122}$$

In special, the expression right above is the equation of a sphere S^3, which allow us to represent U as a sphere.[3] As a result, we obtain

$$U = e^{iy} \begin{pmatrix} \cos\rho\cos\tau + i\sin\phi\sin\rho & \cos\phi\sin\rho + i\cos\rho\sin\tau \\ i\cos\rho\sin\tau - \cos\phi\sin\rho & \cos\rho\cos\tau - i\sin\phi\sin\rho \end{pmatrix}, \tag{4.123}$$

where $y, \phi, \tau \in [0, 2\pi)$ and $\rho \in [0, \pi/2]$. Once we have the operator space, it is time to consider the intermediate states $|\psi(s)\rangle = U(s)|00\rangle$, where $U(s)$ is given by (4.123). Also, it is known that the generators of $\mathcal{U}(2)$ can be taken as

$$L_0 = iI_2, \qquad L_i = i\sigma_i, \tag{4.124}$$

where I_2 is the identity in two dimensions and σ_i are the Pauli matrices.[4] Then, the commutation relations between the generators are

$$[L_i, L_j] = -2\varepsilon_{ij}^k L_k, \qquad [L_0, L_i] = 0, \tag{4.125}$$

which provide us the following form for the Cartan-Killing metric (4.79):

$$K_{IJ} = \delta_{IJ}. \tag{4.126}$$

As a consequence, it is possible to solve (4.81) in order to obtain the control functions $Y_I(s)$ and the cost function (4.83), namely

$$Y^I(s) = \frac{1}{2}\mathrm{Tr}\left[(\partial_s U(s))\, U^{-1}(s)\, L_I\right] \tag{4.127}$$

[3] Here, a and b are not any kind of annihilation operators, just real variables that we are considering to express the complex parameter α.

[4] For the generators of $\mathcal{U}(2)$, let us consider $I = 0, 1, 2, 3$, while $i = 1, 2, 3$.

and

$$\mathcal{D}(U)=\int_0^1 ds\sqrt{\delta_{IJ}Y^I(s)\,Y^J(s)}, \tag{4.128}$$

where $U(s)$ is the one shown in (4.123). By computing explicitly (4.128), we obtain that

$$\mathcal{D}(U)=\int_0^1 ds\sqrt{(\rho')^2+\cos^2\rho\,(\tau')^2+\sin^2\rho\,(\phi')^2+(y')^2}, \tag{4.129}$$

where ρ' refers to the derivative with respect to the curve parameter.

The expression above is the cost function for any operator $U\in\mathcal{U}(2)$. However, if we want the complexity of $|\Omega\rangle$, we need to find the optimal path in the y, ρ, τ and ϕ that minimizes (4.129). Then, the geodesic equations are

$$\begin{aligned} y''&=0,\\ \rho''-\sin\rho\cos\rho\phi'^2+\sin\rho\cos\rho\tau'^2&=0,\\ \tau''-2\tan\rho\rho'\tau'&=0,\\ \phi''+2\cot\rho\phi'\rho'&=0. \end{aligned} \tag{4.130}$$

Instead to solve these equations, we can take advantage to the fact that the metric in (4.129) have at least three Killing vectors $\frac{\partial}{\partial y}$, $\frac{\partial}{\partial\phi}$ and $\frac{\partial}{\partial\tau}$, in such way that

$$\frac{d}{ds}\left(k^\mu\frac{dx_\mu}{ds}\right)=0, \tag{4.131}$$

where $x^\mu(s)=(\tau(s),y(s),\phi(s),\rho(s))$. Then, we obtain three constants of motion

$$\begin{aligned} y'&=c_1,\\ \cos^2\rho\tau'&=c_2,\\ \sin^2\rho\phi'&=c_3, \end{aligned} \tag{4.132}$$

with c_1, c_2 and c_3 being constants to be defined. The equations provided by the constants of motion seem more treatable than the ones in (4.130).

The next step is to consider the boundary conditions. At $s=0$, we have that $U(0)=I$, which lead us to arrange the coordinates y, ρ, τ and ϕ in such way that the $U(s)$ in (4.123) at $s=0$ becomes the identity. As a result, we obtain that the initial vector $x^\mu(0)$ is

$$\tau(0)=0,\qquad y(0)=0,\qquad \phi(0)=\phi_0,\qquad \rho(0)=0. \tag{4.133}$$

For the boundary conditions at $s=1$, we first need to figure out what is the matrix that

accomplish the relation shown in (4.119). One possibility is

$$U(1) = \begin{pmatrix} \cos\theta & i\sin\theta e^{-i\gamma} \\ i\sin\theta & \cos\theta e^{-i\gamma} \end{pmatrix}, \tag{4.134}$$

where γ is an arbitrary phase with $\gamma \in [-\pi, \pi)$. Considering the $U(1)$, we need to arrange the coordinates x^μ again so that $U(s)$ in (4.123) matches (4.134). Then, we obtain that

$$\tau(1) = \theta, \qquad y(1) = -\frac{\gamma}{2}, \qquad \phi(1) = \frac{\pi}{2} - \theta, \qquad \rho(1) = \frac{\gamma}{2}. \tag{4.135}$$

We would hope to solve the equations in (4.130) with the help of (4.132). However, what happens is that the equation for ϕ is trivially solved, which makes it impossible to determinate $\phi(s)$. For the other coordinates, we have

$$y(s) = -\frac{\gamma}{2}s, \qquad \rho(s) = \frac{\gamma}{2}s, \qquad \tau(s) = \theta s, \tag{4.136}$$

in such way that

$$\mathcal{D}(U_{opt}) = \int_0^1 ds \sqrt{\left(\frac{\gamma}{2}\right)^2 + \cos^2\left(\frac{\gamma}{2}\right)\theta^2 + \sin^2\left(\frac{\gamma}{2}\right)(\phi')^2 + \left(\frac{\gamma}{2}\right)^2}. \tag{4.137}$$

However, since γ is an arbitrary phase, it is clear that if we set it to be zero, we will obtain a lower value for the depth, namely

$$\mathcal{C} = \mathcal{D}(U_{opt}) = \frac{1}{2}\arctan\left(\frac{g}{2\omega}\right), \tag{4.138}$$

where we used equation (4.108) in order to obtain the answer in terms of the Hamiltonian parameters. The expression right above is the complexity of the Bogoliubov transformed ground state $|\Omega\rangle$ for a system of two coupled fermionic oscillators. However, the Hamiltonian in (4.102) describes a chain of $N/2$ coupled fermionic oscillators. For each value of k we have a different pair of coupled oscillators. Also, there is not any mix between different k's in the coupling term (4.102), which means that the Hilbert space is of the form $\mathcal{H} = \prod_{k=1}^{\frac{N-1}{2}} \otimes \mathcal{H}_k$. Once the system is completely decoupled between different values of k, the Bogoliubov transformations preserve such feature. As a consequence, the total new vacuum $|\Omega_T\rangle$ after we perform the Bogoliubov transformations on each $k-$oscillator, will be $|\Omega_T\rangle = \prod_{k=1}^{\frac{N-1}{2}} \otimes |\Omega_k\rangle$. Finally, the total complexity of the process will be sum of the complexity of each $|\Omega_k\rangle$, namely

$$\mathcal{C}(|\Omega_T\rangle) = \sum_{n=1}^{\frac{N-1}{2}} \frac{1}{2}\arctan\left(\frac{g(k)}{2\omega}\right), \qquad g(k) = 2\sin\left(\frac{2\pi k}{N}\right). \tag{4.139}$$

The above result is not so illuminating than the one obtained for the complex

scalar field case (4.72). The Bogoliubov transformations applied in this case do not include time, which means that we are not in position to perform some analysis about the time behavior of the complexity. However, in this example, we have demonstrated the procedure to compute complexity for a many-body system step by step. Despite the fact that original discussion was about complexity in QFT, the procedure described above is essentially the same if we don't want to place the QFT on a lattice.

4.4 Complexity of operators

In the previous sections the main properties of the so-called complexity of states were presented, as well as two examples of applications. The core of this definition of complexity is to provide a quantity related to the reference state and the target state. In this sense, the result of the computation is highly dependent on the choice of such states. This could not be different since we are measuring the complexity between two states of interest. On the other hand, the complexity of operators, that was widely discussed in [51, 52], essentially measures the complexity of the time evolution operator

$$U(t) = e^{-iHt}, \tag{4.140}$$

where H is the Hamiltonian of system. At this point, the first main difference between the two approaches of complexity appears. First of all, the time evolution operator $U(t)$ is a crucial piece of information for the study of quantum systems. This operators is responsible for the time evolution of the quantum system, implying that the complexity associated with this operator will carry a direct dependence of time, allowing us to study the time evolution of the complexity itself. Second, while the complexity of states is highly dependent on the choices of reference and target state, the complexity of operators is interested on the time evolution operator, which is an operator relevant for any quantum system. Thus, the complexity of operators seems to have a major degree of generality in comparison with the complexity of states since the time evolution operator is unique given the Hamiltonian of the system.

In order to present the main concepts related to complexity of operators, it is important to highlight that both types of complexity share similar mathematical objects and ideas, despite their conceptual differences. Because of these similarities, the presentation of some objects can seem repetitive, however, it is important to clarify that even similar objects will have different uses depending of which complexity we are talking about.

Consider that we are handling a system that is composed by L lattice sites where we can have bosonic or fermionic degrees of freedom. Then, the Hilbert space of this $\mathcal{H}$

system has the following tensor factorization

$$\mathcal{H} = \mathbb{C}^N \otimes \mathbb{C}^N \otimes \cdots \otimes \mathbb{C}^N, \tag{4.141}$$

where N is the number of bosonic or fermionic degrees of freedom on each site. Once we are talking about operator complexity, it is important to define the *operator space* $\mathcal{U}$ that acts on the Hilbert space $\mathcal{H}$, that is

$$\mathcal{U}(\mathcal{H}) = SU(N^L). \tag{4.142}$$

For example, if our system is a spin chain with two sites, then the operator space is $SU(4)$. The operator space is a key concept in the complexity of operators. Essentially, as we are going to see soon, the geometry of this space will provide key aspects of the complexity.

In order to study geometrical aspects of $SU(N^L)$, it is necessary that we choose a basis for the Lie algebra of the group. At this point, it is time to discuss the very important notion for complexity of operators: *locality*. The idea here is that we need to classify the generators of the Lie algebra as local or non-local. Another way that we can refer to these classes of generators is as simple or hard, respectively. Despite of different nomenclatures, in quantum computing, it is quite standard to choose some simple operators as the elementary gates to be used in building circuits. On the other hand, in the geometric approach, we can pick different types of operators from the operator space. As consequence, it is natural to choose a k-local subspace of the Lie algebra of the unitary group manifold to correspond to *simple directions*. All the other directions that are not in the k-local subspace are considered *hard directions*. As we are going to see in details soon, the way that we will distinguish simple and hard directions will be by the insertion of a penalty over the hard directions.

The question now is what are going to be the rule to choose the k-local subspace? In order to answer this question, let us consider the case of $SU(2)$. It is well known that we can pick the Pauli matrices

$$\sigma_1 = \begin{pmatrix} 0 & 1 \\ 1 & 0 \end{pmatrix}, \quad \sigma_2 = \begin{pmatrix} 0 & -i \\ i & 0 \end{pmatrix}, \quad \text{and} \qquad \sigma_3 = \begin{pmatrix} 1 & 0 \\ 0 & -1 \end{pmatrix} \tag{4.143}$$

as a basis of the $SU(2)$ Lie algebra with commutation relations

$$[\sigma_i, \sigma_j] = 2i\epsilon_{ijk}\sigma_k. \tag{4.144}$$

In fact, for the case of one single qubit, the idea of a k-local subspace seems unnecessary. However, for $L \geq 2$, it is possible to build the basis of $SU(2^L)$ using the Pauli matrices

plus the identity matrix I_2, namely

$$\Big\{I_2, \quad \sigma_1, \quad \sigma_2, \quad \sigma_3\Big\}. \tag{4.145}$$

For example, considering two qubits ($L = 2$), from (4.145) it is possible to generate 16 operators via tensor product, once each qubits contributes with 4 matrices. As a consequence, if we take out the 4×4 identity matrix from this list, we obtain the generators of $SU(4)$, which are given by

$$T_a = \{I_2 \otimes \sigma_i, \quad \sigma_i \otimes I_2, \quad \sigma_i \otimes \sigma_j\}, \quad a = 1, \ldots, 15 \quad \text{and} \quad i, j = 1, \ldots, 3. \tag{4.146}$$

It is possible to repeat this same process for any number of qubits. The total number of ordered tensor products is $(2^L)^2 - 1$, which is precisely the dimension of the Lie algebra $\mathfrak{su}(2^L)$. In this sense, T_A are the generators of $\mathfrak{su}(2^L)$, providing the following commutation relations

$$[T_a, T_b] = i f_{ab}{}^c T_c, \tag{4.147}$$

where $f_{ab}{}^c$ are the structure constants of the Lie algebra. In this sense, the philosophy related to the complexity of states is quite similar to Nielsen's approach for complexity of states: we are going to look for a minimal-length geodesic on $SU(N^L)$ with respect to a right-invariant metric chosen in such way that it penalizes the contribution of non-local directions for the unitary operators.

The criteria for non-local directions is quite simple. Once the generators of the Lie algebra will be build as tensor products between individual generators of the $\mathfrak{su}(N)$, which represents the generators of the group for individual sites. We can introduce then a set of matrices $t_i^{(n)}$ that are composed by the identity matrix I_N and the generators of $\mathfrak{su}(N)$, where $i = 0, 1, 2, \ldots, \dim(\mathfrak{su}(N))$ and n runs over the number of sites. In this context, the k-local subspace is composed by all the generators built with at least k matrices $t_i^{(n)}$.[5] All the remaining generators will form the non-local subspace, whose directions will be penalized in such way that these non-local generators will increase the complexity of the operator more than local generators.

In order to clarify the criteria described right above, let us consider the case of three qubits ($L = 3$). In this situation, the matrices $t_i^{(n)} = \{I_2, \sigma_1, \sigma_2, \sigma_3\}$ can be used to produce the generators of $\mathfrak{su}(8)$ as

$$T_a = t_i^{(1)} \otimes t_j^{(2)} \otimes t_k^{(3)}, \tag{4.148}$$

where $a = 1, 2, 3, \ldots, 63$ and $i = 0, 1, 2, 3$. Here, the generators T_a can be organized in

[5] In this construction, we will always have a combination with only identity matrices that needs to be unconsidered in order match the dimension of $\mathfrak{su}(N^L)$.

the following way:

$$\begin{aligned} \{\sigma_i \otimes I_2 \otimes I_2,\ I_2 \otimes \sigma_i \otimes I_2,\ I_2 \otimes I_2 \otimes \sigma_i\} \quad & \text{1-local generators,} \\ \{\sigma_i \otimes \sigma_j \otimes I_2,\ \sigma_i \otimes I_2 \otimes \sigma_j,\ I_2 \otimes \sigma_i \otimes \sigma_j\} \quad & \text{2-local generators,} \\ \{\sigma_i \otimes \sigma_j \otimes \sigma_k\} \quad & \text{3-local generators.} \end{aligned}$$

In this sense, for the generators shown right above, we can say that local subspace is generated by the 1-local and 2-local operators, which provide 36 local directions. On the other hand, the 3-local operators will provide 27 non-local directions. This analysis for $SU(8)$ explicitly shows what will be the criteria to classify a generator as easy or hard: any operator that is at most 2-local can be considered as generating an easy direction on the manifold, which means that no penalization will be applied over this direction. This choice of criteria comes from quantum computing where the most important gates acts on one or two qubits at most.

It is important to point that the criteria of locality is arbitrary. However, what makes sense is that only a small portion of the generators are considered local, otherwise, the criteria of locality would not make sense if the most part of the generators are considered local. In the case of three qubits, almost 57% of the generators are local. Such fact could allow someone to point that the this fact is contradictory with the statement that most part of the generators should be non-local. The point here is that three qubits is just a small number. Following our criteria for locality, if we consider a system with L qubits, the number of 1-local and 2-local operators are given by

$$N_{1-local} = 3L, \tag{4.149}$$

$$N_{2-local} = \frac{9L(L-1)}{2}, \tag{4.150}$$

respectively. Then, the number of non-local generators (3-local, 4-local, etc.) can be computed by the difference between the dimension of the Lie algebra $2^L - 1$ and the number of local generators (1-local and 2-local). The result is that

$$N_{non-local} = 2^L - \frac{3}{2}(3L-1)L - 1. \tag{4.151}$$

Despite the fact that (4.151) is not that illuminating, if we think on the asymptotic behaviour of (4.150) and (4.151) as function of L, the number of local generators grows polynomially while the growth for the non-local generators are exponential. The conclusion here is that as the dimension of the spin chain increases, the number of non-local generators eventually will dominate, what is in agreement with the assumption that the set of local generators should be quite smaller than the non-local set.

4.4.1 Complexity and geodesics on the operator space

Similarly to what it was already shown during the explanation of the Nielsen's approach for complexity of states, our objective here is to obtain the complexity of $U(t)$ from the identity operator $\mathcal{I}$ through the computation of the geodesic on the operator space $\mathcal{U}(\mathcal{H})$. In this sense, the operators in $\mathcal{U}(\mathcal{H})$ can be written in terms of the generators T_a as

$$U(s) = \overleftarrow{\mathcal{P}} \exp\left[-i \int_0^s ds' V^a(s') T_a\right], \tag{4.152}$$

where T_a are the generators of the Lie algebra of the group, $V^a(s)$ are the velocities that control the motion of $U(s)$ through the directions provided by T_a and s is the curve parameter on the geodesic with $s \in [0, 1]$. The operator $U(s)$ also satisfies the following boundary condition:

$$U(0) = \mathcal{I} \quad \text{and} \quad U(1) = U_{target}, \tag{4.153}$$

where it is important to emphasize that $U_{target} = U(t)$. The metric on $\mathcal{U}(\mathcal{H})$ can be obtained via the Cartan-Killing form

$$K_{ab} = -f_{ac}{}^{d} f_{bd}{}^{c}, \tag{4.154}$$

which can provide a positive-definite metric. However, we still need to apply the penalization over the non-local directions. This process can be done by hand directly in the construction of the metric. Let us start splitting the generators in two groups

$$T_a = \{T_\alpha,\ T_{\dot{\alpha}}\},$$

where T_α refers to all the local generators (1-local, 2-local, 3-local, etc.) and $T_{\dot{\alpha}}$ to all the non-local. The range of α and β will depend on the specific algebra. For example, if the group manifold is $SU(8)$, which means three qubits, $\alpha = 1, 2, \ldots, 36$ and $\alpha = 1, 2, \ldots, 27$. Then, the metric of operator space can be modified from the (4.154) as

$$G_{ab} = \begin{pmatrix} K_{\alpha\beta} & 0 \\ 0 & (1+\mu) K_{\dot{\alpha}\dot{\beta}} \end{pmatrix}, \tag{4.155}$$

where μ is the *cost factor* that penalizes motion in non-local directions. If we set $\mu = 0$, we re-obtain the standard case where all the directions will contribute the same amount for the complexity.

Once we choose the direction that will be penalized, the geodesic on $\mathcal{U}(\mathcal{H})$ can be provided by the Euler-Arnold equation, namely

$$G_{ab} \frac{dV^b}{ds} = f_{ab}{}^{c} V^b G_{cd} V^d, \tag{4.156}$$

where ${f_{ab}}^C$ are the structure constants given in (4.147) and G_{cd} the metric in (4.154). Another equation that must be satisfied by $U(s)$ is the well known matrix equation for the unitary operator

$$\frac{dU(s)}{ds} = -iV^a(s)T_aU(s). \tag{4.157}$$

Lastly, the complexity is given by the geodesic length between the target unitary operator U_{target} and the identity operator $\mathcal{I}$, that is

$$\mathcal{C}(U_{target}) = \min \int_0^1 ds \sqrt{G_{ab}V^a(s)V^b(s)}. \tag{4.158}$$

In order to illustrate the entire process describe right above, we are going to consider the analytical case of one qubit.

4.4.2 Analytical case for one qubit

Considering the case of one qubit, we have the operator space being $SU(2)$, where the generators of the Lie algebra are the Pauli matrices in (4.143). For this Lie algebra, the structures constants are ${f_{ab}}^c = 2\epsilon_{abd}\delta^{dc}$, providing the following Cartan-Killing form:

$$K_{ab} = \delta_{ab}. \tag{4.159}$$

For the case of one qubit there is not a good notion of locality, at least for the Pauli basis. However, it is possible to consider one generator of the Lie algebra as non-local just to have at least one non-local direction. In this sense, the metric (4.155) becomes

$$G_{ab} = \begin{pmatrix} 1 & 0 & 0 \\ 0 & 1 & 0 \\ 0 & 0 & 1+\mu \end{pmatrix}, \tag{4.160}$$

where σ_3 was chosen as the non-local generator.

The next step is to solve the Euler-Arnold equations (4.156), that have the following form for $\mathfrak{su}(2)$:

$$\frac{dV^1}{ds} = 2\mu V^2V^3, \tag{4.161}$$

$$\frac{dV^2}{ds} = -2\mu V^1V^3, \tag{4.162}$$

$$\frac{dV^3}{ds} = 0. \tag{4.163}$$

The system of equations displayed right above can be solved by

$$V_1(s) = C_1 \cos(C_3 \mu s) + C_2 \sin(C_3 \mu s), \tag{4.164}$$

$$V_2(s) = C_2 \cos(C_3 \mu s) - C_1 \sin(C_3 \mu s), \tag{4.165}$$

$$V_3(s) = \frac{C_3}{2}, \tag{4.166}$$

where C_1, C_2 and C_3 are integration constant that need to be fixed. Once we have solved the geodesic equation for all the V_a, which allows us to obtain the tangent vector at any point along the geodesic, it is now possible to compute the complexity between $U(0) = \mathcal{I}$ and $U(1) = U_{target}$, namely

$$\mathcal{C} = \sqrt{(C_1)^2 + (C_2)^2 + \frac{1+\mu}{4}(C_3)^2}. \tag{4.167}$$

The first interesting characteristic of the complexity is that it is s-independent, which leads us to the following conclusion: the complexity depends only of the initial configuration of the tangent vector, provided by C_1, C_2 e C_3, and the cost factor μ.

Now, the task is to compute the values of the integration constants. It can be achieved by imposing the boundary condition $U(1) = U_{target}$, where in our case $U_{target} = e^{-iHt}$. However, to impose the boundary conditions, we need first to obtain the expression of $U(s)$ in terms of tangent vectors V_a. From (4.157), using the information from (4.166), we obtain that

$$U(s) = \begin{pmatrix} \phi(s)\left(\cos(s\omega) - \frac{iC_3(\mu+1)\sin(s\omega)}{2\omega}\right) & -\frac{(iC_1+C_2)\phi(s)\sin(s\omega)}{\omega} \\ \frac{(C_2-iC_1)\phi(-s)\sin(s\omega)}{\omega} & \phi(-s)\left(\cos(s\omega) + \frac{iC_3(\mu+1)\sin(s\omega)}{2\omega}\right) \end{pmatrix}, \tag{4.168}$$

where

$$\phi(s) = e^{\frac{iC_3\mu s}{2}}. \tag{4.169}$$

The constants C_i are inside this new parameter ω that can be interpreted as a characteristic frequency of the systems, namely

$$\omega^2 = (C_1)^2 + (C_2)^2 + \frac{(1+\mu)^2}{4}(C_3)^2. \tag{4.170}$$

The expression for $U(s)$ in (4.168) provides the set of unitary on the path between the identity matrix ($s = 0$) and the target operator ($s = 1$). It is already known that the target operator is the time evolution operator $U(t)$. However, nothing was told about the Hamiltonian so far. For one single qubit, without losing generality, we can consider an Hamiltonian like

$$H = J_1 T_1 + J_2 T_2 + J_3 T_3, \tag{4.171}$$

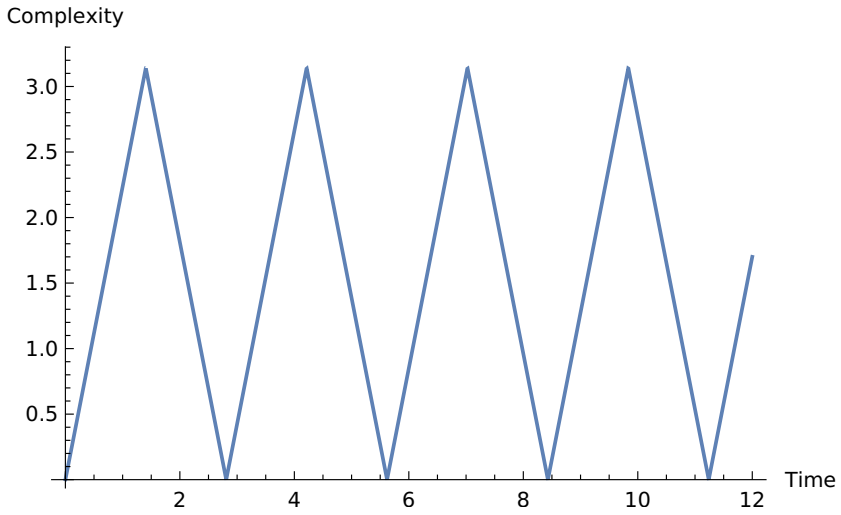

Figure 4.2: Complexity as function of time for $J_1 = 1$, $J_2 = 2$, $J_3 = 0$ and $\mu = 10$. The complexity has an initial linear growth, reaching a maximum value and than keeps oscillating linearly.

where J_1, J_2 and J_3 are projections of H in the directions generated by T_1, T_2 and T_3, respectively. Once H is known, we are able to perform the match between $U(s=1)$ and $U(t)$. Such process results in a system of three equations that can be solved numerically.[6] As a result, we obtain the value of the integration constants and place them in 4.167, obtaining this way the time dependent complexity numerically. In Figure 4.2 it is shown the behavior of complexity for a certain combination of the system parameters. The linear oscillation of the complexity is quite similar to what was presented in [53]. Such behavior is due to the fact that the group $SU(2) \simeq S^3$. After a certain time, the minimal length starts to connect two antipodal points of the sphere. Then, the minimal length switches direction, shrinking until become zero again.

In principle, the formalism presented in this section can be applied for bigger lattices. The problem is that the number of directions on the group manifold increases fast. For example, considering two qubits, the number of generators is 15, which means this same number of coupled differential equations from (4.156). Even solving these differential equations, there is also the problem of setting the integration constants. Instead of find the solutions of (4.156), the integration constants and consequently the complexity, it is possible to explore the behavior of the complexity at early times by analyzing solutions close to the so-called *linear geodesic*.

[6] It was used the function `FindRoot` from `Mathematica` in order to find the value of the constants C_1, C_2 and C_3 that satisfies the matrix equation $U(1) = U_{target}$.

4.4.3 The linear geodesic

Before we get into the discussion about the linear geodesic, it is important to point out that the most difficult part of solving the equations (4.156) is in the cost factor μ. If we set this parameter equal zero, which is called *bi-invariant* case, the equations in (4.156) become

$$G_{ab}\frac{dV^b}{ds} = f_{abc}V^bV^c, \tag{4.172}$$

where it was considered that for $\mu = 0$ the metric G_{ab} reduced to Euclidean metric δ_{ab}. In situations where f_{abc} is completely anti-symmetric, the right hand side of (4.172) becomes zero, implying that

$$\frac{dV^a}{ds} = 0. \tag{4.173}$$

The above equation can be easily solved by $V^a = C^a$, where the integration constants C^a can be fixed by applying the boundary conditions (4.153) with U_{target} being e^{-iHt}. Then, as a result we obtain

$$C^aT_a = Ht + 2\pi k, \qquad k \in \mathbb{Z}. \tag{4.174}$$

With the above result, the complexity in (4.158) can be rewritten as

$$\mathcal{C}(t) = \min_{k_n} \sqrt{\frac{1}{N^L}\sum_{n=1}^{N^L}\left(E_nt + 2\pi k_n\right)^2}, \tag{4.175}$$

where E_n are the energy eigenstates of the Hamiltonian, $\{k_1, \ldots, k_{N^L}\}$ are integers that sum to zero due to the traceless condition of $V(s)$ and N and L are the number of bosonic or fermionic degrees of freedom on each site and lattices of the chain, respectively.

For the cases where (4.156) cannot be easily solved, the linear geodesic approach becomes useful. This approximation consists in the assumption that at early times the complexity grows linearly through the local directions generated by T_α. Eventually, the non-local directions will start to take part of the process, which could be understood as the limit of the linear geodesic. Mathematically speaking, the velocities in this case are given by

$$V^\alpha = v^\alpha \qquad \text{and} \qquad V^{\dot{\alpha}} = 0, \tag{4.176}$$

where v^α are constants to be fixed by the boundary conditions.

It was pointed in (4.171) a specific decomposition of H over the T_a generators for the case of one qubit. However, such decomposition can be generalized for any system, namely

$$H = J^aT_b, \qquad J^a = \frac{1}{N^L}Tr\left(HT^a\right). \tag{4.177}$$

Here, we can make the assumption that quadratic Hamiltonians have decomposition only over local directions, since non-local direction could be related with high order terms of

the theory. In this sense, for the case of quadratic Hamiltonians, the v^α constants become

$$v^\alpha = J^\alpha t. \tag{4.178}$$

Once we assumed that the linear geodesic is the correct minimum, the complexity acquires a similar, but simpler, form than (4.175), namely

$$\mathcal{C}(t) = t\sqrt{\frac{1}{N^L}\sum_{n=1}^{N^L} E_n^2}. \tag{4.179}$$

The expression above presents a linear growth for the complexity, agreeing with holographic calculations [11, 12, 18]. The next step is to understand how far we can go with the assumption that the linear geodesic is the appropriate behavior of the minimum related to the complexity of the system.

4.5 Conjugate Points

The linear geodesic is quite adequate to describe the early time behavior of complexity. However, it is well-known that there is limit for the linear growth of complexity, which saturates to its maximum at $t \sim e^N$. After such time, the complexity fluctuates around its maximum value [54]. As a consequence, the linear geodesic cannot be the correct minimum indefinitely. At some point, another curve on the group manifold will take the place of correct minimum. In order to figure out this process for the linear geodesic, we can study the so-called *conjugate points* on $\mathcal{U}$. Let $V(s)$ be the geodesic determined by the Euler-Arnold equations (4.156). As a consequence, we can think on $U(s) : [0,1] \to \mathcal{U}$ as the geodesic on the group manifold. That said, if there exists a variation δ through the geodesic curve, namely $U(\eta, s) : [-\delta, \delta] \times [0,1] \to \mathcal{U}$, such that $U(\eta, s)$ obeys the geodesic equation at first order in η, $U(0,s) = U(s)$, $U(\eta, 0) = \mathcal{I}$ and $U(\eta, 1) = U(1) + \mathcal{O}(\eta^2)$. Conjugate points along a geodesic segment mean that the segment is a saddle point, not a minimum. Therefore, conjugate points are an obstruction to a geodesic segment being locally minimizing.

In order to find conjugate points, we look for a velocity perturbation $\delta V(s)$, also called a Jacobi field, which obeys a first order differential equation known as the Jacobi equation, with adequate boundary conditions. As a direct consequence of the perturbation $\delta V(s)$, there will be a first order change δU in the target unitary operator. Setting the δU perturbation to zero will provide a boundary condition for the Jacobi equation, which is equivalent to find a conjugate point.

The Jacobi equation, in this context, is obtained by studying the first order correction of the Euler-Arnold equation, around the original unperturbed geodesic. In

our case, the original geodesic is the linear one $V = Ht$, which will receive a velocity perturbation

$$Ht \to Ht + \delta V(s). \tag{4.180}$$

If we place the right above perturbation in Euler-Arnold equation (4.156), we obtain the Jacobi equations as

$$\begin{aligned} i\frac{d\delta V_L(s)}{ds} &= \mu t[H, \delta V_{NL}(s)]_L, \\ i\frac{d\delta V_{NL}(s)}{ds} &= \frac{\mu t}{1+\mu}[H, \delta V_{NL}(s)]_{NL}, \end{aligned} \tag{4.181}$$

where the subscripts L (local) and NL (non-local) denote projection into the local ($\mathcal{A}_L$) and non-local ($\mathcal{A}_{NL}$) subspace, namely

$$\begin{aligned} \delta V_L &= \frac{1}{N^L}\sum_{\alpha} Tr\left(\delta V T^{\alpha}\right) T_{\alpha}, \\ \delta V_{NL} &= \frac{1}{N^L}\sum_{\dot{\alpha}} Tr\left(\delta V T^{\dot{\alpha}}\right) T_{\dot{\alpha}}, \end{aligned} \tag{4.182}$$

where T_{α} and $T_{\dot{\alpha}}$ are bases for the local and non-local subspace, respectively.

4.5.1 Solution of the Jacobi equations

In order to solve the Jacobi equations (4.181), notice that in the second equation there is the commutator of a non-local projection δV_{NL} with the Hamiltonian, projected over the non-local subspace. Such commutator can be generalized as a super-operator $C : \mathcal{A}_{NL} \to \mathcal{A}_{NL}$, defined as

$$C(X) = [H, X]_{NL}, \tag{4.183}$$

where X is a non-local operator. The introduction of the super-operator $C(X)$ will be useful in order to solve the non-local equation in (4.181). Consider that exists a new basis $\tilde{T}_{\dot{\alpha}}$ for the non-local subspace where $C(\tilde{T}_{\dot{\alpha}})$ is diagonal, namely

$$C(\tilde{T}_{\dot{\alpha}}) = [H, \tilde{T}_{\dot{\alpha}}]_{NL} = \lambda_{\dot{\alpha}}\tilde{T}_{\dot{\alpha}}, \tag{4.184}$$

where it is possible to write $\delta V_{NL} = \sum_{\dot{\alpha}} \delta\tilde{V}^{\dot{\alpha}}\tilde{T}_{\dot{\alpha}}$ in the tilde basis. With the decomposition (4.184), the non-local equations in (4.181) become

$$i\frac{d\delta\tilde{V}^{\dot{\alpha}}}{ds} = \frac{\mu t}{1+\mu}\lambda_{\dot{\alpha}}\delta\tilde{V}^{\dot{\alpha}}, \tag{4.185}$$

with no summation over $\dot{\alpha}$ on the right-hand side. The solution of the above equation is given by

$$\delta\tilde{V}^{\dot{\alpha}}(s) = \delta\tilde{V}^{\dot{\alpha}}(0)\exp\left(\frac{-i\mu\lambda_{\dot{\alpha}}s}{1+\mu}\right), \tag{4.186}$$

where $\delta\tilde{V}^{\dot{\alpha}}(0)$ are integration constants. If we place the above solution in the local equation of (4.181), we obtain that

$$i\frac{d\delta V_L(s)}{ds} = \mu t\sum_{\dot{\alpha}}\delta\tilde{V}^{\dot{\alpha}}(0)\exp\left(\frac{-i\mu\lambda_{\dot{\alpha}}s}{1+\mu}\right)[H,\tilde{T}_{\dot{\alpha}}]_L, \tag{4.187}$$

whose the solution is

$$\delta V_L(s) = \delta V_L(0) - i\mu t\sum_{\dot{\alpha}}\delta\tilde{V}^{\dot{\alpha}}(0)\frac{\exp\left(\frac{-i\mu t\lambda_{\dot{\alpha}}s}{1+\mu}\right)-1}{\frac{-i\mu t\lambda_{\dot{\alpha}}s}{1+\mu}}[H,\tilde{T}_{\dot{\alpha}}]_L. \tag{4.188}$$

In the above solution, $\delta V_L(0)$ are integration constants due the local Jacobi equation.

Notice that the solutions in (4.186) and (4.188) depend on the existence of the tilde basis $\{\tilde{T}_{\dot{\alpha}}\}$. It is possible to obtain this basis from (4.184) assuming that there exists a relation between the basis $\{\tilde{T}_{\dot{\alpha}}\}$ and $\{T_{\dot{\alpha}}\}$ of the form

$$\tilde{T}_{\dot{\alpha}} = \Lambda_{\dot{\alpha}}{}^{\dot{\beta}}T_{\dot{\alpha}}, \tag{4.189}$$

where $\Lambda_{\dot{\alpha}}{}^{\dot{\beta}}$ is obtained from the relation

$$\Lambda_{\dot{\alpha}}{}^{\dot{\gamma}}\left(iJ^{\alpha}f_{\alpha\dot{\gamma}}{}^{\dot{\rho}}\right)\Lambda^{*}_{\dot{\rho}}{}^{\dot{\gamma}} = D_{\dot{\alpha}}{}^{\dot{\beta}}. \tag{4.190}$$

In the right above equation, $D_{\dot{\alpha}}{}^{\dot{\beta}}$ is a diagonal matrix with the $\lambda_{\dot{\alpha}}$ in its diagonal. In other words, the $\Lambda_{\dot{\alpha}}{}^{\dot{\gamma}}$ will provide to us the basis $\{\tilde{T}_{\dot{\alpha}}\}$ as well as the eigenvalues of the super-operator $C(\tilde{T}_{\dot{\alpha}})$.

4.5.2 Conjugate time

The idea is to use the solutions (4.186) and (4.188) to determine the appearance of the conjugate point. This can be accomplished by understanding the first order perturbation to the unitary $U(1)$ provided by δV, namely

$$U(1) = \mathcal{P}\exp\left(-i\int_0^1 ds(Ht+\delta V(s))\right) = e^{-iHt} - i\delta U(1), \tag{4.191}$$

where $\delta U(1)$ is the first order term from the expansion of $U(1)$ in a Dyson series,

$$U^{-1}\delta U(1) = \int_0^1 ds e^{iHts}\delta V(s)e^{-iHt}. \tag{4.192}$$

Considering the expression right above, a conjugate point is obtained from the condition

$$U^{-1}\delta U(1) = 0. \tag{4.193}$$

If we place the solutions (4.186) and (4.188) in (4.192), it is possible to consider $U^{-1}\delta U(1)$ as a super-operator $\mathbf{Y}_{(\mu)} : \delta V(0) \to U^{-1}\delta U(1)$, whose the action is given by

$$\begin{aligned}\mathbf{Y}_{(\mu)}\left(\delta V(0)\right) = \int_0^1 ds e^{iHts}\Bigg[\delta V_L(0) - i\mu t\sum_{\dot\alpha}\delta\tilde V^{\dot\alpha}(0)\frac{\exp\left(\frac{-i\mu t\lambda_{\dot\alpha}s}{1+\mu}\right)-1}{\frac{-i\mu t\lambda_{\dot\alpha}s}{1+\mu}}[H,\tilde T_{\dot\alpha}]_L \\ + \delta\tilde V^{\dot\alpha}(0)\exp\left(\frac{-i\mu\lambda_{\dot\alpha}s}{1+\mu}\right)\Bigg]e^{-iHts}.\end{aligned} \tag{4.194}$$

In this super-operator language, a conjugate point corresponds to a zero mode of $\mathbf{Y}_{(\mu)}$. In general, the zero mode conditions will provide an equation of the form $\Phi(\mu, g_1, \ldots, g_n, t) = 0$, where $g_1, \ldots, g_n$ are the Hamiltonian parameters. If it is possible to solve this equation for t, either analytically or numerically, we obtain the so-called conjugate time t_c, which is the instant of time where the first conjugate point appears.

4.5.3 Bi-invariant case

Finding the zero modes of $\mathbf{Y}_{(\mu)}$ for general values of μ is analytically difficult. It can be done numerically using the method proposed in [55], but it still is a hard process. On the other hand, the bi-invariant case ($\mu = 0$) is much simpler, allowing us to obtain the conjugate points exactly. For the bi-invariant case, the expression (4.194) becomes

$$\mathbf{Y}_{(0)}(\delta V(0)) = \int_0^1 ds e^{iHts}\delta V(0)e^{-iHt}, \tag{4.195}$$

where this simplified form is due the fact that $\mu = 0$ all generators are considered to be local (or easy).

It is not difficult to realize that the eigenoperators of $\mathbf{Y}_{(0)}$ are the energy eigenstates projectors $|m\rangle\langle n|$. Placing these projectors in (4.195), we obtain that

$$\mathbf{Y}_{(0)}(|m\rangle\langle n|) = \phi_{mn}(t)\,|m\rangle\langle n|\,, \qquad \phi_{mn}(t) = \frac{e^{i\Delta mnt}-1}{i\Delta mnt}, \tag{4.196}$$

where $\phi_{mn}(t)$ are the eigenvalues of $\mathbf{Y}_{(0)}$ and $\Delta mn = E_m - E_n$. If we impose the zero mode condition for $\phi_{mn}(t)$, we obtain a family of conjugate points that are given by the condition

$$t_{mn} = \frac{2\pi}{\Delta mn}. \tag{4.197}$$

The linear geodesic develops a number of conjugate points that is as larger as the number of eigenstates of the Hamiltonian, with $E_m \neq E_n$, at the times given by (4.197). We are

interested on the first time at the first conjugate points appears. Then, the conjugate time t_c is given by

$$t_c = \frac{2\pi}{E_{max} - E_{min}}, \tag{4.198}$$

where E_{max} and E_{min} corresponds to the higher and lower eigenvalues, respectively.

The analysis of the first conjugate point is relevant for understand how long it takes to the complexity saturates. It is expected that t_c is sensitive to changes on the Hamiltonian parameters, which is a promising connection between the physical behavior of the system and the abstract geometry of the group manifold.

4.5.4 Perturbative case

In the bi-invariant case, the conjugate points appear for certain times t_{mn} that are given by (4.197). It was already pointed out that it could be a difficult task to find a similar rule for the general case ($\mu \neq 0$). However, instead of making ($\mu = 0$), it is possible to consider small values of μ and perform some perturbation theory for this parameter. Small values of μ essentially mean that there is still a differentiation between local and non-local directions, however, in terms of penalization of choosing non-local generators, this difference is quite small, more precisely speaking, $\mu \ll 1$.

We can start rewriting the velocity perturbation $\delta V(s)$ as

$$\delta V(s) = \delta V^{(0)}(s) + \mu \delta V^{(1)}(s) + \mu^2 \delta V^{(2)}(s) + \mathcal{O}(\mu^3). \tag{4.199}$$

If we place (4.199) in (4.181), it is possible to solve the Jacobi equation order to order in μ. The zero-th order equation is quite simple,

$$\frac{d}{ds}\delta V^{(0)}(s) = 0 \;\rightarrow\; \delta V^{(0)}(s) = \delta V^{(0)}(0), \tag{4.200}$$

which is nothing less than the already known bi-invariant case for the conjugate points analysis. The new results will come from the first order correction, namely

$$\frac{d}{ds}\delta V_L^{(1)}(s) = -it[H, \delta V_{NL}^{(0)}(0)]_L, \tag{4.201}$$

$$\frac{d}{ds}\delta V_{NL}^{(1)}(s) = -it[H, \delta V_{NL}^{(0)}(0)]_{NL}, \tag{4.202}$$

whose the solution is

$$\delta V^{(1)}(s) = \delta V^{(1)}(0) - ist[H, \delta V_{NL}^{(0)}(0)]. \tag{4.203}$$

If we place (4.200) and (4.202) together, we obtain the full solution of $\delta V(s)$ up to first order on μ, which is

$$\delta V(s) = \delta V^{(0)}(0) + \mu \left(\delta V^{(1)}(0) - ist[H, \delta V_{NL}^{(0)}(0)] \right). \tag{4.204}$$

Once we have the perturbative solution, it is time to figure out some relation for the development of conjugate points. In this sense, we could try to obtain a family of conjugate points that are similar to the ones provided by (4.197). It can be done by finding the zero modes of $\mathbf{Y}_{(\mu)}$ perturbatively, order to order, namely

$$\langle m|\mathbf{Y}_{(\mu)}(\delta V(s))|n\rangle = \int_0^1 ds e^{its\Delta_{mn}}\Big[\langle m|\delta V^{(0)}(0)|n\rangle + \mu\langle m|\left(\delta V^{(1)}(0) - ist\Delta_{mn}\delta V^{(0)}_{NL}(0)\right)|n\rangle\Big], \tag{4.205}$$

where we are considering the matrix elements of $\mathbf{Y}_{(\mu)}$ in order to make the result simpler. The next step is to perform the integral in (4.205), resulting in

$$\langle m|\mathbf{Y}_{(\mu)}(\delta V(s))|n\rangle = \phi_{nm}(t)\langle m|\left(\delta V^{(0)}(0) + V^{(1)}(0)\mu|n\rangle\right) - \mu t\frac{\partial\phi_{nm}(t)}{\partial t}\langle m|\delta V^{(0)}_{NL}(0)|n\rangle. \tag{4.206}$$

It is reasonable to expect that the times t_{mn}, for this perturbative case, have the form

$$t_{mn} = t^{(0)}_{mn} + \mu t^{(1)}_{mn} + \mu^2 t^{(2)}_{mn} + \mathcal{O}(\mu^3), \tag{4.207}$$

where $t^{(0)}_{mn}$ are nothing less than the set of bi-invariant conjugate points and $t^{(n)}_{mn}$ for $n \geq 1$ are the higher order corrections. By placing (4.207) in (4.206) and imposing the zero modes condition, we obtain that the first order correction for t_{mn} is

$$t^{(1)}_{mn} = t^{(0)}_{mn}\frac{\langle m|\delta V^{(0)}_{NL}(0)|n\rangle}{\langle m|\delta V^{(0)}(0)|n\rangle}. \tag{4.208}$$

From the bi-invariant case, it is already known that $\delta V^{(0)}(0) = |m\rangle\langle n|$, which can provide a significant simplification on the denominator of (4.208). Then, the final expression for the times t_{mn} is

$$t_{mn} = t^{(0)}_{mn}\left(1 + \mu\langle m|\delta V^{(0)}_{NL}(0)|n\rangle\right). \tag{4.209}$$

For the perturbative case, the first order correction depends on the matrix elements of the non-local projection of $|m\rangle\langle n|$, which is not trivial to compute. Additionally, the so-called conjugate time t_c corresponds to the lesser value provided by (4.209).

4.6 Complexity of operators and Phase Transitions

Our goal here is to lay hands on the tools developed so far to study the relation between complexity of states and quantum phase transitions. There are already some works where the authors explore phase transitions in the context of complexity of states

[42, 43, 44], however, complexity of states was not duly explored on this direction. In a nutshell, phase transitions represent abrupt changes that occur in the equilibrium state of the system, at specific points, due the change of certain parameters. Thermal (classical) phase transitions occur at a specific temperature T_c, named critical temperature. On the other hand, quantum phase transitions occur at zero temperature due the change of some parameter β which measures the relative weight of two competing terms in an Hamiltonian. At certain critical value β_c, the ground state of the system changes abruptly.

The investigation here will consist on realizing if the complexity toolbox is capable to 'feel' a quantum phase transition. It is expected that two quantities manage to do such task: the complexity by itself and the conjugate time t_c. In order to accomplish this task, the system that will be considered is the one-dimensional XX-Model. The choice of this system is due to two facts: 1) This model was exhaustively studied, which means that are many already known results about it; 2) There is a connections between the XX-Model and the Bose-Hubbard Model (BHM) [56] in the so-called hard-core boson limit [57].

The BHM is a bosonic model on periodic chain with L sites, whose Hamiltonian is

$$H = -J\sum_{i=1}^{L}\left(a_i^\dagger a_{i+1} + a_i a_{i+1}^\dagger\right) + \frac{U}{2}\sum_{i=1}^{L} n_i(n_i-1), \qquad n_i = a_i^\dagger a_i, \tag{4.210}$$

where the first term is the kinetic, or hopping, term that controls the jump of particles between adjacent sites, while the second term is the repulsive local potential ($U > 0$) term at a single site due to particle-particle interaction. What is interesting in our context is the fact that the BHM displays a quantum phase transition between a superfluid phase and a Mott insulator phase as one changes the ratio U/J of the parameters.

The problem here is that the BHM is not a model of qubits: at the L sites of the chain it is possible to have an arbitrary number of bosons, instead of just the two values of the qubit. However, in the limit of large U, namely the strong coupling limit or hard-core boson limit, we can assume that there are no many fluctuation on the number of bosons, which is equivalent to have either 0 or 1 particle at each site. Consequently, the model can be mapped to an $SU(2)$ spin-1/2 model, which is the XX-Model that we are going to discuss next.

4.6.1 XX-Model

The XX-Model makes part of a important class of exactly soluble models that are very important in condensed matter physics and statistical mechanics. These models can be put together in what we call of XY-Model. Consider a one-dimensional spin chain with L sites, each described by Pauli operators σ_a^α, with $a = 1, \ldots, L$ and $\alpha \in \{x, y, z\}$.

The general Hamiltonian for the XY-Model is given by

$$H = -\sum_{i=1}^{L} \left[J_x \sigma_i^x \sigma_{i+1}^x + J_x \sigma_i^y \sigma_{i+1}^y + h\sigma_i^z \right], \tag{4.211}$$

where the first two terms describe a nearest-neighbor interaction in the xy plane, while the last one describes a magnetic field pointing in the z direction. The model is called XY because the interaction is anisotropic, which is usually defined as

$$J_x = J\left(\frac{1+\gamma}{2}\right), \qquad J_y = J\left(\frac{1-\gamma}{2}\right), \tag{4.212}$$

where $\gamma \in [0, 1]$ is called the anisotropy parameter and J is a constant. If $\gamma = 0$ the couplings in the x and y directions become equal and we refer to it, instead, as the XX-model, namely

$$H = -\sum_{i=1}^{L} \left[J\left(\sigma_i^x \sigma_{i+1}^x + \sigma_i^y \sigma_{i+1}^y\right) + h\sigma_i^z \right]. \tag{4.213}$$

On the other hand, if $\gamma = 1$, the y part of the interaction vanishes and we are left with

$$H = -\sum_{i=1}^{L} \left[J\sigma_i^x \sigma_{i+1}^x + h\sigma_i^z \right], \tag{4.214}$$

which is called transverse field Ising model (TFIM).

There are a lot that we can say about these models, however, we are going to focus on the quantum phase transition of the XX-Model. In order to analyse such phenomena, we are going to consider as order parameter the average spin of the system, which we will refer to as *magnetization*, namely

$$m = \frac{1}{L}\sum_{i=1}^{L} \langle \sigma_i^z \rangle, \tag{4.215}$$

where $\langle \sigma_i^z \rangle$ is the expected value of σ_i^z for the ground state. The magnetization takes values in the range $m \in [-1, 1]$, which are the quantum phases of the system. If $m = -1$, all spins are downward. On the other hand, if $m = 1$, all spins are upward.

The magnetization is susceptible to the changes on h/J, like the complexity and the conjugate time are expected to be. In this sense, our strategy will be to make a parallel between these three quantities. We want to see if the complexity and t_c a similar sensibility to the changes of h/J than the magnetization.

4.6.2 Numerical analysis

We will start with a detailed analysis of three qubits ($L = 3$) for the XX-Model in the bi-invariant case ($\mu = 0$), where we have 63 generators with 36 being local and 27 non-local. The XX-Model is an example of H being purely local, which fits perfectly in the formalism developed so far. For our model, it is possible to compute the magnetization and conjugate time t_c for three qubits. The result is shown in the Figure 4.3, where we clearly see the phase transition of the model.

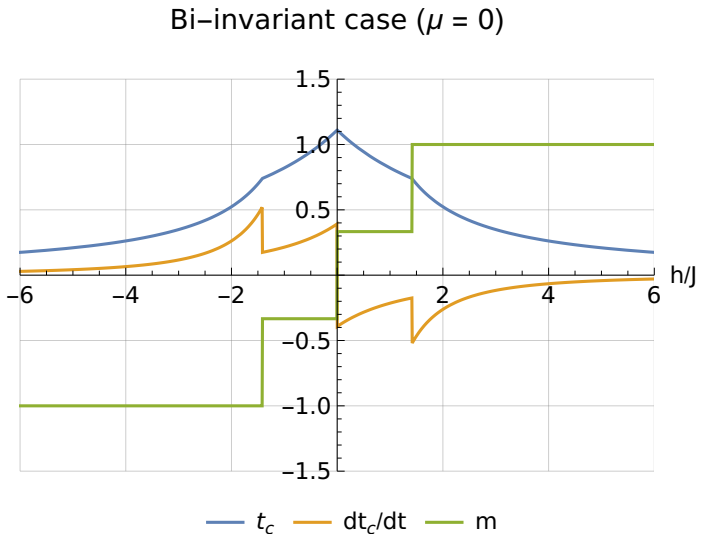

Figure 4.3: Comparison between conjugate time, its derivative and magnetization in the XX-Model for three qubits.

In Figure 4.3, the green curve represents the magnetization m of the model. For $|h/J| > 1.4$, all spins are oriented to the same direction (upward or downward), while for $|h/J| < 1.4$ we have a no-orientated configuration for the spins. At points where the magnetization changes abruptly, we observe kinks in the conjugate time t_c (blue curve). These kinks are discontinuities in t_c that seems to appear only when the ordering of spins changes. In order to check if these kinks aren't numerical errors, we also plotted the derivative of t_c (orange curve), which have notable discontinuities at the same points than the kinks of t_c.

The fact that t_c is sensitive to the phase transitions is not a big surprise. It is known that quantum phase transitions are related to change of the ground state. If we go back to (4.198), we see that t_c is essentially a function of the gap between lowest and highest energies. When the ground states abruptly changes, so does its energy, implying a similar change in t_c. These changes in energies of the system are better understood if we take a look at the level crossing of the model, which is shown in Figure 4.4. For $h/J \sim 1.4$ we see the last crossing for lowest and highest energies. Then, from this point on, there is no crossing anymore, which corresponds to the upward spin case. A similar

effect happens for $h/J \sim -1.4$.

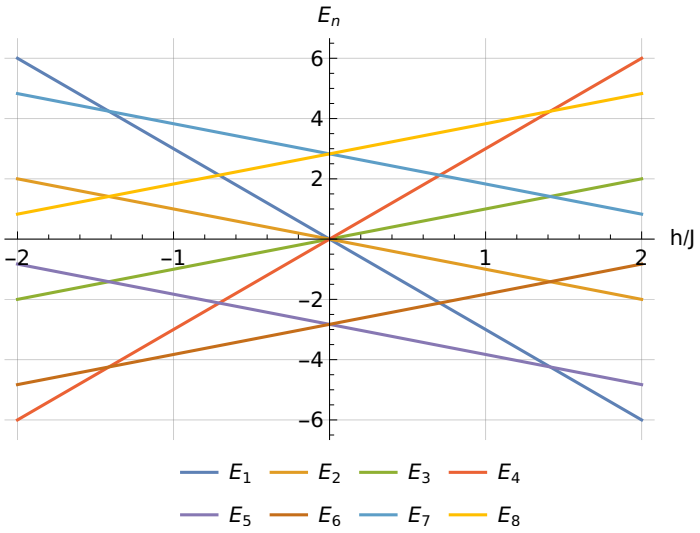

Figure 4.4: Level crossing of the XX-Model for three qubits.

On the other hand, for $\mu \ll 1$, we do not have the kinks of t_c so well located than in the bi-invariant case, as can be seen in Figure 4.5. What happens is a small displacement of the kinks due the first correction provided by μ. We still have the kinks close to points where the magnetization changes abruptly, however, it is not safe anymore to claim that the discontinuities from t_c are related to the phase transition.

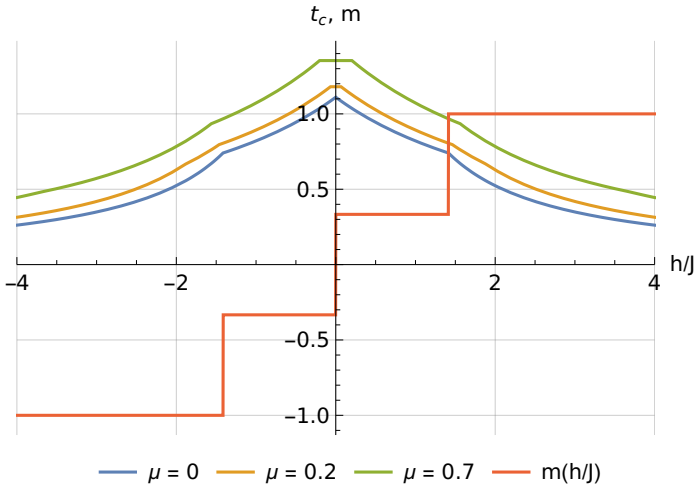

Figure 4.5: Conjugate time in the perturbative case ($\mu \ll 1$).

What seems to be case is that the bi-invariant conjugate time provides a good correspondence with the phase transition of the XX-model. On the other hand, when we consider the perturbative conjugate point, this correspondence get worse as we increase μ. It shouldn't be really surprising because the μ parameter is not in the Hamiltonian, which means that changing this parameter will not interfere on the energies of the sys-

tem. The μ parameter introduces in our problem an anisotropy between simple and hard directions on the group manifold, which potentially will have some effects on the final complexity. However, it is missing a connection between μ and some physical quantity of the model. Some possibility would arise in models with higher order terms where H isn't quadratic anymore. These high order terms will be related to non-local generators and a combination of the coupling constants associated to these terms could be used to build the dimensionless parameter μ. In this sense, the bi-invariant conjugate time is adequate for the study of quantum phase transitions in quadratic systems.

Another interesting plot that could be analysed is the bi-invariant complexity (4.175). For three qubits, the complexity as function of time is shown in Figure 4.6. Indeed, the complexity saturates at some point, with the time required for the complexity reaches the peak decreasing as h/J increases. This is evidence that at least the saturation time is related to the conjugate time. On the other hand, the complexity does not present a behavior that characterizes some sensibility to the phase transitions. Even the kinks are not enough in this case, meaning that they probably are effects of an irregular oscillation due the small number of qubits.

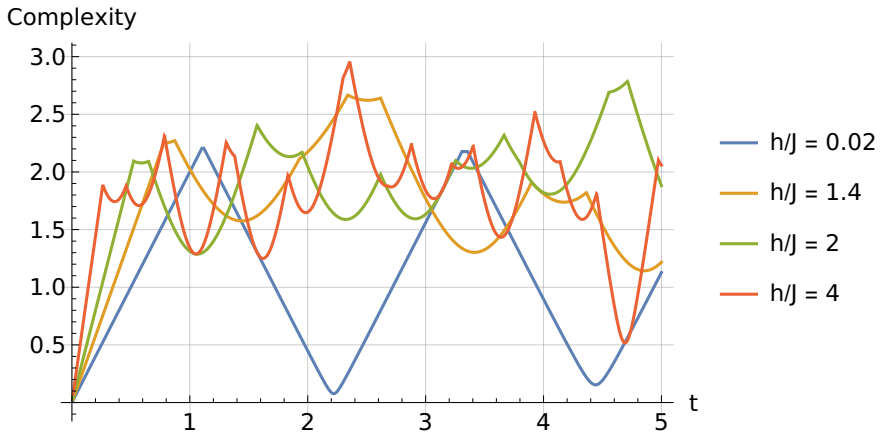

Figure 4.6: Complexity as function of time for different values of h/J.

Lastly, it could be pointed that the correspondence between t_c and the magnetization is just because the small number of qubits. However, it was obtained a similar result for five qubits, as it is shown in Figure 4.7. The difference here is that are five kinks instead of three, but still similar to which was obtained in the previous case. Even so, these kinks are matching the magnetization change, presenting discontinuities on it derivative.

The increasing of qubits number also improved the behavior of complexity as function of time, which is shown in Figure 4.8. On this case, the saturation value for $\mathcal{C}$ seems to be almost the same for different values of h/J. Also, the amplitude of oscillation after the saturation becomes smaller in comparison to what we obtained for three qubits. Apparently, increases the number of qubits tends to make the complexity after the satu-

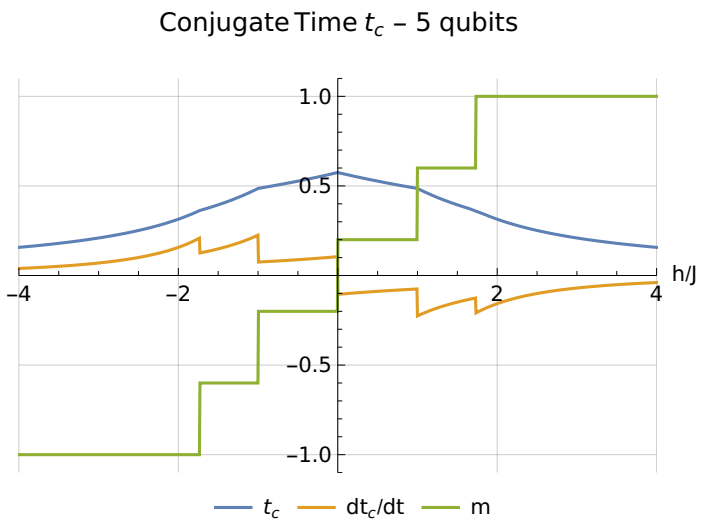

Figure 4.7: Comparison between conjugate time, its derivative and magnetization in the XX-Model for five qubits.

ration less dependent of h/J. Saturation time keeps in accordance to the conjugate time t_c, like in the previous case.

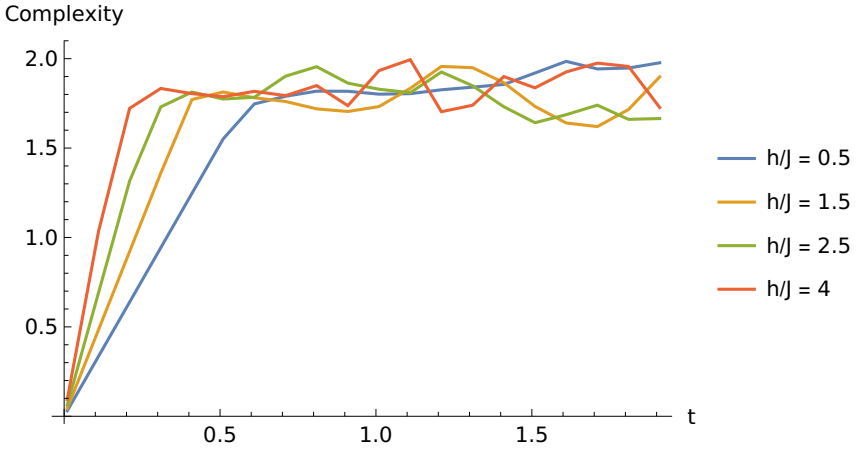

Figure 4.8: Saturation of the complexity for five qubits in the XX-Model.

The study of conjugate points related to quantum phase transitions generated satisfactory results, specially for the bi-invariant case. In order to keep improving these results, we could keep looking for strategies to increase the number of qubits. The dimension of matrices grows quite fast as the number of qubits increases, which is a problem that could be suppressed using different computational methods or even other techniques to obtain the spectra of H. Another possible path to improve results would be to consider the analysis of conjugate points in momentum space, which perhaps is more adequate since the spin chains in general are studied in momentum space.

Final remarks

Since the first works by Susskind [17, 18] about the CA conjecture, a significant progress on the understanding of holographic complexity was made [23]. This quantity now is being explored from different perspectives, specially in the context of quantum mechanics, which was one of our goals here. Additionally, it is possible to point more recent new developments in the studies of complexity called Krylov complexity, which essentially consists in measuring the spreading of a quantum state in the so-called Krylov basis [58]. Despite the fact that this new proposal to compute complexity is closer to complexity of states than operators, there is at least one study where the Krylov complexity is used [59] in the context of phase transitions.

From the holographic complexity point of view, we demonstrate how to apply the CA conjecture to the MT Model for perturbative solutions of the model, up to order a^2. There is a possible extension of this analysis that would be to consider complexity of the model at order a^4. In this situation, the model presents conformal anomaly. So, the question would be about effects of the anomaly on the complexity. However, it will be expected some computational difficulties to handle the model, specially to obtain solutions for the equations of motion at order a^4. Additionally, it will be important to evaluate these solutions at the horizon and boundary of the AdS space-time, which are important points in order to compute thermodynamic quantities of the model and complexity as well. In any case, despite technical difficulties that could appear, computing the computational complexity for the MT Model at order a^4 would be an interesting research project.

The complexity, from the QFT side, seems to be an interesting quantity to study certain properties of quantum systems. When we considered the complexity of the TFD state for the charged scalar field theory, we obtained that the time derivative of the complexity has an expression similar to the Lloyd's bound for the charged AdS-Schwarzschild black hole. This is an indicative that there is, at least in some level, a correspondence between the holographic diagnostic for complexity and what was obtained for it using only quantum mechanic tools.

For the free fermions in $1 + 1$, the complexity of the Bogoliubov transformed vacuum provided us with an overview about the basic techniques that are necessary to compute complexity for quadratic Hamiltonian. The complexity for fermionic systems was not explored as extensively as in comparison to bosonic systems. This provides some

perspectives about studying complexity for other fermionic systems. Also, the complexity for supersymmetric systems is less explored field, as well as the case of interacting theories [25].

From the complexity of operators perspective, it was developed an interesting formalism with clear rules to compute the required quantities (complexity, conjugate time, etc). However, the computation become difficult to handle quite fast. Even the general solutions of the Euler-Arnold equations are hard to obtain for two qubits. Part of these difficulties come up with a suitable basis of easy and hard operators as the number of qubits grows. Avoiding matrix representation for the generators as much as possible might be also a valuable strategy in order to make the computations more suitable.

Computational difficulties directed us to the study of conjugate points, which seems to be promising at least for the study of phase transitions. We also obtained the complexity behavior as function of time, in special, its saturation at t_c. At this stage, it is fair to point out that great part of the computational difficulties appear because the introduction of cost factor μ. Despite the fact that this parameter provides a separation between easy and hard operators, it is still a parameters placed by hand that makes the problem more complicated. Figure out what are the cases where turn on μ is relevant will be a relevant question in future development. There is also a audacious approach which consists in to consider different μ for any locality, making to use operators with higher locality more and more expansive in term of complexity amount.

Bibliography

[1] G. 't Hooft, *Dimensional reduction in quantum gravity*, *Conf. Proc. C* **930308** (1993) 284–296, [gr-qc/9310026].

[2] L. Susskind, *The World as a hologram*, *J. Math. Phys.* **36** (1995) 6377–6396, [hep-th/9409089].

[3] J. M. Maldacena, *The Large N limit of superconformal field theories and supergravity*, *Adv. Theor. Math. Phys.* **2** (1998) 231–252, [hep-th/9711200].

[4] A. Einstein, B. Podolsky, and N. Rosen, *Can quantum-mechanical description of physical reality be considered complete?*, *Phys. Rev.* **47** (May, 1935) 777–780.

[5] J. S. Bell, *On the Problem of Hidden Variables in Quantum Mechanics*, *Rev. Mod. Phys.* **38** (1966) 447–452.

[6] P. Calabrese and J. L. Cardy, *Entanglement entropy and quantum field theory*, *J. Stat. Mech.* **0406** (2004) P06002, [hep-th/0405152].

[7] S. Ryu and T. Takayanagi, *Holographic derivation of entanglement entropy from AdS/CFT*, *Phys. Rev. Lett.* **96** (2006) 181602, [hep-th/0603001].

[8] S. Ryu and T. Takayanagi, *Aspects of Holographic Entanglement Entropy*, *JHEP* **08** (2006) 045, [hep-th/0605073].

[9] J. Maldacena and L. Susskind, *Cool horizons for entangled black holes*, *Fortsch. Phys.* **61** (2013) 781–811, [arXiv:1306.0533].

[10] J. Watrous, *Quantum Computational Complexity*, *arXiv e-prints* (Apr., 2008) arXiv:0804.3401, [arXiv:0804.3401].

[11] L. Susskind, *Computational Complexity and Black Hole Horizons*, *Fortsch. Phys.* **64** (2016) 24–43, [arXiv:1403.5695]. [Addendum: Fortsch.Phys. 64, 44–48 (2016)].

[12] L. Susskind, *Entanglement is not enough*, *Fortsch. Phys.* **64** (2016) 49–71, [arXiv:1411.0690].

[13] J. Maldacena, S. H. Shenker, and D. Stanford, *A bound on chaos*, *JHEP* **08** (2016) 106, [arXiv:1503.01409].

[14] Y. Sekino and L. Susskind, *Fast Scramblers*, *JHEP* **10** (2008) 065, [arXiv:0808.2096].

[15] D. Stanford and L. Susskind, *Complexity and Shock Wave Geometries*, *Phys. Rev. D* **90** (2014), no. 12 126007, [arXiv:1406.2678].

[16] L. Susskind, *Entanglement is not enough*, *Fortsch. Phys.* **64** (2016) 49–71, [arXiv:1411.0690].

[17] A. R. Brown, D. A. Roberts, L. Susskind, B. Swingle, and Y. Zhao, *Holographic Complexity Equals Bulk Action?*, *Phys. Rev. Lett.* **116** (2016), no. 19 191301, [arXiv:1509.07876].

[18] A. R. Brown, D. A. Roberts, L. Susskind, B. Swingle, and Y. Zhao, *Complexity, action, and black holes*, *Phys. Rev. D* **93** (2016), no. 8 086006, [arXiv:1512.04993].

[19] M. A. Nielsen, *A geometric approach to quantum circuit lower bounds*, *arXiv e-prints* (Feb., 2005) quant–ph/0502070, [quant-ph/0502070].

[20] M. A. Nielsen, M. R. Dowling, M. Gu, and A. C. Doherty, *Quantum Computation as Geometry*, *Science* **311** (Feb., 2006) 1133–1135, [quant-ph/0603161].

[21] M. R. Dowling and M. A. Nielsen, *The geometry of quantum computation*, *arXiv e-prints* (Dec., 2006) quant–ph/0701004, [quant-ph/0701004].

[22] S. Chapman, M. P. Heller, H. Marrochio, and F. Pastawski, *Toward a Definition of Complexity for Quantum Field Theory States*, *Phys. Rev. Lett.* **120** (2018), no. 12 121602, [arXiv:1707.08582].

[23] D. Carmi, S. Chapman, H. Marrochio, R. C. Myers, and S. Sugishita, *On the Time Dependence of Holographic Complexity*, *JHEP* **11** (2017) 188, [arXiv:1709.10184].

[24] A. Bernamonti, F. Galli, J. Hernandez, R. C. Myers, S.-M. Ruan, and J. Simón, *Aspects of The First Law of Complexity*, *J. Phys. A* **53** (2020) 29, [arXiv:2002.05779].

[25] A. Bhattacharyya, A. Shekar, and A. Sinha, *Circuit complexity in interacting QFTs and RG flows*, *JHEP* **10** (2018) 140, [arXiv:1808.03105].

[26] R. Khan, C. Krishnan, and S. Sharma, *Circuit Complexity in Fermionic Field Theory*, *Phys. Rev. D* **98** (2018), no. 12 126001, [arXiv:1801.07620].

[27] L. Fortnow and S. Homer, *A short history of computational complexity*, *Bulletin of the EATCS* **80** (01, 2003) 95–133.

[28] A. M. Turing et al., *On computable numbers, with an application to the entscheidungsproblem*, *J. of Math* **58** (1936), no. 345-363 5.

[29] M. Nielsen and I. Chuang, *Quantum Computation and Quantum Information: 10th Anniversary Edition*. Cambridge University Press, 2010.

[30] L. Trevisan, *Lecture notes on computational complexity*, *Notes written in Fall* (2002).

[31] E. D. Demaine, S. Hohenberger, and D. Liben-Nowell, *Tetris is Hard, Even to Approximate*, *arXiv e-prints* (Oct., 2002) cs/0210020, [cs/0210020].

[32] R. M. Karp, *Reducibility among combinatorial problems*, in *Complexity of computer computations*, pp. 85–103. Springer, 1972.

[33] J. M. Maldacena, *Eternal black holes in anti-de Sitter*, *JHEP* **04** (2003) 021, [hep-th/0106112].

[34] A. R. Brown and L. Susskind, *Second law of quantum complexity*, *Phys. Rev. D* **97** (2018), no. 8 086015, [arXiv:1701.01107].

[35] D. Stanford and L. Susskind, *Complexity and Shock Wave Geometries*, *Phys. Rev. D* **90** (2014), no. 12 126007, [arXiv:1406.2678].

[36] S. Lloyd, *Ultimate physical limits to computation*, *Nature* **406** (Aug., 2000) 1047–1054, [quant-ph/9908043].

[37] D. Mateos and D. Trancanelli, *The anisotropic N=4 super Yang-Mills plasma and its instabilities*, *Phys. Rev. Lett.* **107** (2011) 101601, [arXiv:1105.3472].

[38] D. Mateos and D. Trancanelli, *Thermodynamics and Instabilities of a Strongly Coupled Anisotropic Plasma*, *JHEP* **07** (2011) 054, [arXiv:1106.1637].

[39] S. A. Hosseini Mansoori, V. Jahnke, M. M. Qaemmaqami, and Y. D. Olivas, *Holographic complexity of anisotropic black branes*, *Phys. Rev. D* **100** (2019), no. 4 046014, [arXiv:1808.00067].

[40] L. Lehner, R. C. Myers, E. Poisson, and R. D. Sorkin, *Gravitational action with null boundaries*, *Phys. Rev. D* **94** (2016), no. 8 084046, [arXiv:1609.00207].

[41] R. Cheng, *Quantum Geometric Tensor (Fubini-Study Metric) in Simple Quantum System: A pedagogical Introduction*, *arXiv e-prints* (Dec., 2010) arXiv:1012.1337, [arXiv:1012.1337].

[42] F. Liu, S. Whitsitt, J. B. Curtis, R. Lundgren, P. Titum, Z.-C. Yang, J. R. Garrison, and A. V. Gorshkov, *Circuit complexity across a topological phase transition*, *Phys. Rev. Res.* **2** (2020), no. 1 013323, [arXiv:1902.10720].

[43] Z. Xiong, D.-X. Yao, and Z. Yan, *Nonanalyticity of circuit complexity across topological phase transitions*, *Phys. Rev. B* **101** (2020), no. 17 174305, [arXiv:1906.11279].

[44] N. Jaiswal, M. Gautam, and T. Sarkar, *Complexity and information geometry in the transverse XY model*, *Phys. Rev. E* **104** (2021), no. 2 024127, [arXiv:2005.03532].

[45] J. Preskill, *Lecture notes for physics 229: Quantum information and computation*, *California Institute of Technology* **16** (1998).

[46] S. Chapman, H. Marrochio, and R. C. Myers, *Complexity of Formation in Holography*, *JHEP* **01** (2017) 062, [arXiv:1610.08063].

[47] W. K. Wootters, *Statistical Distance and Hilbert Space*, *Phys. Rev. D* **23** (1981) 357–362.

[48] M. Sinamuli and R. B. Mann, *Holographic Complexity and Charged Scalar Fields*, *Phys. Rev. D* **99** (2019), no. 10 106013, [arXiv:1902.01912].

[49] A. B. Klimov and S. M. Chumakov, *A group-theoretical approach to quantum optics: models of atom-field interactions*. John Wiley & Sons, 2009.

[50] K. Goto, H. Marrochio, R. C. Myers, L. Queimada, and B. Yoshida, *Holographic Complexity Equals Which Action?*, *JHEP* **02** (2019) 160, [arXiv:1901.00014].

[51] V. Balasubramanian, M. Decross, A. Kar, and O. Parrikar, *Quantum Complexity of Time Evolution with Chaotic Hamiltonians*, *JHEP* **01** (2020) 134, [arXiv:1905.05765].

[52] V. Balasubramanian, M. DeCross, A. Kar, Y. C. Li, and O. Parrikar, *Complexity growth in integrable and chaotic models*, *JHEP* **07** (2021) 011, [arXiv:2101.02209].

[53] V. Balasubramanian, M. Decross, A. Kar, and O. Parrikar, *Quantum Complexity of Time Evolution with Chaotic Hamiltonians*, *JHEP* **01** (2020) 134, [arXiv:1905.05765].

[54] A. R. Brown, L. Susskind, and Y. Zhao, *Quantum Complexity and Negative Curvature*, *Phys. Rev. D* **95** (2017), no. 4 045010, [arXiv:1608.02612].

[55] V. Balasubramanian, M. DeCross, A. Kar, Y. C. Li, and O. Parrikar, *Complexity growth in integrable and chaotic models*, *JHEP* **07** (2021) 011, [arXiv:2101.02209].

[56] H. A. Gersch and G. C. Knollman, *Quantum cell model for bosons*, *Phys. Rev.* **129** (Jan, 1963) 959–967.

[57] E. Altman and A. Auerbach, *Oscillating Superfluidity of Bosons in Optical Lattices*, *prl* **89** (Dec., 2002) 250404, [cond-mat/0206157].

[58] V. Balasubramanian, P. Caputa, J. M. Magan, and Q. Wu, *Quantum chaos and the complexity of spread of states*, *Phys. Rev. D* **106** (2022), no. 4 046007, [arXiv:2202.06957].

[59] P. Caputa and S. Liu, *Quantum complexity and topological phases of matter*, *Phys. Rev. B* **106** (2022), no. 19 195125, [arXiv:2205.05688].